Optimal Design Synthesis of Multi Speed Gear Trains

Murugiah Narayana Moorthy

A Thesis
in
The Department
of
Mechanical Engineering

Presented in Partial Fulfillment of the Requirements
for the Degree of Master of Applied Science at
Concordia University
Montreal, Quebec, Canada

July 1995

ISBN 0-612-05137-4

Canada

ABSTRACT

OPTIMAL DESIGN SYNTHESIS OF MULTI SPEED GEAR TRAINS

MURUGIAH NARAYANA MOORTHY
Concordia University, 1995

Gear train systems that possess uncertain characteristics due to manufacturing, assembling, and operating conditions are analyzed based on a systematic optimum design synthesis. The efficiency and reliability of the system are described by probabilistic variables based on minimum mass and maximum transmitted power. The torsional vibratory response is analyzed through possible individual realizations of mounting of component gears on shafts. Kinematic parameters are generated for minimum overall size and error in the gear ratios. To overcome the practical difficulty of repeated analyses of different design layouts of a gear drive application, a new computer aided design methodology is proposed for generating all possible speed diagrams.

ACKNOWLEDGEMENTS

My sincerest gratitude goes out to my thesis advisor, Dr. T. S. Sankar under whose guidance this research thesis was completed before his leaving the University. His ideas and contribution were instrumental in the development and final results of my research work. A special debt of thanks is owed to the thesis supervisor Dr. V. Latinovic for his advice and assistance during the final stage of my work. In particular, I thank Dr. R. Ganesan for many of his useful suggestions in the reliability and dynamic portions of the work presented here and his advice has been very valuable. I also would like to recognize Dr. A.S. Kumar who has been most supportive of my work.

I wish to thank the NSERC for the financial support in the form of research assistantship through different grants awarded to Dr. T. S. Sankar.

I would also like to thank my parents Mr and Mrs Murugiah for their unwavering support, patience and understanding. Special thanks to my friends Dr. Kasi Periyasamy and Dr. R. Ranganathan for their encouragement.

LIST OF ILLUSTRATIONS

LIST OF TABLES

NOMENCLATURE

α	Flexibility
B	Speed range ratio
C	Damping
d	Turning or boring diameter
D_i	Center distance of i^{th} transmission stage
DV	Dunkerley value
E(i)	Algebraic constant relating input and output speed positions
F	Constraint function
FW	face width
G1	Total number of single gear sets.
G2	Total number of 2 gear sets
G3	Total number of 3 gear sets
g( )	Density function
i	Transmission stage order
J	Inertia
J	Equivalent inertia
J_C	Equivalent inertia for cluster
J_G	Equivalent inertia for gear
K	Stiffness
K	Equivalent stiffness
K_B	Factor derived for bending stress
K_C	Stress concentration factor
K_D	Dynamic load factor
K_W	Factor derived for wear stress
K_C	Equivalent coupling stiffness

K_I	Equivalent stiffness of the input shaft
K_O	Equivalent stiffness of the output shaft
K_S	Equivalent stiffness between wheels mounted shafts
K_{int}	Net value for optimized shaft stiffness
KE	Kinetic energy
k_1	Weighting factor
k_2	Weighting factor
L	Number of transmission stages
M_t	Transmitting torque
m	Module
N	Number of spindle speeds
n	Rotating speed of workpiece
$N_I(i)$	Number of input speeds for i^{th} transmission stage
$N_O(i)$	Number of output speeds for i^{th} transmission stage
NG	Number of gear sets
NS	Number of shafts
NV	Number of design variables
NSR	Number of shafts required
P	Transmitted power
PE	Potential energy
R	Reliability
R_i	Reliability of i^{th} element
R_{sys}	System reliability
R_{max}	Maximum gear ratios laid by design standards
R_{min}	Minimum gear ratios laid by design standards
R(i,j)	Gear ratio of j^{th} gear set in i^{th} transmission stage
S_B	Bending strength

s_B	Induced bending stress
S_W	Wear strength
s_W	Induced wear stress
S	Mean value of strength
s	Mean value of induced stress
S(i,l)	l^{th} speed ratio of i^{th} transmission stage
SF	Speed frequency
T	Torque
T_{max}	Maximum number of teeth laid by design standards
T_{min}	Minimum number of teeth laid by design standards
T_p	Number of pinion teeth
T_w	Number of wheel teeth
$T_p(i,1)$	Number of pinion teeth in i^{th} transmission stage of reference transmission path
$T_p(i,1)$	Number of pinion teeth of 1^{th} gear set in i^{th} transmission stage
$T_w(i,1)$	Number of wheel teeth in i^{th} transmission stage of reference transmission path
$T_w(i,1)$	Number of wheel teeth of 1^{th} gear set in i^{th} transmission stage
V_l	Lowest possible speed of wheel
$V_I(i,j)$	j^{th} input speed of i^{th} transmission stage
$V_O(i,k)$	k^{th} output speed of i^{th} transmission stage
x	Design variable
y	Lewis factor
z	Standardized variable for normal distribution curve
Z(i)	Number of gear sets in the i^{th} transmission stage
α	Pressure angle
δ	Tolerance value for gear ratio deviation

ε	Deviation on the gear ratio
Φ	Objective function
ϕ	Step ratio
$\varphi^{-1}(R)$	Normal variate corresponding to reliability
λ_i	Eigen value
ω_i	Natural frequency
ρ	Material density
ξ	Excess stress value
θ	Angular displacement
$\dot{\theta}$	Angular velocity
$\ddot{\theta}$	Angular acceleration
V	Cutting speed
σ	Standard deviation
ζ_{op}	Operational efficiency limit

TABLE OF CONTENTS

CHAPTER 1

INTRODUCTION

1.1 Design needs

Mechanical systems such as machine tools in manufacturing, precision tools, turbogenerators, high speed rotodynamic systems, etc. require the capability of producing a wide range of operating speeds. This demands the proper selection of a particular speed from within the spectrum of operating speeds. Such an objective is achieved in industrial machines by the use of multi-speed gear trains, that are located between the drive unit (power source) and spindle. A complete design of multi-speed gear trains is carried out based on the following qualitative and quantitative information:

1. Speed of the drive unit (input speed)
2. Speeds on the spindle (output speed)
3. Space limitations
4. Power transmitting capacity
5. Weight limitations
6. Reliability of the components
7. Vibrational safety
8. Operating conditions (i.e. temperature, lubrication, etc.)

A decision about the structure itself is to be made before deciding on these variables, considering the intended use.

The selection of speeds on drive unit and spindle is normally identified so that the designer can decide on the range of various different speeds, among which a particular speed for a given operation is to be picked up. Then the multi-speed gear train is designed to provide this range of output speeds from a single input speed of drive unit and this stage of design is known as *kinematic design*. A decision about the speeds on shafts, spacing

between mating gears and the number of teeth of different gears is generally the output of the kinematic design. The auxiliary information about the driving and the driven gears as well as the speeds transferred through each gear set, is also provided as an additional output of the kinematic design.

The power transmission capability and reliability of a gear train are controlled by one or more of several possible failure phenomena, such as tooth breakage, tooth wear, scoring, pitting fretting, etc. These failures are caused, when the induced stresses increase above the strength of the gear train component corresponding to a particular failure mode during power transmission. Hence, the components are to be designed for their geometrical properties, whereas the selection of a suitable material is to be carried out keeping in view the intended use. This brings in the second stage of the design process, the *strength design*. The kinematic design serves as the starting point of the strength design. The decision about the face widths of all the gear sets to satisfy wear strength, bending strength and other safety requirements, is the output of the strength design.

Furthermore, as can be deduced form the above descriptions, the kinematic design can reliably be based on a deterministic framework. But, on the other hand, the strength design, by its inherent character, need to be carried out on a probabilistic framework. This is because both the actual loads and the load capability of the gear train are fundamentally probabilistic in nature. The use of safety factor in the design of gear systems, has for long been accepted in practice and indirectly accounts for these kinds of uncertainties. It has been well recognized that this uncertainty severely affects the performance of the entire gear systems and better analysis is needed in design of gears. But the statistical nature of these design safety factors themselves has been recognized only in recent times. Any deviations, which might be caused by motion of the gears relative to one another, tooth profile or spacing errors, fluctuations in applied loads, variations in strength parameters like tooth stiffness, etc. are seen to produce combinations of frequency and amplitude modulation of the mesh frequency. The hunting is the tooth failure phenomenon that is encountered in

most cases due to the strength parameter fluctuations. This is highly dangerous with respect to operational safety and it produces an audible amplitude modulation of the gear mesh frequency. So, a complete probabilistic treatment can only be a natural recourse to design gear trains for a prescribed reliability and service life.

The reflection of these kinds of uncertainties can be clearly seen on the gear vibration signature. Considering two gears of different size, the transmission error gives rise to, (i) the interaction force on both the gears (ii) a difference in their linear displacements. This error is a time dependent function over the operating cycle of the machine and is basically stochastic in nature. A wide array of problems can always be attributed to the unavoidable, ever-present, inherent randomness in the gear systems. Stochasticity is always present at all stages of design of gear systems, particularly in specifications, configurations, tooth geometries, material selection, etc. All these contribute to large fluctuations and hence a drastic reduction in the service life and thereby in the premature failure of the gear trains.

A complex broad vibration spectrum, beginning with frequencies well below the shaft rotational speeds and extending to several multiples, is known as the gear mesh frequency. This gear mesh frequency, is defined, as being equal to the number of gear teeth times the shaft rpm. The obvious important role played by the natural frequency and the number of teeth for a given gear rotating speed is now evident. When the load varies during one complete revolution, gear systems develop torsional vibrations. Torsional vibrations are also caused depending on the torsional stiffness of the shaft and the rotary inertia. The critical effect of the number of teeth can also be observed from the noise spectrum of an operating gear. Gear systems are also subjected to common vibration problems arising due to rotating mass imbalance caused by misalignment or shaft deflection.

In addition to these, there are quite a few problems that are unique to gears such as pitch line runout, pitting, fretting, etc. Fair among them have their origin of occurrence at the tooth contact where cyclic dynamic stresses are caused by gearing action.

1.2 Some definitions of gear train configuration

General definitions and details of gears and gear trains are available in numerous gear literature. However as a pre-requisite, some basic definitions are reviewed in this section. Throughout the present investigation, spur gears are selected as the component for consideration because of their precision and design simplicity. Spur gears are gears, in which the tooth form is an involute, the pressure angle is constant, the teeth dimensions are identical in all planes of rotation and the teeth lie parallel to the axis of rotation. Further more, the ability to transmit high speeds and loads with high precision allows spur gears to be used commonly in the design of machine tools [23]. In a power transmitting gear set, the driving gear known as the *pinion* is located on the input shaft, transmitting the rotational speed and torque to the output shaft through the driven gear known as the *wheel*. Because the axis of rotation of both shafts are parallel, this type of arrangement is called as *parallel shaft gear arrangement* and the shortest line between the axes is termed as the *center distance*. The ratio of the rotational speeds of wheel to the pinion is known as *speed ratio*. In the course of a design for multiple speeds of output shaft, it may be desirable to use several gears and shafts. This type of arrangements are termed as multi-speed multi-shaft gear trains. In such a case, the speeds on the output shaft, which is connected to the spindle, are called *spindle speeds*. Typical mathematical rules exist for the number of spindle speeds and the ratio between the successive speeds on the multi-speed gear trains of industrial machine tools in use.

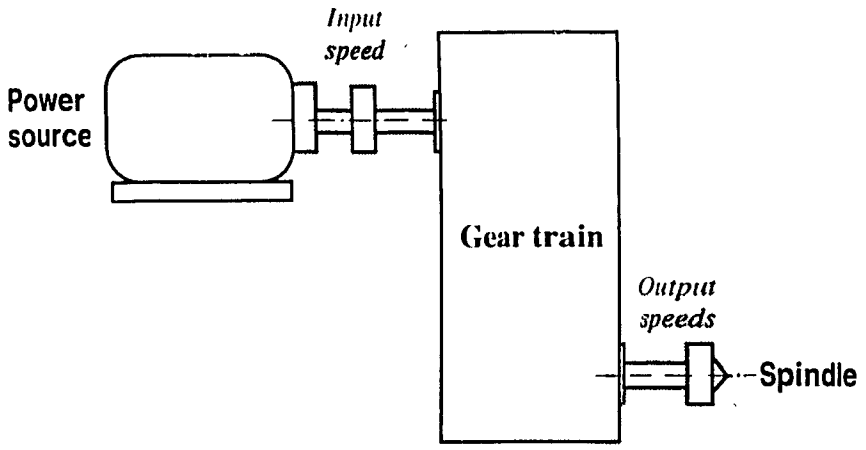

Figure 1.1 Location of the multi-speed gear train in an industrial machine tool

Physical location of the gear train of an industrial machine tool is shown in Figure 1.1. In general, a multi-speed gear train provides the required spindle speeds through various sectors which are termed as *transmission stages*. In each transmission stage, input speed is transformed through a cluster mechanism or a single gear set. By shifting the cluster to different mesh positions, the engagement pattern of the mating gears is changed, resulting in a new spindle speed. Normally, the cluster mechanism contains two or three gear sets with different pitch diameters. The number of gear sets in a given transmission stage is obtained according to the *transmission formula* of the gear train. The transmission formula is defined as the numerical expression in the form of a product equation and relates the number of gear sets in the gear arrangement with the number of spindle speeds. The left hand side (L.H.S.) of transmission formula shows the number of spindle speeds produced, and the right hand side (R.H.S.) of transmission formula indicates the number of gear sets in each transmission stage and the order of occurrence. For a 18 speed gear train with 3 transmission stages, the transmission formula is given as: 18 = 3 * 3 * 2. This corresponds to 18 speed gear train with 4 shafts, *kinematic arrangement* which is shown in Figure 1.2.

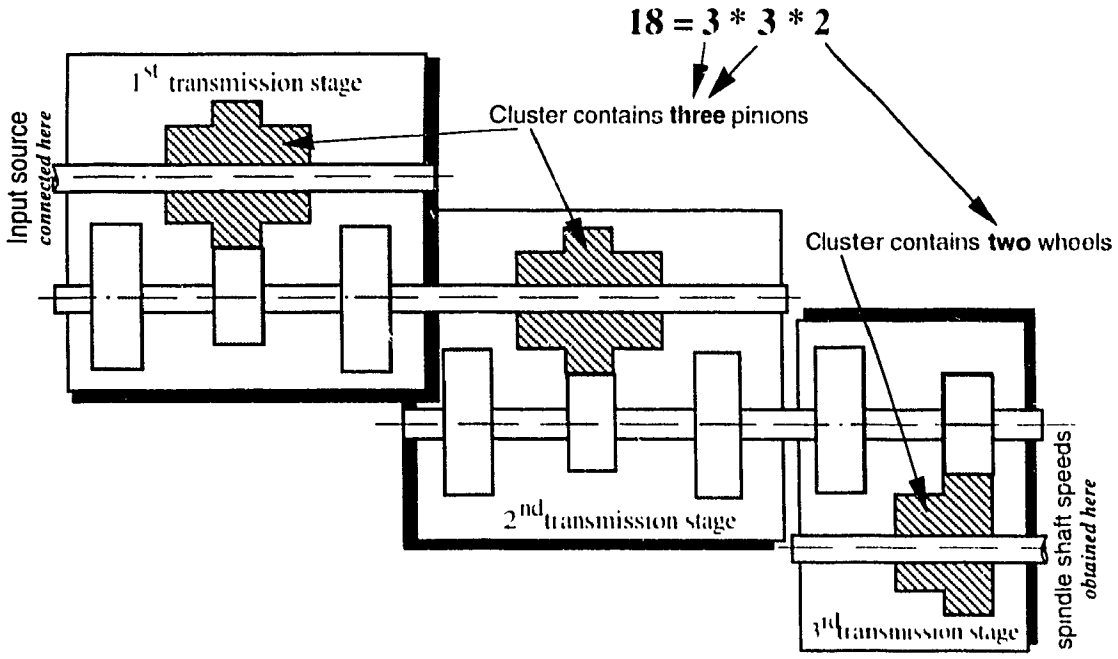

Figure 1.2 Kinematic arrangement of a 18 = 3 * 3 * 2 gear train

The order of transmission stages from drive unit to spindle is not unique for a specified number of spindle speeds. This order can be changed to yield a improved dynamic behavior of the entire gear system. Similarly, interchanging the non-identical transmission stages will alter the speed distribution pattern of the gear train as well as the layout of the kinematic arrangement. When a gear train is in its operational regime, each of the spindle speed produced is obtained by engaging a new combination of mating gears. The mesh position of all pinions and wheels of the gear train is termed as the *engagement pattern* for the corresponding spindle speed. Each engagement pattern is normally identified with an integer which is refered to as the *transmission path index*.

1.3 Thesis organization

The prime concern of the present investigation is to introduce a comprehensive design synthesis of parallel shaft multi-speed gear trains of industrial machine tools by which improved design tasks such as accurate speeds on the spindle, reduced space limitations, increased power transmitting capacity, reduced weight limitations, reliable components and vibrational safety are secured. Although many researchers have previously attempted to investigate these design tasks separately, most of them overlooked other viable designs that may be possible for a given set of initial specifications. The present investigation describes an efficient and improved way of integrating a systematic design methodology for the above mentioned design tasks with nonlinear programming technique of optimization.

To facilitate an automated design synthesis of gear trains, a computer aided solution for producing all possible speed diagrams is developed in Chapter 2. The overall design synthesis of gear trains presented here consists of three stages: kinematic design, strength design and the torsional vibration safety analysis. In the kinematic design, all layouts that can produce the desired spindle speeds from a specified input speed, are checked for a possible design with a minimum overall size of the gear train. This is presented in Chapter 3, where the procedure for the option of optimum number of teeth with the minimum gear ratio error of all gears is developed. This kinematic design is carried out essentially in a deterministic approach. However, the stochastical type of errors introduced due to both the manufacturing defects as well as the material property variability are considered in the next stage of design, i.e. the strength design. Here, a probabilistic approach is formulated wherein the variability is included in terms of the ranges of the above mentioned errors. Strength design thus becomes a problem of optimum design subject to random parameters. The variability of gear train parameters determined by the kinematic design also affects the component reliability and service life. So, a prescribed level of reliability has to be specified and achieved at the design stage. This leads to an additional constraint in the

optimization problem. Therefore, based on the reliability concept, an optimum strength design of a optimum kinematic design is developed in Chapter 4. The torsional vibration safety is achieved through a detailed investigation of all possible dynamic system configurations. Different spindle speeds are obtained by changing the engagement pattern of the mating gears, that ultimately alters the dynamic system configuration and results in a mobile distribution of inherent inertia. Not all the kinematically distinct dynamic configurations of same engagement pattern have the same order of sensitivity. A solution algorithm for obtaining optimum shaft stiffnesses of a gear train is required, considering all possible dynamic configurations of each engagement pattern, to avoid the torsional resonance of the system. Such a method is presented in Chapter 5, where all possible dynamic configurations of all engagement patterns are identified for the solution.

1.4. Relevant Historical Development

Mechanical devices similar to gears were stated to have been first used by world's ancient civilizations such as Greeks, Egyptians, Chinese and Tamils. The earliest written description of gears is said to be made by Aristotle in 4th century B.C., but the real beginning of gearing was in 250 B.C., with Archimedes [48]. He used gears to simulate astronomical ratios and also in the mechanisms for use in war. Many models that use gears are found in the manuscripts of Leonardo da Vinci, written between 1493 and 1497. The artistic talent and engineering genius of Leonardo da Vinci in this area are evident in his studies of the design of tooth profile and various gearing arrangements, that were centuries ahead of their time. Chinese south pointing chariot, early Roman clocks and cyclometer are just a few examples where gears were used in the beginning of the first century A.D.[17].

In early times, gears were adopted for a long time without any technical improvements. Poor tooth contact and large backlash were common in these early gears and this required a greater understanding on the kinematic behavior of such devices. To this end, much of the developments were focused on effect of the physical shape of the

gear teeth while transmitting power. The gear tooth form was soon modified to transfer the rotational motion smoothly. During the period of 1450 to 1750, the mathematical analysis of gear tooth profiles and theories on geared mechanisms were formulated. By 1700, the cycloidal tooth form and involute form were proposed to maintain the constant relative angular velocity in gearing. Involute tooth then became commonly acceptable because of its two advantages over cycloidal, namely: (1) errors in the center distance produces no effect on the kinematics of involute gear tooth, and (2) surface curvature of involute tooth form allows transmission of a constant load as compared to cycloidal. Since the industrial revolution in the mid-19th century, the art of gear design blossomed and gear design became more based on scientific principles. In early part of the twentieth century, many more improvements were made to the involute gear tooth form. As a result, spur and helical gears became the major power transmitting components. By this time, parallel shaft gear trains were slowly introduced in transportation systems. By 1916 after the arrival of specialized machine tools, the need for multi-speed gear trains that have the capability of transmitting high torques and high rotational speeds became a necessity. As the demand for better manufacturing quality of gear trains arose, the requirement for higher performance reliability, and lower cost became the prime concern of many gear designers. Unfortunately, there are still many unsolved problems that exist in the domain of multi-shaft, multi-speed gear trains, solutions for which will be the subject of investigation for many more years to come [17, 48, 56, 59].

Most noteworthy analytical solutions for the design of various gears, gearing systems and their behaviors are discussed in a wide range of references [1, 23, 24, 28, 45, 54]. It is understood that the conventional analytical methods lead to overdesign since they are based on the concept of safety factors as these theories fail to predict critical stress and vibration levels accurately. Although, the basic principles have not changed in recent years, the design of gears and gear trains has undergone significant changes and improvements. To this end, the computer-aided simulations and exact solutions that allow

designer to synthesize and analyze gears and gear trains have been developed. These solutions are now widely used to improve the existing geometry of gears in reliable and efficient design of the gear trains. One such a computer-aided solution for gear geometry is given by Staph [46], which studies the effect of the parameter which influences mostly the involute gear geometry, namely the contact ratio. This study concludes that high contact ratios for involute spur gears favour lower bending stress in teeth and produce large friction, induced heat and flash temperatures.

Gears in mesh never operate under smooth, continuous load. Factors such as manufacturing errors in tooth profile and circular pitch, tooth deflections under load, and mass unbalance all interact to create a fluctuating dynamic load. Attempts have been made to study the dynamic load through various techniques such as modal analysis [26] and statistical analysis by [53]. Modifications to tooth profile can affect the dynamic behavior of the mating gear system [14, 50, 51]. An improved dynamic model was proposed by Yang et al [61], in which the backlash in mating gears was taken into account. The same model was later improved by considering also the deformations arising due to bending, axial compressions and coluomb friction [60].

Considerable effort has been devoted during the recent past, to develop efficient computational methods for the kinematic and strength designs of gear trains based on the concept of deterministic approach, but similar efforts are lacking for reliable stochastic design of gear trains. Highly versatile finite element methods have for long been in use for strength analysis of gears [32, 55]. However, little attention has been paid in developing appropriate automated design schemes for multi-speed gear trains. One such computer-aided design synthesis of spur gears and multi-speed gear trains is reported in [15] and [27] respectively. In this method, the computer aided solutions are made more effective by the implementation of numerical optimization methods. The numerical optimization procedure provides a thorough search of all possible designs in the feasible space to select the best parameters for an efficient design. It starts by identifying the design variables to be

chosen, the constraints on the anticipated design and the objective function by which the best design will be selected. A detailed optimum design of standard spur gear set is presented in [42, 43] by considering those aspects of stress related failures such as scoring, pitting, bending and the feasible gear geometry condition of involute interference. The model presented in [43] is modified considering AGMA codal previsions for geometry and dynamic factors by Carroll et al [10]. The authors then replaced the constraint of involute interference with the condition of under-cut prevention and solved the problem in a dimensionless design space [11].

Keeping in view the design synthesis of gear trains, White [57] is the first author to present an analytical module for the kinematic characteristics. However, this module can only be applicable for a selected type of gear train. An improved model is presented in reference [58] adopted for different gear arrangements, but it obviously has many drawbacks. Osman et al [34] improved the model developed by White in reference [57] by adopting an optimization procedure to design nine speed gear train with ten gears, resulting in optimal values for pitch diameters and the ratio of minimum spindle speed to input speed. In order to automate the optimization procedure using the model in reference [34] for different types of gear trains, Bush [8] and Bush et al [9] formulated an alternative method. This investigation combines the volume minimization with the maximization of the shaft stiffness based on kinematic design parameters such as gear ratio and pitch diameters. The recent work by Osman et al [33] provides a generalized design procedure based on the optimal speed ratio. The procedure examines kinematic design of a 12 speeds composite gear train with 3 shafts and 12 gears. The obvious drawback in the work is that the variable representing the number of teeth is treated as non integer.

While minimizing the cost through reduction of weight of component gear sets of the gear train, the effects on parameters such as overall gear ratio, pressure angle, contact ratio, induced stresses, face widths, and number of pinion teeth are examined in reference [12]. A computer aided design approach to determine all possible number of teeth for a

multi-shaft gear train that can produce a specific spindle speed from a specified speed of the drive unit is reported in [5] and [6]. This work was modified to accommodate an additional condition on the center distance specification in [7]. These works [5, 6, 7] used no optimization techniques. An optimization method that yields minimum values for the center distance, speed deviations on all shafts and masses along with maximum transmitted power is presented in reference [39] satisfying wear and bending stress constraints.

While transmitting the power from one rotating shaft to another, the gear teeth in contact contribute to energy dissipation. A perfect form of the teeth without any defects, would cause very little or negligible vibration and as a result of this, a negligible cyclic dynamic loading [4, 49]. In reality, a complex nature of vibration response could be observed which would severely affect the safety of the gear systems [9]. Rattle problems are also commonly encountered in gear systems due to vibro-impacts experienced [36]. From the all vibration related gear failures reported in the past, one important characteristic can be observed, namely, the inherent uncertainty associated with the failure modes. Uncertainty is implied in the definition of gear system dynamic parameters, material properties, operational speeds and environmental conditions, etc [37]. In this context it is clear that a statistically based design synthesis of gear trains, would allow one to conduct the design of component gears on the basis of computational schemes that reflect, to a great extent, real life conditions. A probabilistic approach will not only make use of these modern advancements, in a most efficient manner, but also will make the design conducted for a desired confidence level. Such a method based on reliability constraints in the design of a multi-speed gear train is reported in reference [40].

A steady, vibration free operation of the gear train in a machine system largely depends on its torsional natural frequency [8]. The component gears are to be placed on the shafts at selected locations defined by the shaft stiffness where torsional vibrations are expected to be a minimum. For this purpose, the component gears are sought to posses

minimum inertia [44]. A study of a single gear set mounted on torsionally deformable shaft is presented in reference[29]. An efficient method for avoiding the torsional vibrations in multi-speed gear trains through the proper selection of optimum shaft stiffness is proposed by Narayana Moorthy, Ganesan and Sankar [31].

All of the above surveyed literature deals with only spur gears. It has been generally accepted that the helical gears offer better performance characteristics than spur gears. A report on computer aided helical gear design is given in reference [22]. The literature survey, however, indicates that there is no much work available on the selection of bearings or in the area of alignments, unbalance and runouts of component gear sets in gear trains. Design of housing for the gear trains is another area which may lead to reduction in noise and vibrations but is yet to draw attention of researchers.

CHAPTER 2

An automated generalized procedure for generating all possible speed diagrams

2.1 Introduction

Establishment of speed diagram is essentially a combination of iterative and graphical design procedure where the designer decides on basic parameters such as speed ratios in which the component gears are to operate, input speed of drive, spindle speeds and other parameters related to the of the kinematic design of gear train system. Such a procedure is time consuming and prone to errors. The computer aided method for determining speed diagrams described in this chapter eliminates many of the difficulties experienced in this procedure. A wide range of tasks involving the design of gear trains can be handled by the proposed procedure. It also reduces the computing time to a few minutes with complete interactive progress to final design and specification of the gear train outline. Examples illustrating the various options available to the designer are revealing efficiency and the simplicity of the procedure.

2.2 Fundamentals on cutting speeds

Cutting speeds and feeds in machine tool applications are dictated by various instantaneous machining conditions. The use of multipurpose and universal machine tools that are most common in the modern manufacturing industry are operated under complex machining conditions. Thus, a range of useful speeds are to be provided by the design of such type of machines, wherein the multi-speed gear trains are widely used to satisfy the requirements. Since the tool life and the operational cost of the manufacturing process largely depend on the accuracy with which the required output speed is obtained,

improvements over the speed determination of a gear train are continuing challenge. To this end, the intended use of gear train is one of the first concerns.

Considering the cutting process, which is accomplished by the turning or boring diameter d (mm) of workpiece revolving at a rotating speed n (rpm), the cutting speed V (m/min) is given by,

$$V = \frac{\pi * d * n}{1000} \approx \frac{d * n}{320} \tag{2.1}$$

or

$$n = \frac{320 * V}{d} \tag{2.2}$$

For a machine tool a range of workpiece diameters to be produced is usually preselected at d_{min} and d_{max}. Depending on what cutting tools and workpiece materials are going to be machined, a range of cutting speeds is preselected at V_{min} and V_{max}. The minimum and maximum spindle speeds in revolutions per minute may, then, be defined as [23]:

$$n_{min} = \frac{320 * V_{min}}{d_{max}} \tag{2.3}$$

$$n_{max} = \frac{320 * V_{max}}{d_{min}} \tag{2.4}$$

The speed range ratio B which is defined as the ratio between the maximum and minimum spindle speeds required is given by,

$$B = \frac{n_{max}}{n_{min}} \tag{2.5}$$

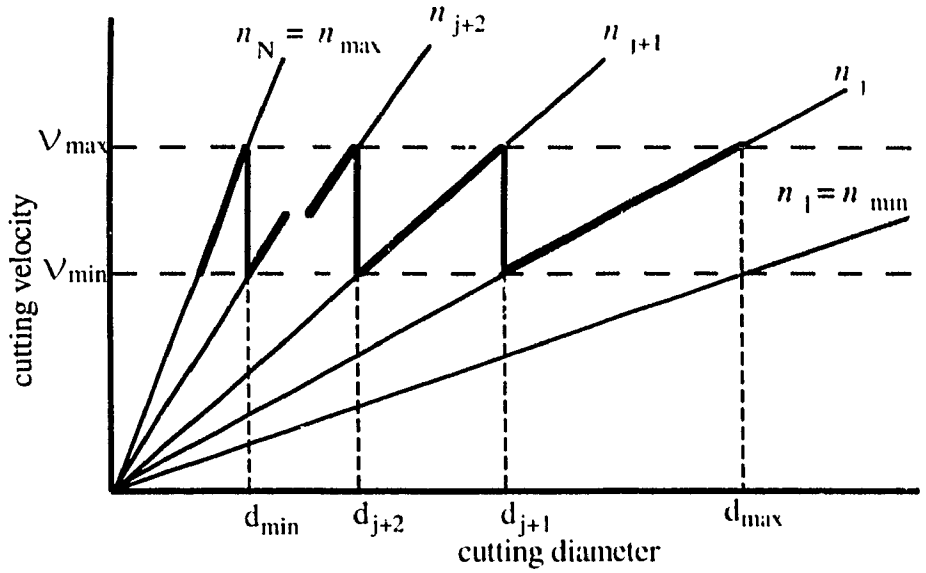

Figure 2.1 Cutting speeds for geometric speed progressions [23]

If the cutting speeds are plotted as the function of cutting diameter d, a linear relationship appears for different rotational speeds $n_1, n_2, \ldots n_N$. as shown in the Figure 2.1. These rotational speeds are governed by n_{max} and n_{min}. As required, the proposed gear train is to be designed to cover the above mentioned speed range ratio B.

$$n_{j+1} = \frac{320 * V_{max}}{d_{j+1}} = \frac{320 * V_{min}}{d_{j+2}} \quad , \qquad j = 1,2,..N. \tag{2.6}$$

Since, it is not possible to obtain an optimum rotational speed continuously to achieve optimal cutting speed, it is common practice to provide a number of spindle speeds (steps) which will provide rotational speeds that give near the optimal cutting speed within the specified operational efficiency limit ζ_{op} [34]. This allows machining of a workpiece of a certain diameter range, using cutting speeds between the established limits.

$$\zeta_{op} = \frac{V_{min}}{V_{max}} \tag{2.7}$$

where V_{min} and V_{max} are defined as actual cutting speed and optimal cutting speed respectively.

The step between two consecutive spindle speeds in a speed range n_{j+1}, n_j is given as:

$$\frac{n_{j+1}}{n_j} = \frac{V_{max}}{V_{min}} = \phi = \frac{1}{\zeta_{op}} \tag{2.8}$$

The constant ϕ is called the step ratio. Equation (2.8) shows that the spindle speeds are in geometric progression with the reduction ratio which is always a constant and equal to $(\phi - 1) / \phi$. In this way, if one spindle speed is changed to the next, the reduction ratio is always maintained the same. A series of spindle speeds are standardized for a given machine tool [23]. Most commonly used spindle speeds are named as R20 series of the preferable numbers and shown in Table 2.1. Based on the R20 series, sub-series R20/2, R20/3, R20/4 are obtained by selecting the second, third, and forth speed series respectively. The sub-series have a step ratio as a power of ϕ - ϕ^2, ϕ^3 and ϕ^4 .

Nominal rev min^{-1}										Limiting rev min^{-1} of the R20 series			
Basic series R20	Sub series									Due to Mechanical variables		Due to mechanical and electrical variables	
	R 20/2	R 20/3			R 20/4		R 20/6						
ϕ =1.12	ϕ =1.25	ϕ =1.4			ϕ =1.6		ϕ = 2			-2%	+3%	-2%	+6%
1	2	3			4	5	6			7	8	9	10
100										98	103	98	106
112	112	11.2				112	11.2			110	116	110	119
125			125							123	130	123	133
140	140			1400	140				1400	138	145	138	150
160		16								155	163	155	168
180	180		180			180		180		174	183	174	188
200				2000						196	206	196	212
224	224	22.4			224		22.4			219	231	219	237
250			250							246	259	246	266
280	280			2800		280			2800	276	290	276	299
315		31.5								310	326	310	335
355	355		355		355			355		348	365	348	376
400				4000						390	410	390	422
450	450	45				450	45			438	460	438	473
500			500							491	516	491	531
560	560			5600	560				5600	551	579	551	596
630		63								618	650	618	669
710	710		710			710		710		694	729	694	750
800				8000						778	818	778	842
900	900	90			900		90			873	918	873	945
1000			1000							980	1030	980	1060

Table 2.1 Rotational speed ranges for machine tools (DIN 804)

The following relationship can be derived using equations (2.3) to (2.8)

$$n_{max} = \phi^{N-1} * n_{min} \tag{2.9}$$

where N is number of spindle speeds.

i.e.

$$\phi^{N-1} = \frac{n_{max}}{n_{min}} = B \tag{2.10}$$

Table 2.2 shows the speed range ratio B and the number of spindle speeds N, for different types of machine tools [24].

Type of Mchine tool	B	N
Planing machines	6 - 10	6 - 9
Lathes	50 - 200	12 - 18
Milling and boring machines	Up to 400	Up to 36
Presses	1	1

Table 2.2 Values of B and N for selected machine tools (Lynwander, [24])

2.3 Layout diagram and speed diagram

Layout diagram is a graphical representation showing all proposed speed ratios of the gear train. In the layout diagram, the speed ratios of mating gears are represented by mesh lines which are drawn to join speed positions between the lines representing the shafts. With the layout diagram, one can directly see how the speeds are changing from input shaft towards spindle and which gear sets are used to produce the required output speeds. Adopting the layout diagram representation, mesh lines with negative slope indicate decreasing speeds and that with positive slope indicate increasing speeds. It is observed that the largest output speeds in all transmission stages are produced through the largest speed ratios, using gear sets that provide the corresponding speed ratios. In a similar way, the lowest output speeds in all stages are obtained using the lowest speed ratios using the gear sets with lowest gear ratios. All other speeds are obtained by the combination of appropriate speed ratios that are shown in the layout diagram.

Since equation (2.8) shows that the spindle speeds are in geometric progression, the speeds in the layout diagram are plotted on a logarithmic scale on speed axis. On the

other axis, the shafts are represented as equally spaced parallel lines. The ratio of successive output speeds in the line represented by the spindle is equal to the step ratio ϕ. For intermediate shafts, the ratio of successive speeds may not be equal to ϕ, but may be an integral power of ϕ. For an intermediate shaft, if all speed positions are not at equal distance, the shaft is said to have a discontinuity.

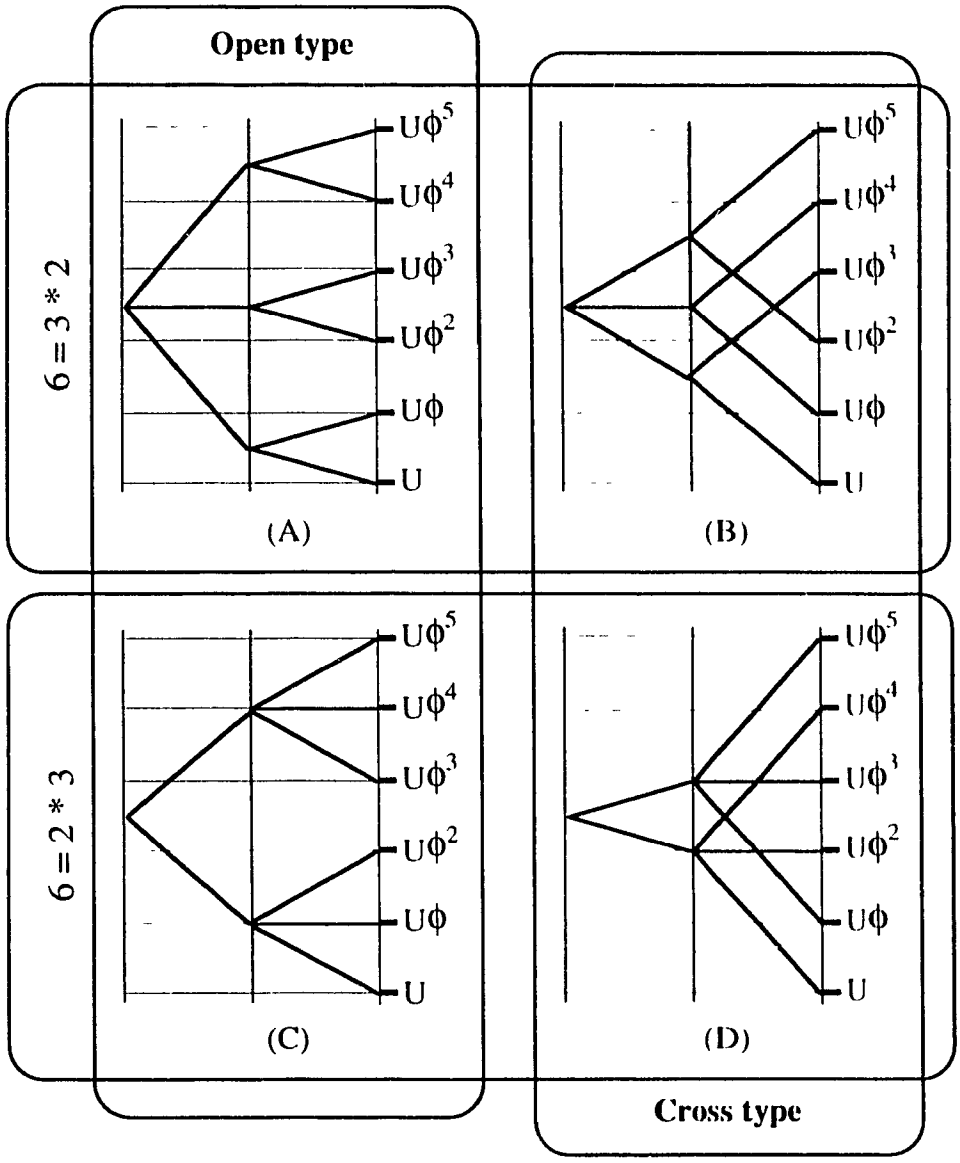

Figure 2.2 Layout diagrams of a 6 speed gear train

For a specific transmission formula of gear train with given N, B and ϕ, a known number of different layout diagrams can be achieved. For example, Figure 2.2 (A) and (B) show two different types of layout diagrams that are possible for a kinematic arrangement of gear train with transmission formula 6 = 3 * 2, where U represents the ratio of the smallest spindle speed to drive unit speed. These layout diagrams are conventionally classified as open type or cross type. When the mesh lines do not cross each other, the distribution pattern is called open type. If the they cross each other, the pattern is called cross type. In some arrangements, a combination of these two types can also be observed. Similarly, Figure 2.2 (C) and (D) illustrate an open and cross layout diagram of the other possible kinematic arrangement of a 6 speed gear train with transmission formula 6 = 2 * 3.

The design parameters, such as the number of teeth, pitch diameters and gear ratios, are determined from the speed requirements that are given in the layout diagram. Literature survey reveals that attempts have been made to incorporate the layout diagrams into the kinematic design analysis of gear trains. White [57] presents a mathematical model which relates the pitch diameters of a 9 speed gear train with step ratio ϕ. The method was then further expanded by Sanger [58], Osman et al [34], Bush et al [9] and Osman et al [33]. So far most of the design analyses are carried out for pre-selected layout diagrams. However, a complete study on the design of gear trains always requires a design procedure combined with different layout diagrams. Dande and Gupta [15] reported an automated design synthesis which covers various aspects of different layout diagrams. Unfortunately the procedure is not fully automated and the drawback is that all information about the layout diagram is to be inputted in a data form.

After performing kinematic design analysis for a specific layout diagram, a complete information about the kinematic characteristics is posted to form another graphical representation, known as the speed diagram. The speed diagram clearly indicates actual speeds of all shafts along with the actual gear ratios of all gears. It is to be noted that, for a given layout diagram and a specified set of required spindle speeds from a drive unit, a

number of speed diagrams can be achieved. Thus, the resulting range of possibilities should be considered for optimal design synthesis of a gear train, because the optimal design can be achieved from any one of the speed diagrams.

To effectively study different kinematic arrangements for multi-speed gear trains, therefore it is desirable to be able to generate an automated design procedure for all possible speed diagrams based on specified speed requirements. Such a computer aided procedure is presented in this chapter. The input data required for the procedure are (1) number of the spindle speeds, (2) number of shafts required, (3) drive unit speed, (4) all spindle speeds and (5) largest speed ratio value in each transmission stage. The procedure computes all intermediate shaft speeds for the given input data, and as a result, all possible speed diagrams are identified.

2.4 Maximum number of possible kinematic arrangements

Conventionally, the transmission formula of a gear train with N spindle speeds is written as,

$$N = \prod_{i=1}^{L} Z(i) \qquad (2.11)$$

where i indicates the transmission stage order, Z(i) is the number of gear sets in the i^{th} transmission stage and L is the number of transmission stages.

For a specified number of spindle speeds N, the value of L is obtained from the factorization of N. This factorized value should satisfy the requirement about the minimum number of transmission stages for the given N. From this, the number of shafts NS is given as,

$$NS = L + 1 \qquad (2.12)$$

Practical considerations reveal that the number of shafts specified by the designer may exceed this value. Specifying the number of shafts required (by the designer) by NSR, it can be observed that if NSR is greater than NS, then transmission stages with

single gear sets are added (Z(L+1) = 1) till NS = NSR. If NS is greater than NSR, the specified design is not possible to achieve.

For a prescribed set of N and NS, relocation of transmission stages leads to different kinematic arrangements. Having chosen a kinematic arrangement with L transmission stages, L! number of forms of equation (2.11) can be obtained, where L! is the factorial of L. Among these set of arrangements wherein more than one transmission stages that have same number of gear sets can be observed, thus resulting in identical transmission formulas. Thus, the maximum number of possible kinematic arrangements is equal to the number of non identical combinations of transmission formulas. This then gives,

$$\text{Number of maximum possible kinematic arrangements} = \frac{L!}{G1! * G2! * G3!} \qquad (2.13)$$

where G3 and G2 are respectively the total number of 3 and 2 gear sets and G1 is the total number of single gear sets.

To illustrate the above described procedure, the following steps are given. For brevity and clarity, a 6 speed 4 shaft gear train is considered for the illustration.

Step 1. Specify the required number of spindle speeds and the number of shafts required: N = 6; NSR = 4

Step 2. Establish a transmission formula: N= Z(1) * Z(2); 6 = 3 * 2

Step 3. Find the number of transmission stages L: L = 2

Step 4. Find the number of shafts NS: NS = L + 1 = 3

Step 5. Check if the number of shafts NS established in step 4 is equal to number of shafts required NSR. If yes go to step 7; else continue.

Step 6. Add additional transmission stages with single gear set (Z(i) = 1), i = NS +1 to NSR: Z(3) = 1; L = 3

Step 7. Rewrite transmission formula: N= Z(1) * Z(2) * Z(3); 6 = 3 * 2 * 1

Step 8. Find all possible combinations of the transmission formula obtained in the step 7:

$6 = 3 * 2 * 1$	$6 = 2 * 3 * 1$
$6 = 3 * 1 * 2$	$6 = 2 * 1 * 3$
$6 = 1 * 3 * 2$	$6 = 1 * 2 * 3$

Step 9. Eliminate the identical combinations of the transmission formula.: *nil*

Step 10. Store all non-repeating transmission formulas as all possible kinematic arrangements.

2.5 Maximum number of possible layout diagrams

The number of input speeds for i^{th} transmission stage $N_I(i)$ is calculated by dividing the number of output speeds, $N_O(i)$, by the number of gears of i^{th} transmission stage $Z(i)$. The number of input speeds for the i^{th} transmission stage is thus equal to the number of output speeds of the $(i-1)^{th}$ transmission stage.

i.e. $$N_I(i) = \frac{N_O(i)}{Z(i)} \tag{2.14}$$

$$N_O(i-1) = N_I(i) \tag{2.15}$$

Denoting by $V_I(i,j)$ and $V_O(i,k)$, respectively, the input and output speeds of i^{th} transmission stage where j runs from 1 to $N_I(i)$ and k runs from 1 to $N_O(i)$; the speed ratios between any $V_O(i,k)$ and $V_I(i,j)$ are denoted as $S(i,l)$, with a range from 1 to $Z(i)$:

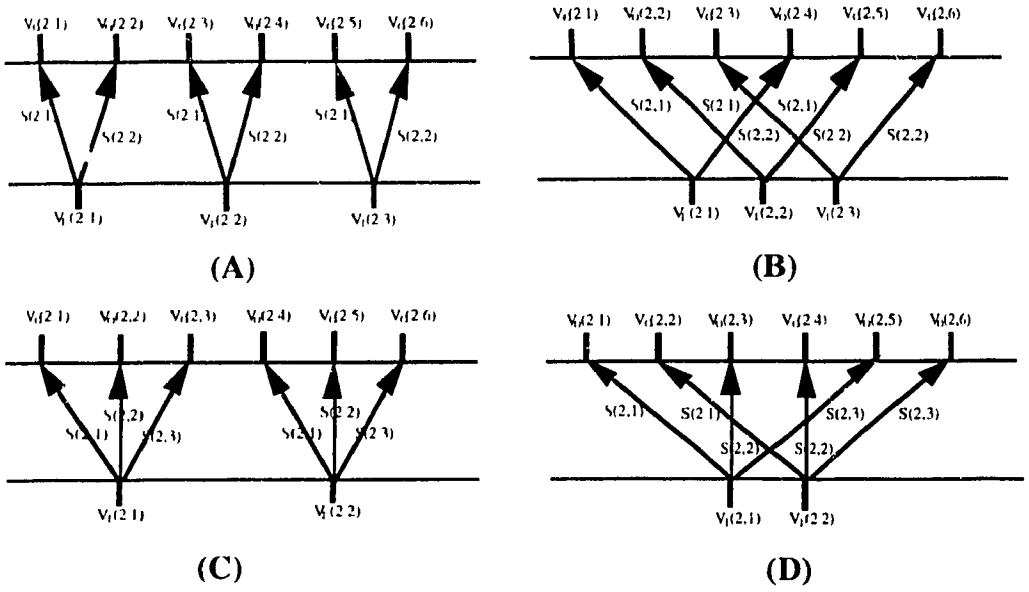

Figure 2.3 Speed distribution through 2 and 3 speed change gear set

Considering the layout diagrams of 6 = 3 * 2 and 6 = 2 * 3 gear trains, Figure 2.3 shows how a set of $V_O(i,k)$ and $V_I(i,j)$ are linked in the layout diagram by mesh lines. Figure 2.3 (A) and (B) show the speed distribution in the 2nd transmission stage of a 6 = 3 * 2 gear train. The 2nd transmission stage contains 2 gear sets that yield 6 different output speeds ($V_O(2,k)$, k =1,2,..,6) from 3 different input speeds ($V_I(2,j)$, j =1,2,3) using the speed ratios S(2,1) and S(2,2). Here the S(2,1) and S(2,2) are in decreasing order of magnitude. Largest output speed $V_O(2,1)$ is created by the largest input speed, $V_I(2,1)$, using speed ratio S(2,1). The same input speed, $V_I(2,1)$, creates one more output speed out of five output speeds $V_O(2,k)$, k = 2,3,..,6) using the speed ratio S(2,2). Figures 2.3 (C) and (D) show the speed distribution in the 2nd transmission stage of a 6 = 2 * 3 gear train. The 2nd transmission stage has 3 gear sets, the speed ratios of which are denoted by S(2,1), S(2,2) and S(2,3) in decreasing order of magnitude. All the 6 different output speeds ($V_O(2,k)$ k=1,2,..,6) are created from 2 different input speeds ($V_I(2,j)$, j =1,2). Thus, the largest output speed $V_O(2,1)$ is created from the largest input speed, $V_I(2,1)$, using the speed ratio S(2,1). The same input speed is expected to create

two more output speeds which are selected from the set of output speeds, $V_O(2,k)$, k= 2,3,..,6 using the speed ratios S(2,2) and S(2,3).

It can now be seen that all output speed positions relative to their input speeds are distributed symmetrically portraying a well defined graphical pattern with equal positional distance. Obviously, a certain rule is followed in the speed distribution of output speeds. If all input/output speeds are indexed, an algebraic constant E(i) can be introduced to relate the output speed positions with an input speed. Assuming that the k^{th} output speed is identified, the next output speed position k for the same input speed is given by k = k+E(i). The constant E(i) is of equal value for all output speeds of i^{th} transmission stage.

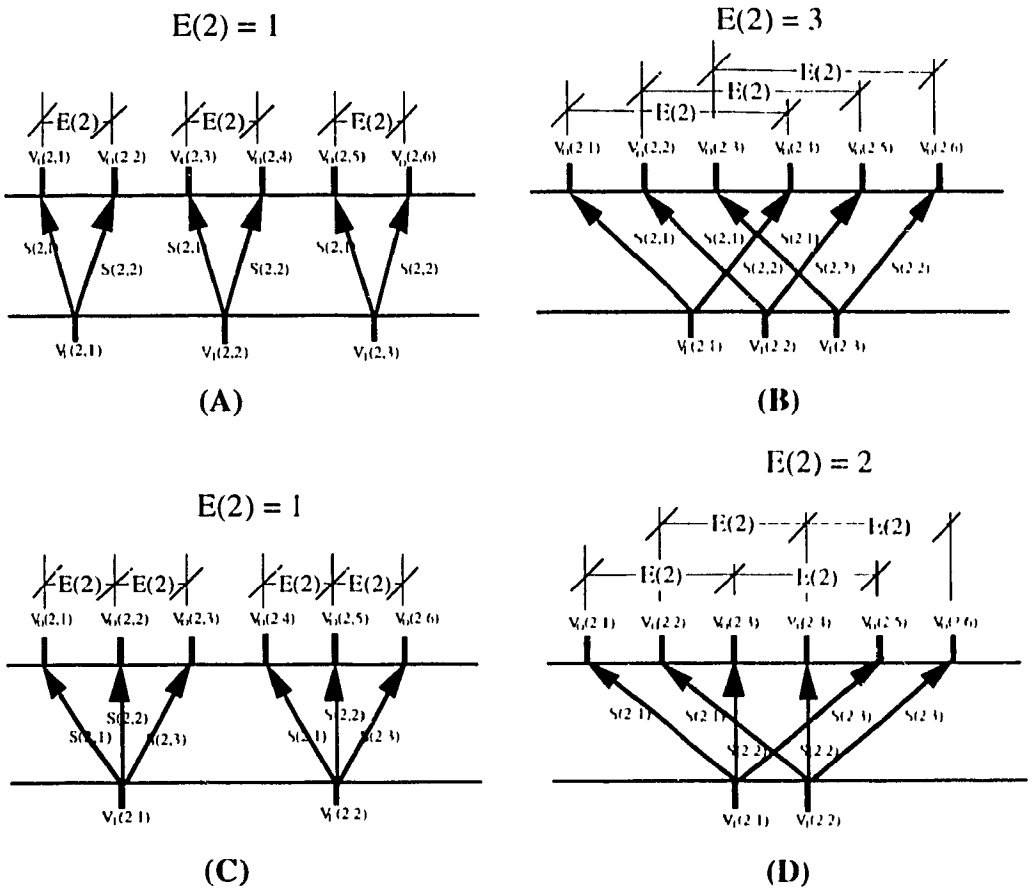

Figure 2.4 Speed distribution through 2 and 3 speed change gear set with E(i)

In Figure 2.4 (A) output speed positions (1,2); (3,4) and (5,6) are joined with input speed positions 1, 2 and 3 respectively, resulting in the value of constant E(2) to be equal to 1. In Figure 2.4 (B) output speed positions (1,4) (2,5) and (3,6) are joined with input speed positions 1 and 2 respectively, resulting the value for the constant E(2) =3. In Figure 2.4 (C) output speed positions (1, 2, 3) and (4, 5, 6) are joined with input speed positions 1 and 2 respectively resulting in the value 1 for the constant E(2). In Figure 2.3 (D) output speed positions (1, 3, 5) and (2, 4, 6) are joined with input speed positions 1,2 and 3 respectively resulting in the value 2 for the constant E(2).

This reveals that the E(i), which is responsible for different layout diagrams, may be viewed as constant indicator for i^{th} transmission stage of a given kinematic arrangement. A systematic approach of calculating the values for E(i) using transmission formula is explained below. Consider a 6 speed, 3 shaft gear train, possible layout diagrams of which is shown in Figure 2.2. The possible two transmission formulas are given as,

$$6 = 3 * 2$$

$$6 = 2 * 3$$

Case (A) *Select 6 = 3 * 2 arrangement:*

For 2^{nd} transmission stage:

number of output speeds $N_O(2) = 6$

number of input speeds $N_I(2) = \frac{N_O(2)}{Z(2)} = \frac{6}{2} = 3 = N_O(1)$

possible E(i) values:

$\frac{N_O(2)}{Z(2)}$	$\frac{N_O(2)}{Z(2) * Z(1)}$
$\frac{6}{2}$	$\frac{6}{2 * 3}$
3	1

For 1st transmission stage:

number of output speeds $N_O(1) = 3$

number of input speeds $N_I(1) = \frac{N_O(1)}{Z(1)} = \frac{3}{3} = 1$

possible E(i) value:

$\frac{N_O(1)}{Z(1)}$
$\frac{3}{3}$
1

Case (B) *Select 6 = 2 * 3 arrangement:*

For 2nd transmission stage:

number of output speeds $N_O(2) = 6$

number of input speeds $N_I(2) = \frac{N_O(2)}{Z(2)} = \frac{6}{3} = 2 = N_O(1)$

possible E(i) values:

$\frac{N_O(2)}{Z(2)}$	$\frac{N_O(2)}{Z(2) * Z(1)}$
$\frac{6}{3}$	$\frac{6}{3 * 2}$
2	1

For 1st transmission stage:

number of output speeds $N_O(1) = 2$

number of input speeds $N_I(1) = \frac{N_O(1)}{Z(1)} = \frac{2}{2} = 1$

possible E(i) value is given as,

$$\frac{No(1)}{Z(1)}$$

$$\frac{2}{2}$$

1

Transmission Formula	1st transmission stage	2nd transmission stage
6 = 3 * 2	1	3 1
6 = 2 * 3	1	2 1

Table 2.3 Possible E(i) values for a 6 speed gear train

The possible values of E(i) for both kinematic arrangements are given in Table 2.3. Using the combination of the E(i), all possible layout diagrams can now be constructed. Similarly, using the above mentioned method, E(i) values for a 18 speed 4 shaft gear train are calculated and tabulated in Appendix A, followed by a Table for a 18 speed 5 shaft gear train.

2.6 All possible speed diagrams

For each layout diagram, a corresponding speed diagram can be achieved, incorporating specified set of drive unit speed, spindle speeds and given speed ratios. A method for finding the speed diagrams of a 6 = 3 * 2 cross type is presented here having known the layout diagram, drive unit speed $V_I(1,1)$, all spindle speeds $V_O(2,1)$ to $V_O(2,6)$ and largest speed ratios S(1,1), S(2,1).

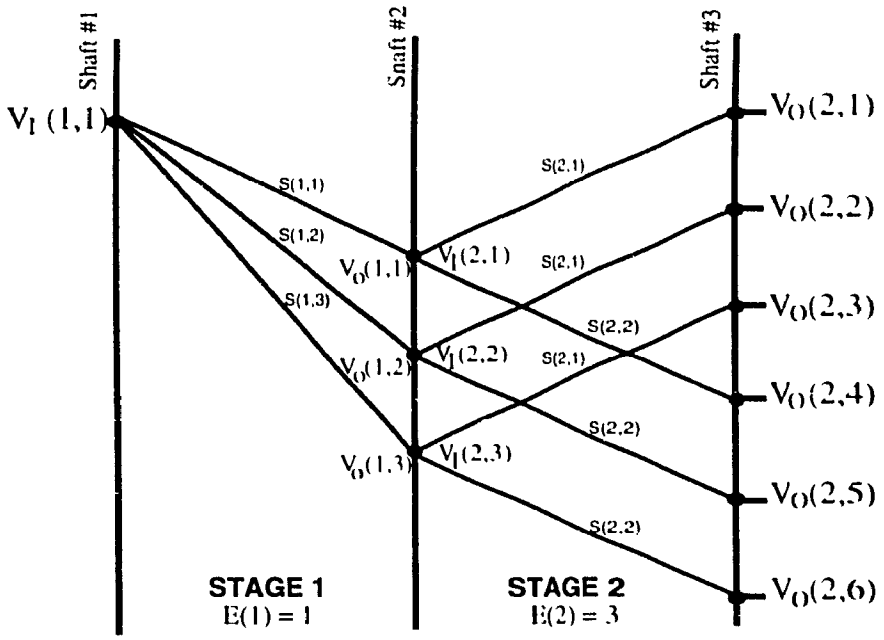

Figure 2.5 Speed diagram of a 6 speed 3 * 2 cross type

It can be seen from Figure 2.5 that $V_O(2,1)$ is the largest output speed and it is created from drive unit speed $V_I(1,1)$ using both speed ratios S(1,1)and S(2,1)

$$V_O(2,1) = V_I(1,1) * S(1,1) * S(2,1) \qquad (2.16)$$

The largest input speed on shaft # 2 is calculated using the following formula:

$$V_I(2,1) = \frac{V_O(2,1)}{S(2,1)} \qquad (2.17)$$

The other output speeds, created from the same input speed $V_I(2,1)$ are selected using E(i) value. Since E(i) value for second stage is given as 3, the input speed $V_I(2,1)$ produces the 4th speed $V_O(2,4)$ on output shaft #3. The speed ratio S(2,2) to obtain the speed $V_O(2,4)$ from $V_I(2,1)$ is then given by,

$$S(2,2) = \frac{V_O(2,4)}{V_I(2,1)} \qquad (2.18)$$

Once the output speeds $V_O(2,1)$ and $V_O(2,4)$ are identified with an input speed $V_I(2,1)$, the next unidentified highest speed $V_O(2,2)$ is expected to be produced from the next highest input speed of shaft 2, which is $V_I(2,2)$. Knowing the layout diagram, it is deduced that the gear set with speed ratio S(2,1) produces $V_O(2,2)$ from the input shaft speed $V_I(2,2)$ and it is given by,

$$V_I(2,2) = \frac{V_O(2,2)}{S(2,1)} \tag{2.19}$$

The next output speed on shaft 3 for the above input speed $V_I(2,2)$ is $V_O(2,5)$. The speed ratio $V_O(2,5) / V_I(2,2)$ will be equal to S(2,2). In the same way $V_I(2,3)$ can be calculated as:

$$V_I(2,3) = \frac{V_O(2,3)}{S(2,1)} \tag{2.20}$$

Further $V_O(2,6)/V_I(2,3)$ will be equal to S(2,2). All these calculated input speeds for 2nd transmission stage $V_I(2,k)$, k=1,2,3 are equal to the output speeds for the 1st transmission stage $V_O(1,j)$, j=1,2,3 respectively and further are produced from the drive unit speed $V_I(1,1)$, using the speed ratios S(1,1), S(1,2) and S(1,3).

$V_I(1,1)$ is calculated or verified using following equation,

$$V_I(1,1) = \frac{V_O(1,1)}{S(1,1)} \tag{2.21}$$

The S(1,2), S(1,3) are calculated as,

$$S(1,2) = \frac{V_O(1,2)}{V_I(1,1)} \tag{2.22}$$

$$S(1,3) = \frac{V_O(1,3)}{V_I(1,1)} \tag{2.23}$$

This approach is easy to apply for different kinematic arrangements of multi-speed gear drives. Based on this approach, an automated computer aided procedure along is developed to establish all possible speed diagrams and is presented next.

2.7 Recommended generalized procedure for finding all possible speed diagrams

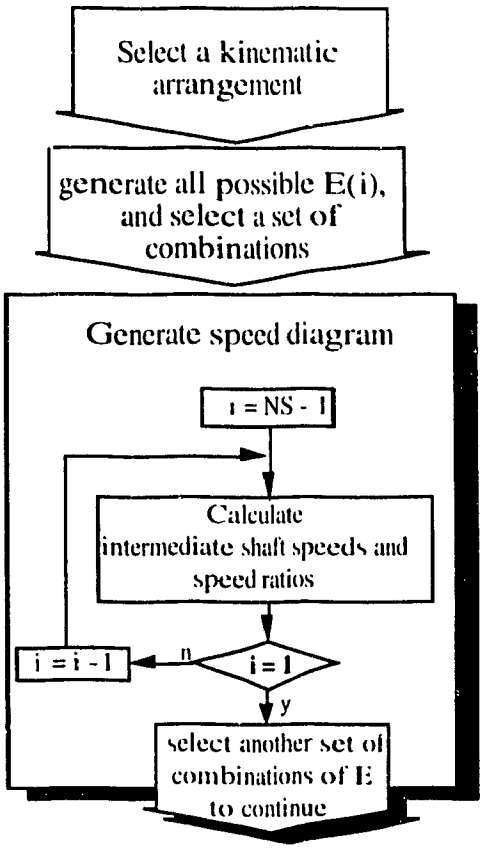

Figure 2.6 Procedure for speed diagrams for a selected E(i)

The generalized procedure finding all possible speed diagrams involves a method of calculating all intermediate shaft speeds and speed ratios for different layout diagrams. Figure 2.6 shows a flowchart for generating speed diagrams through each

transmission stage. The step by step instructions for calculating speeds and speed ratios of i^{th} transmission stage is described below:

For i^{th} transmission stage,

Number of gear pairs = Z(i)

Number of output speeds = $N_O(i)$

Output speeds of $(i+1)^{th}$ shaft = $V_O(i,j)$, j = 1, 2,..., $N_O(i)$

(Output speeds are set in descending order)

Number of input shaft speeds $N_I(i) = \frac{N_O(i)}{Z(i)}$

Input speeds on i^{th} shaft = $V_I(i,k)$, k = 1, 2,..., $N_I(i)$

The maximum speed ratio is specified with S(i,1)

Step 1. Select the maximum output speed $V_O(i,j)$ on $(i+1)^{th}$ shaft .

Step 2. Divide the maximum output speed by maximum speed ratio of i^{th} stage S(i,1) and find maximum input speed $V_I(i,k)$ of i^{th} shaft.

Step 3. Identify the (Z(i) - 1) output shaft speeds produced from maximum input speed $V_I(i,k)$ using E(i) value.

Step 4. calculate speed ratios for i^{th} stage.

$$2^{nd} \text{ larger speed ratio} = \frac{V_O(\, i,\, j+E(i)\,)}{V_I(\, i,k\,)}$$

$$3^{rd} \text{ larger speed ratio} = \frac{V_O(\, i,\, j+2*E(i)\,)}{V_I(\, i,k\,)} \quad (\text{ This applies only if } Z(i) = 3)$$

Step 5. select maximum output speed $V_O(i,j)$ skipping all output speeds considered in step 1 and step 3.

Step 6. Divide output speed obtained in step 5 by S(i,1) and find the next maximum input speed

$V_I(i,k)$ of i^{th} shaft.

Step 7. Identify the (Z(i) -1) output shaft speeds produced from the next maximum input speed $V_I(i,k)$ using E(i).

Step 8. Verify speed ratios S(i,2) and S(i,3)

$$2^{nd} \text{ larger speed ratio } S(i,2) = \frac{V_O(i, j+E(i))}{V_I(i,k)}$$

$$3^{rd} \text{ larger speed ratio } S(i,2) = \frac{V_O(i, j+2*E(i))}{V_I(i,k)} \quad (\text{This applies only if } Z(i) = 3)$$

Step 9. Select maximum output speed $V_O(i,j)$, skipping all output speeds considered in step 1, step 3 and step 5.

Step 10. Repeat steps 6, 7 and 8 until all output speeds from ($V_O(i,j)$ are selected.

2.8 SPDIAG (speed diagram) program description

Using the above procedure, an automated computer aided interactive graphical program (SPDIAG) is developed to determine and plot all possible speed diagrams. Input parameters for this procedure are:

1. Number of output shaft speeds: N.
2. Number of shafts required: NSR.
3. Values of output shaft speeds: $V_O(NSR-1, n)$, n = 1, 2,..., N.
4. Largest speed ratios for all transmission stages: S(i,1), i = 1, 2,..., NSR -1.

From the input data N and NSR, the program first establishes a transmission formula . Using that transmission formula, the maximum possible kinematic arrangements are identified. Then for each kinematic arrangement, all possible E(i) values are computed. Using these E(i) values, all possible speed diagrams are generated known the values of

spindle speeds V_O(NSR-1,n), where n = 1 to N and largest speed ratios S(i,1) for all transmission stages. The flowchart of SPDIAG is shown in Figure 2.7.

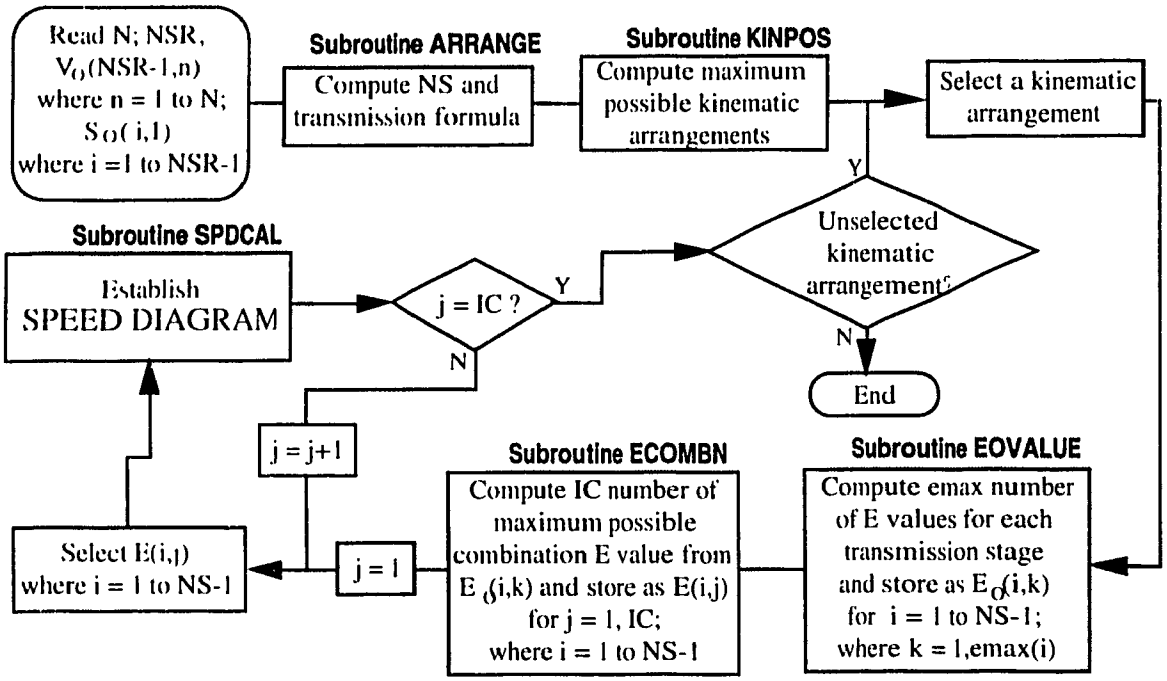

Figure 2.7 Flowchart of the program SPDIAG

The main program SPDIAG calls 5 subroutines to complete the task. Brief description of the main program and the subroutines are given below:

Main program SPDIAG

1. *Read number of spindle speeds N;*

   (ii) Number of shafts required NSR;

   (iii) Spindle shaft speeds V_O(NSR-1,n), n =1,N and

   (iv) Largest speed ratios S_O(i,1) for all transmission stages (for i = 1, NSR-1).

2. Call subroutine **ARRANGE**

3. Call subroutine **KINPOS**

4. For each kinematic arrangements

   4.1 call subroutine **EOVALUE**

4.2 call subroutine **ECOMBN**

4.3 for each combinations of E(i,j) (that is, j runs from 1 to IC);

4.31 set E(i,j) for i = 1, NS-1

4.32 call subroutine **SPDCAL**

5. End

Subroutine ARRANGE

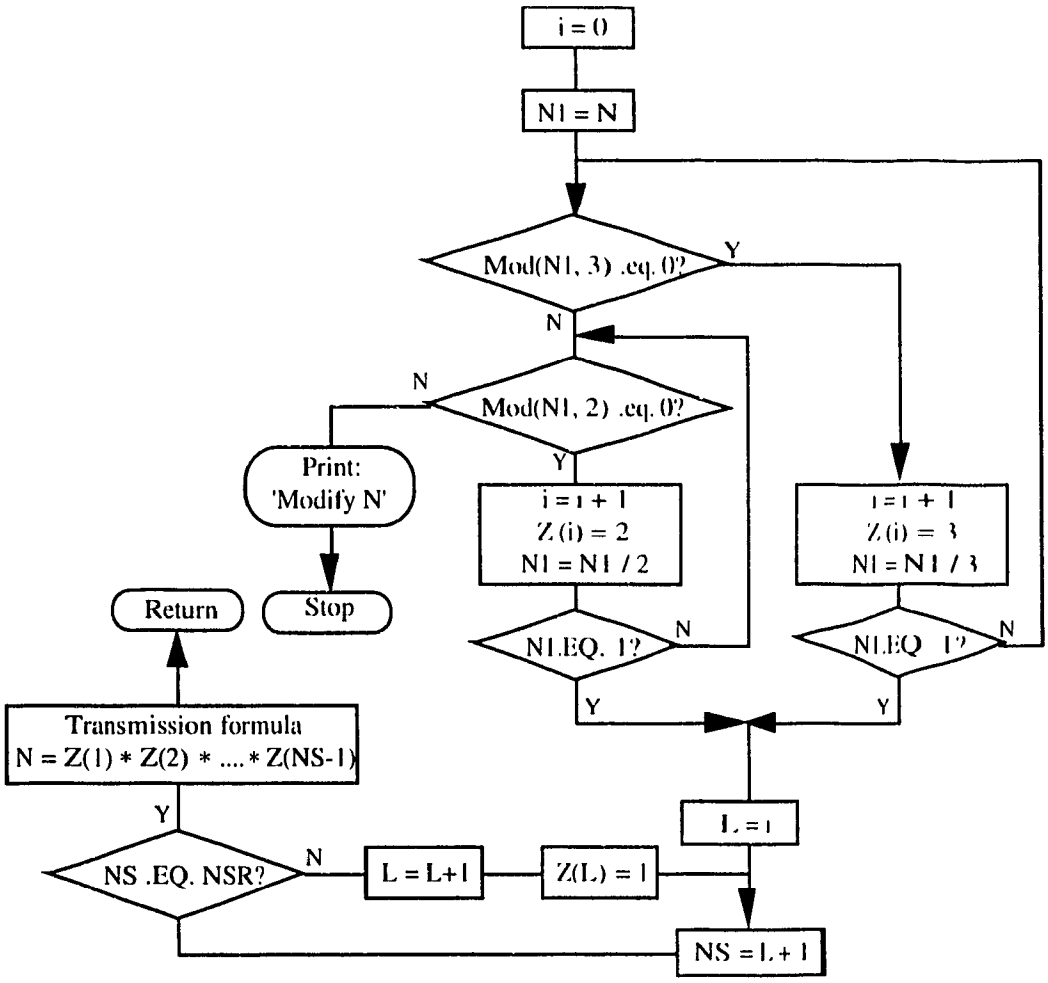

Figure 2.8 Computational scheme of subroutine ARRANGE

The subroutine ARRANGE performs the following steps:

1. Establishes a transmission formula for the given value of N
2. Calculates the number of shafts NS

   If calculated number of shafts value is equal to number of shafts required, then assigns NS = NSR, else adds additional transmission stages with single gear sets till the condition NS = NSR, is satisfied.
3. Rewrites transmission formula for NS
4. Returns

Flowchart of the subroutine ARRANGE is given in Figure 2.8. The algorithm signals an error message "Modify N" followed by the termination of the program, if an unrealistic N is inputed.

Subroutine KINPOS

The subroutine KINPOS performs the following steps:

1. Establishes all possible transmission formulas
2. Identifies and eliminates repeated transmission formulas
3. Rewrites non repeating transmission formulas as possible kinematic arrangements
4. Returns

Subroutine EOVALUE

The subroutine EOVALUE performs the following steps:

1. Creates a two dimensional array
2. computes $E_O(i,k)$ for each transmission stage which is converted into E(i,j) values later.
3. Eliminates repeated $E_O(i,k)$ of i^{th} stage and determines emax(i) that is the number of non repeated $E_O(i,k)$ of i^{th} stage.
4. Returns

Flowchart of the subroutine EOVALUE is given in Figure 2.9.

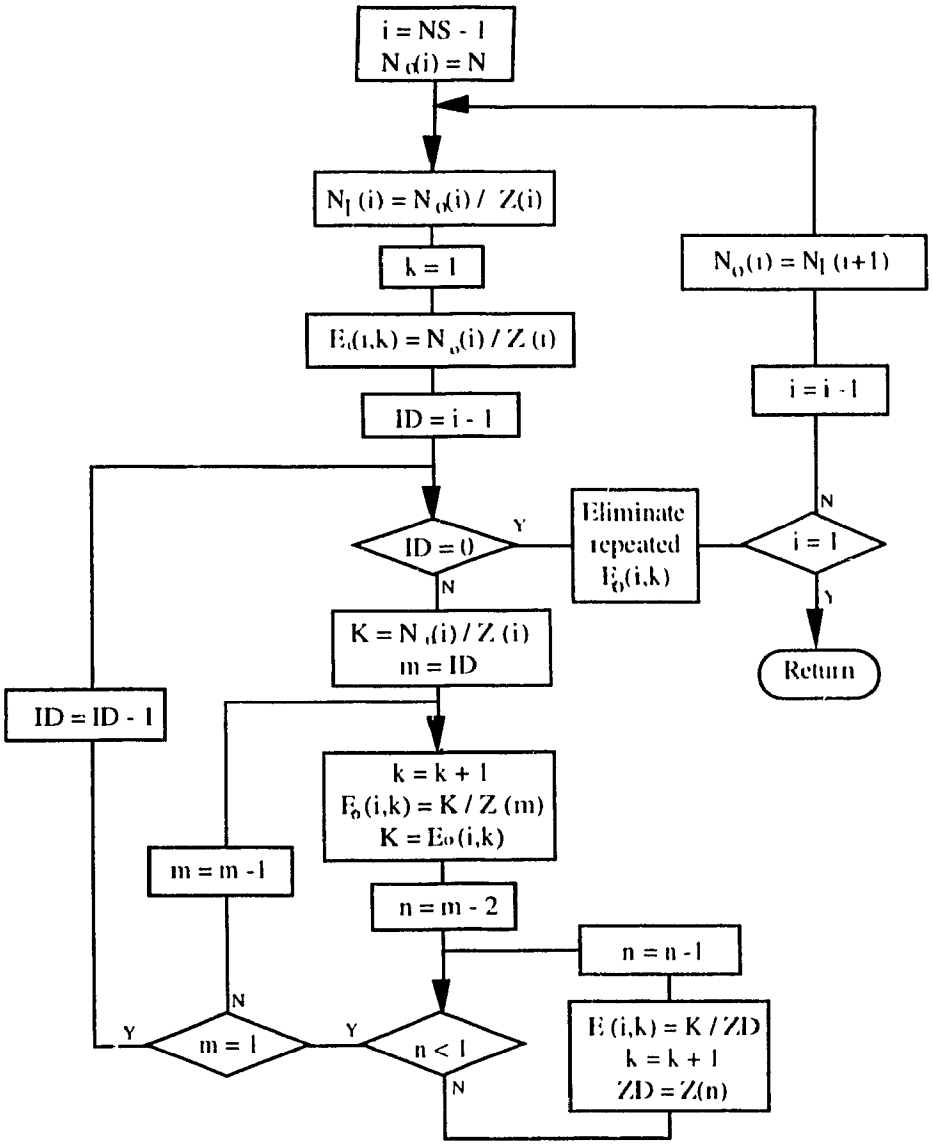

Figure 2.9 Computational scheme of subroutine EOVALUE

Subroutine ECOMBN

The subroutine ECOMBN performs the following steps:

1. Computes all possible combinations of $E_O(i,k)$ for i = 1to NS-1; where k = 1 to emax(i)
2. Computes the total number of different combinations IC
3. Stores the resulting values as E(i,j) for j = 1 to IC; where i = 1 to NS - 1
4. Returns

Subroutine SPDCAL

The subroutine SPDCAL performs the following steps:

1. Using the given output shaft speeds $V_O(NS-1,n)$ where n =!,N and largest speed ratios RTO1(i) for all transmission stages;
   1.1 Computes all speeds of each shafts
   1.2 Computes all speed ratios other than given.
   1.3 Compares the input speed computed on the shaft 1 with the given input source speed
2. Returns

2.9 Demonstration results

To demonstrate the full potential of the developed method, all possible speed diagrams for a 18 speed 4 shaft gear train are generated. The input parameters for the task is tabulated in Table 2.4. The results are plotted using the above mentioned computer aided program SPDIAG and shown in Figure 2.10(A), 2.10(B) and 2.10(C).

Number of spindle shaft speeds	Values of spindle shaft speeds	Number of shafts required	Largest speed ratios	
			Transmission stage	Numerical value
18	1391.170 1220.588 1070.691 939.2025 823.8618 722.6857 633.9349 556.0833 487.7923 427.8880 375.3403 329.2459 288.8122 253.3440 222.2316 194.9400 171.0000 150.0000	4	1	0.729780
			2	1.312500
			3	1.037037

Table 2.4 Input data for SPDIAG

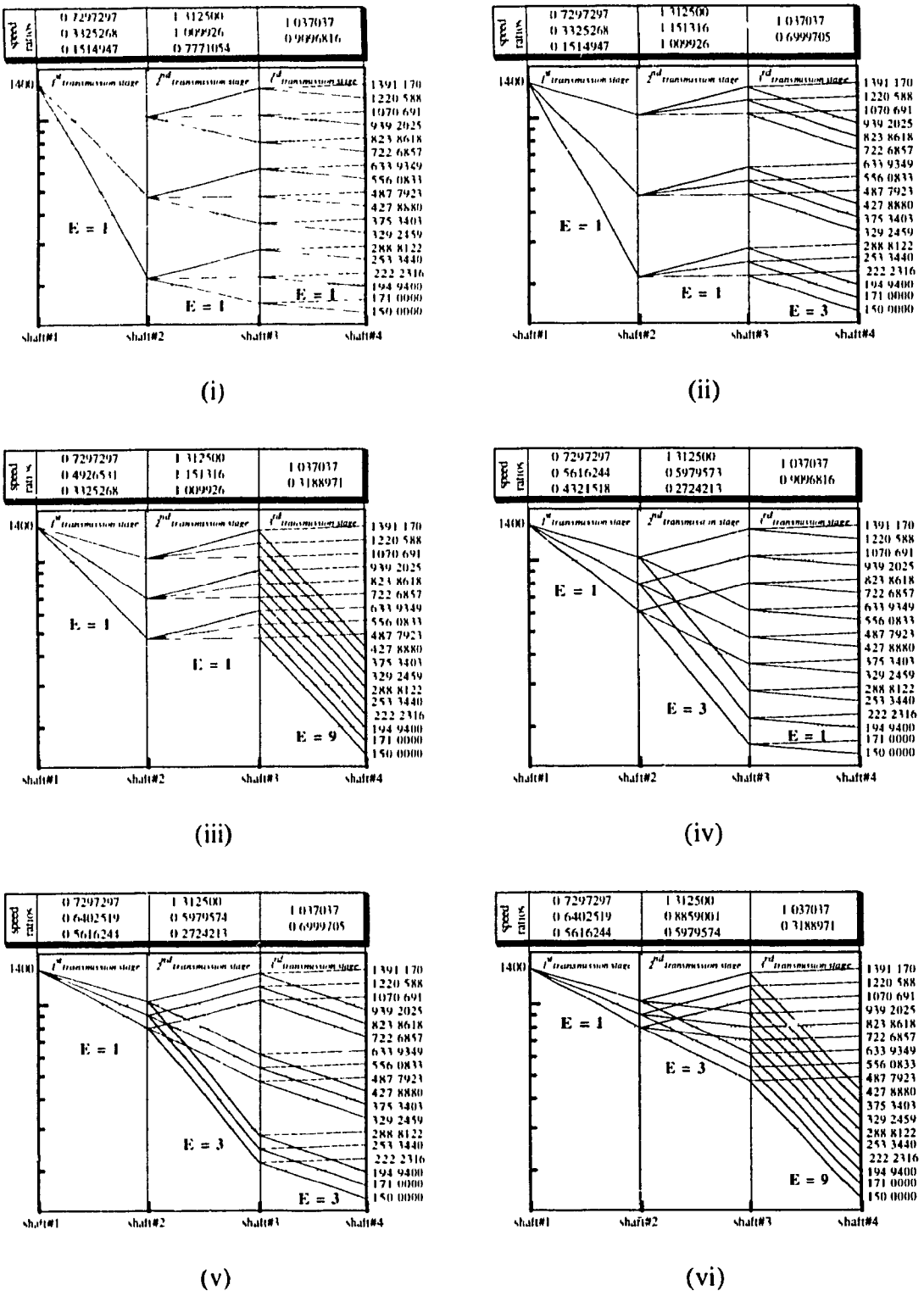

Figure 2.10 (A) Speed diagrams of 18 = 3 * 3 * 2 gear train

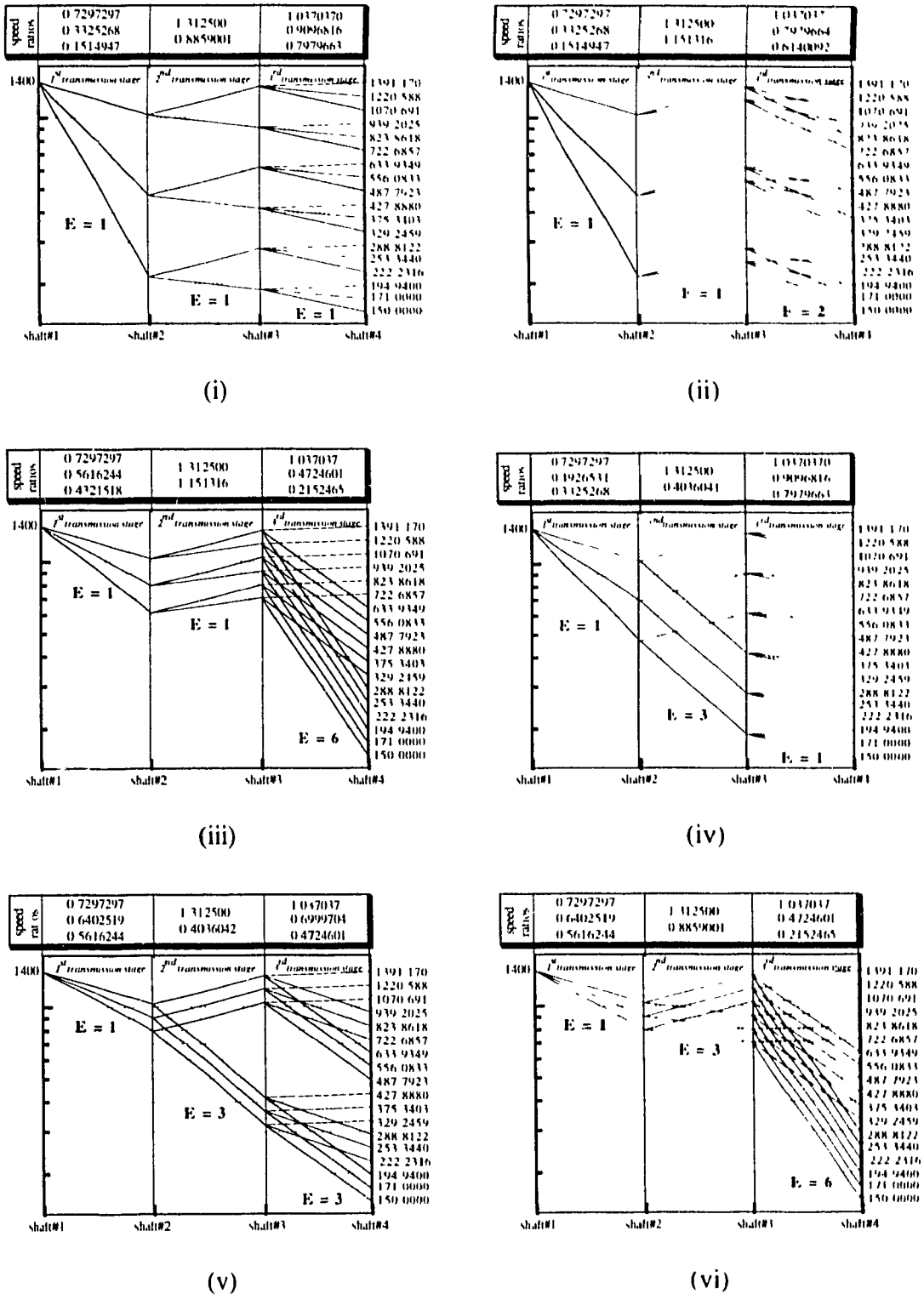

Figure 2.10 (B) Speed diagrams of 18 = 3 * 2 * 3 gear train

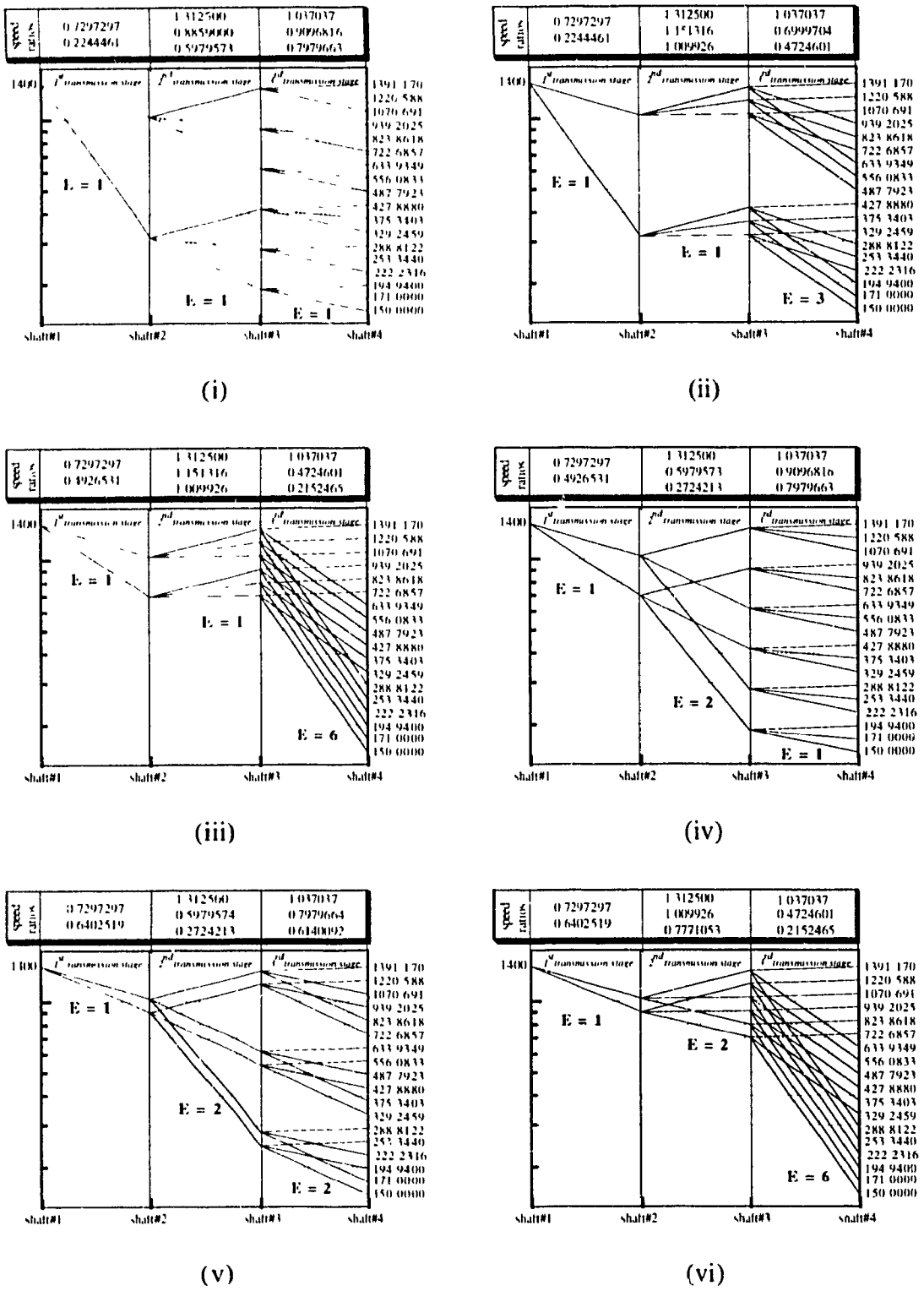

Figure 2.10 (C) Speed diagrams of 18 = 2 * 3 * 3 gear train

2.10 Conclusion

A computer aided method for determining all possible speed diagrams is developed and presented in this chapter. The method presented herein has several advantages. It easily deals with any number of output speeds and any number of shafts required and it accommodates all types of layout diagrams. If discontinuities are observed in any of the layout diagram, the method automatically adjusts to such conditions without requiring any additional input parameters. Changing the input values for the largest speed ratios allows the designer to examine different speed diagrams with same speed specifications. This advantage can be useful for incorporating all possible speed diagrams in a kinematic analysis. In some cases, when speed ratios of transmission stages are interchanged, this method becomes a useful tool to examine speed diagrams.

CHAPTER 3

Kinematic design of multi-speed gear trains

3.1 Introduction

Design of a gear train requires appropriate strategies to achieve increased durability, compactness, precision, low noise and low vibration levels of component gear units. The durability and longevity of gears are determined by the hardness of gear teeth material and the capability to resist stress reversals induced in them. It is possible to manufacture durable gears by using gear fabricating material such as high hardened steel or medium hardened steel. The other factor that governs the durability of gears is the heat treatment. Heat treatment can increase the service life of a gear set up to ten times without increasing its size or weight. Compactness of gears is obtained through selecting hardened gear materials or reducing the dimensions of gears or a combination of both. The dimensions of medium-hardened gears can be considerably reduced sometimes as much as two times, by changing to high hardened gear material. The important design factors that play a major role in reducing gear dimensions are the gear ratios, the number of teeth of pinion, module, pressure angle and the ratio between facewidth and pitch diameter. Gear trains with precision gears are widely used in instrumentation, automatic controls, machine tools, high speed units etc. Precision gears satisfy high design standards and they require refined analysis, design, fabrication and assembling criteria. Further, the noise generated by the gear train is basically related to the transmission error of the component gear units. This transmission error is caused by the deflections of gear teeth due to operational loads, tooth profile, spacing between teeth, and runout errors resulting from the manufacturing process. The vibrations that are manifested during operation are caused by inertia, compliance and damping of the individual components of the vibratory system.

In multi-speed gear trains, each spindle speed is produced by a number of selected gears. The series of selected mating gears is termed as the transmission path of the particular spindle speed. Component gears in each transmission path are designed to satisfy the operational requirements, wherein these requirements are given in terms of transmitted power, input / output speeds and desired speed ratios from the layout diagram. Smaller gears satisfying the prescribed operational requirements are most desirable in use, because they operate smoothly due to smaller inertial loads and pitch line velocities as well as due to their compactness, lesser cost and the easiness in manufacturing. The cost not necessarily follows linear dependence with gear dimensions, especially if the smaller gear size is made durable by heat treatment. However, the trade-off generally favors the minimized gear dimensions. Obviously, smaller gears will use less material for the gear elements and for the surrounding housing. If the same life and reliability is achieved in a smaller package, a more economical design is achieved.

In general, the problem of design synthesis of gear trains involves minimized volume and manufacturing cost but not at the expense of a safer level of strength. This requirement automatically translates the problem of design into a problem of optimization. One advantage of using an optimization procedure is that, it enables the designer to consider a spectrum of possible designs. The procedure starts by listing the design parameters available, the equality constraints to be satisfied, the inequality constraints that define the limit of acceptable designs and the objective function that is used to compare the design task of each possible design on a specified merit basis. The relevant constraints are listed as: (1) Force constraints (bending and wear capacities, vibrational safety constraints, etc.) (2) Tooth geometry constraints (limit on ratio of facewidth to pitch diameter, contact ratio to be more than the minimum defined for the selected gear, no involute interference i.e. - gear tooth cannot be undercut, etc.) (3) Dimensional constraints (outside diameter of the gear cannot be less than the shaft diameter, gear ratios must be within the allowable values, gear ratio product of all gear sets must be equal to the overall speed ratio of the

corresponding transmission path, etc.). Thus, the volume, center distances, gear sizes, gear ratio deviations, etc. are designed to have their respective optimal values. In a parallel shaft gear arrangement this means essentially that volume optimization is to be achieved by the minimization of both the length and width of the gear train individually. The length of the gear train in a parallel shaft gear arrangement is usually defined by shaft lengths needed to meet torsional strength requirements and the width is a sum of center distances between the shafts; it is also affected by the largest gears on the first and last shafts. In order to minimize the width of a gear train, the overall center distance between the shafts and the radius of the largest gears on input and output shafts are to be minimized jointly [34]. However, extrema of center distances between shafts are limited at least at their minimum value, by the codal provisions[54]. That is so because, the center distance between shafts is a sum of the number of teeth on the pinion and wheel whereas these two in turn are subjected to the feasibility of manufacture. The problem of optimization is thus to take into account all these complicating factors. Most of the optimization methods that are currently available for the design of gear trains, are capable of dealing only with a selected kinematic arrangement with specified layout diagram. When the same methods are adapted for other types of kinematic arrangements or layout diagrams, most of them become inevitably inefficient and complicated.

3.2 Formulation of the kinematic design problem

Failures arising due to manufacturing process uncertainty are more crucial in practical high speed gear arrangements and the analysis of which would provide opportunities of reducing the reliability of the entire dynamic system. For instance, misalignment of gear teeth is encountered due to errors or variations in center distance of the mating gears and this causes many stress related failures. These variations can always constitute an ensemble of a stochastic process when identical mass products are considered. In addition, randomness can be observed in speeds, transmitted power, gear ratio,

facewidth, tooth geometry, material properties, etc. It is very practical to address a wide range of factors which causes the uncertainties in the gear system in the design stage itself. Carroll and Johnson [11] present a solution procedure for the optimal design of spur gear set, minimizing the pitch diameter of the pinion in a dimensionless design space, subject to stress and undercut constraints. The optimal design of gear geometry is found depending only on gear ratio and strength properties of gear materials. Although the gear ratio is specified as an input data, the procedure assumes a tolerance to the gear ratio in order to keep the number of teeth as an integer. Due to this assumption, an adjustment is again to be made to the facewidth to achieve a feasible safe design.

The problem of determining gear ratios for the component gear sets of a transmission path is attempted in Reference [5]. The desired overall speed ratio of the transmission path is assumed as a rational fraction of integer numbers within a tolerance. The denominator and the numerator are then factorized into several integer numbers so as to produce the desired number of transmission stages. Combination of these integers in the denominator and the numerator is treated as gear ratios in the transmission path. The value equal to the sum of the squared variation of gear ratio of each transmission stage, is defined to select the best combination. The method is expanded by the authors in Reference [7] to adopt the center distance requirement where a numerical scanning method finds all gear sets with a specified gear ratio and / or center distance within some tolerances. Both of these reports [5, 7] are straight forward design approaches and do not use any optimization procedures.

Deterministic design investigation of a 18 speed 5 shaft gear train with a pre-selected layout diagram is studied by Rao et al [39]. The design synthesis is performed in two steps and both are staged in the form of multi-objective minimization approach. In the first step, the formulation involves two objective functions as the design task. They are the minimization of the sum of speed deviations from specified values in all speeds including the intermediate shaft speeds and the minimization of overall center distance of the gear

train. The number of teeth of gears are treated as design variables and the lower bound on number of teeth for both pinion and wheel is selected as the constraints for the first step. The second step involves the minimization of mass and the maximization of transmitted power simultaneously, satisfying bounding parameters to the facewidths and the allowable limitations on induced bending and wear stresses. Both the facewidth and transmitted power are selected as the design variables for the second step. Furthermore, the above study uses the methodology presented in Reference [15] to compute the integer values for the number of teeth. The results of the above investigation have a number of drawbacks that are listed below: (1) For a practical design of a gear train, the spindle speeds and their variations are more important than the intermediate speeds. Thus, the minimization of speed deviations in intermediate speeds leads to uneconomical designs. (2) Selection of module for the component gear sets is the designers choice, based on application and manufacturing conditions of the intended gear train. This makes one of the given results, that is module versus sum of speed deviations, to be not useful. (3) It is clear from basic equations [54] that the center distance is directly proportional to the module. By carefully examining the solution procedure for designing multi-speed gear trains, it becomes explicit, that one gear set is determined first as a reference, based on which the center distance and the other gears in the current transmission stage are designed. Such reference gear sets in each transmission stage form a reference transmission path that is responsible for the overall center distance of the gear train. If a same module is assigned for all component gear sets, overall center distance obviously has a linear relationship with the selected module. The other result from the optimization of the first step provides such a linear curve, which affects the definition of optimum parameters. (4) Probabilistic nature of the gear train parameters is not addressed in solving the force constraints. (5) As indicated earlier, a pre-selected kinematic arrangement and layout diagram are investigated, which hinders the options of checking all other possible layout diagrams of all possible kinematic arrangements.

Moreover, the above mentioned references clearly show inefficiency in the problem formulation and computational methods of multi-speed gear trains, resulting in a need for a new solution method to avoid the undesirable variations in gear parameters such as gear ratio, center distance and facewidths. It is known that, the gear ratio always remains as a constant, when the number of teeth of pinion and wheel are treated as deterministic prime numbers in the design procedure. Since the center distance has a linear dependence with the module and the sum of the number of teeth of both pinion and wheel, variations in the center distance can cause variations in module. Treating the module and facewidth as random parameters and number of teeth as deterministic variable can thus increase the efficiency of the solution procedure. The selection of number of teeth can only affect the kinematic characteristics of the gear train, and the random parameters can be solved separately in order to satisfy the force constraints.

The primary requirement for the optimization strategy in this chapter, is the selection of the number of teeth for each gear, so that a gear train will provide a gear ratio equal to the corresponding speed ratio. Minimum volume or minimum center distances is obtained from the optimization. The constraints are imposed on mesh conditions for each transmission stage and maintaining limitations on number of gear teeth, acceptable module values, etc. Solving this type of constrained problem is difficult when larger number of output speeds are considered. The problem involves large number of design variables and generally does not permit minimization in simple single objective modules. Thus a multi-objective formulation becomes necessary to solve the problem.

The entire minimization scheme is performed sequentially in two steps. The first step is performed to minimize the overall center distance of a reference transmission path. The number of teeth values of this reference transmission path are selected as integer design variables and are constrained by the desired input to output speeds, codal provisions for gear ratios and the number of teeth. There are 2 * (NS - 1) number of design variables that are selected to form the reference transmission path.

Once the number of teeth value of the reference transmission path is obtained, all other speed ratios can be computed using the method described in Chapter 2. The second minimization procedure determines number of teeth of all gears other than that in reference transmission path. The deviation between ideal and actual gear ratios is selected as the objective function for minimization. The center distance of each gear set is incorporated as an equality constraint by making it to be equal to the center distance of the reference gear set that is obtained in the corresponding transmission stage. For an economical solution, a standard tooth system made by standard tooling is sought. Codal provisions provides a limited number of module, standard pressure angle and standard addenda and dedenda. The codal provisions for the present study is governed by AGMA standards.

3.3 Formulation of the optimal design

The optimization procedure is composed of two steps, namely the minimization of overall center distance and the minimization of gear ratio deviations. The number of teeth is kept as an integer design variable and the design space is limited by the equality and inequality constraints. The relevant objective functions and constraints are now presented in the following sections.

3.3.1 Step 1: Minimization of overall center distance

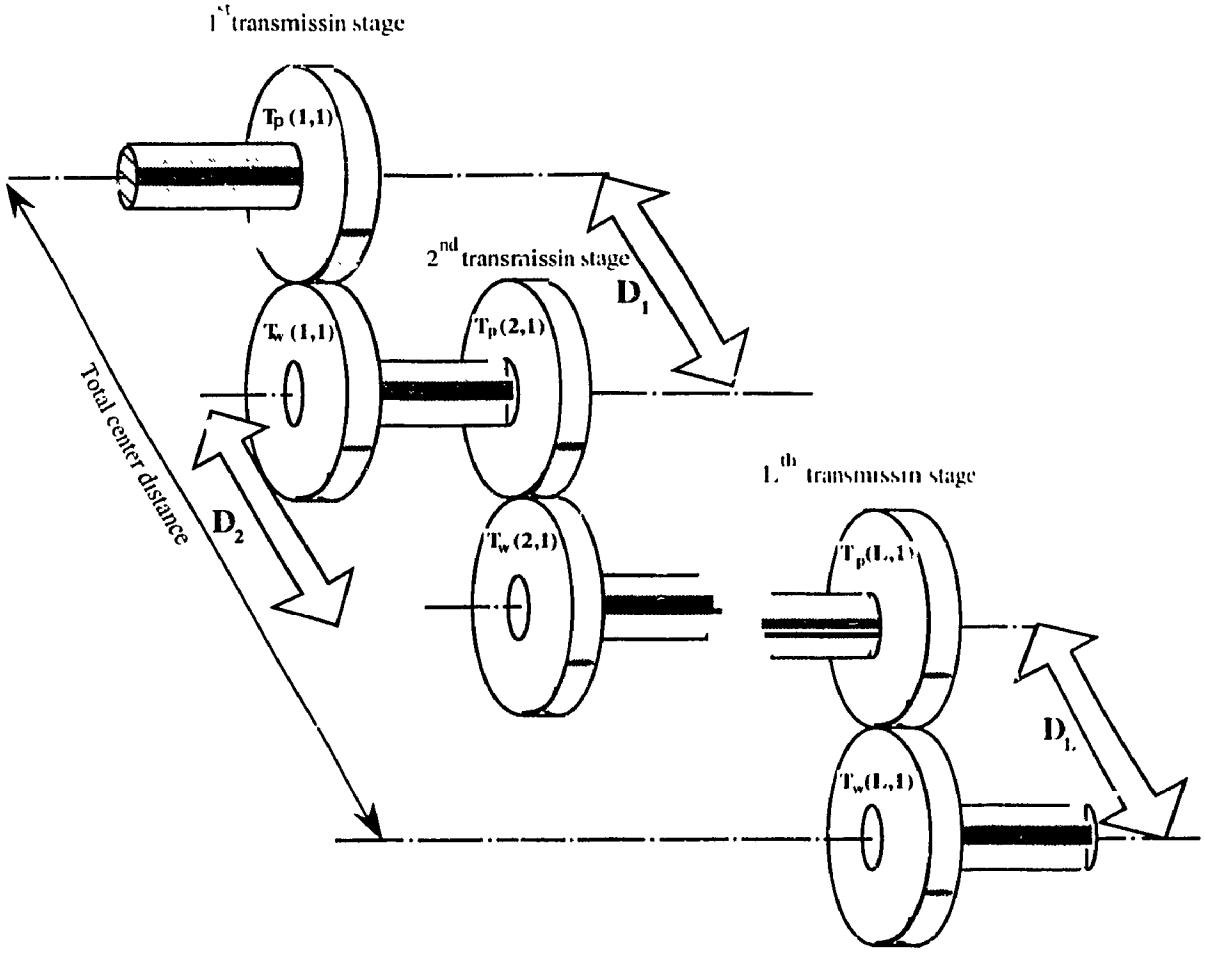

$$\text{Total center distance} = \sum_{i=1}^{L} D_i \;;\; D_i = \frac{m * C_i}{2} \;;\; C_i = T_p(i,1) + T_w(i,1)$$

Figure 3.1 Parallel multi-shaft gear train

With reference to the parallel multi-shaft gear train, a design approach for the optimum value of overall center distance is implemented. Figure 3.1 shows schematically the arrangement of a multi-shaft gear train with (L+1) number of gears mounted on (L+1)

number of shafts. For this gear train, the overall center distance is the sum of the center distances found in all L number of transmission stages. Thus,

$$\text{Overall center distance} = \sum_{i=1}^{L} D_i \tag{3.1}$$

where D_i is the center distance of i^{th} transmission stage.

The objective function

All gear sets in the reference transmission path are assumed to have same module m. Although the module is probabilistic in nature, in the present deterministic formulation the mean of the module is taken as a constant m. The objective function Φ now takes the following form:

$$\textit{Minimize} \qquad \Phi = \sum_{i=1}^{L} \frac{m}{2} * [T_p(i,1) + T_w(i,1)] \tag{3.2}$$

or alternately, after substituting the design variables it takes the form,

$$\textit{Minimize} \qquad \Phi = \sum_{i=1}^{L} \frac{m}{2} * [x(2i-1) + x(2i)]$$

where x(2i-1) and x(2i) respectively represent the design variables assigned for the number of pinion and wheel teeth of i^{th} transmission stage.

The constraints

Two types of constraints arise due to taking into account the speed ratio requirement and gear ratio limitations. The reference transmission path produces the largest spindle speed $V_O(L,1)$ from the drive unit speed $V_I(1,1)$ using L number of speed ratios. If the product of all gear ratios (T_p / T_w) in the reference transmission path is made equal to the quotient $V_O(L,1)$ / $V_I(1,1)$, the corresponding output speed $V_O(L,1)$ will have zero speed deviation. Thus, this condition can be set as an equality constraint. That is,

$$F_1 = \prod_{i=1}^{L} \frac{T_p(i,1)}{T_w(i,1)} - \left| \frac{V_O(L,1)}{V_I(1,1)} \right| = 0 \qquad (3.3)$$

Upon substituting the design variables, this reduces to,

$$F_1(x) = \prod_{i=1}^{L} \frac{x(2i-1)}{x(2i)} - \left| \frac{V_O(L,1)}{V_I(1,1)} \right| = 0 \qquad (3.4)$$

However, gear ratios $T_p(i,1) / T_w(i,1)$ are to be governed by their limiting values $R_{max}(i)$ and $R_{min}(i)$ that are laid by design standards. The standard values for $R_{max}(i)$ and $R_{min}(i)$ are given by Townsend in the reference [54], as any value from 0.5 to 2.0. Knowing that all torsional natural frequencies that arise during the operation of the gear train are to be checked with the rotating speeds in the reference transmission path, the specification of the value for $R_{max}(i)$ is important in the kinematic design stage. The specification of smaller values for $R_{max}(i)$ will yield smaller rotating speeds in the reference transmission path that will improve the operational safety of the gear train. Thus, additional 2*L number of inequality constraints can be formulated to keep the gear ratios within the beneficial limitations.

$$F_k = R_{min}(i) - \frac{T_p(i,1)}{T_w(i,1)} \leq 0 \qquad (3.5)$$

$$F_{k+1} = \frac{T_p(i,1)}{T_w(i,1)} - R_{max}(i) \leq 0 \qquad (3.6)$$

Substituting the design variables these turn into

$$F_k(x) = R_{min}(i) - \frac{x(2i-1)}{x(2i)} \leq 0 \qquad (3.7)$$

$$F_{k+1}(x) = \frac{x(2i-1)}{x(2i)} - R_{max}(i) \leq 0 \qquad (3.8)$$

where i = 1,2,...,L and k = 2i -1

By minimizing the overall center distance, optimal values of $T_p(i,1)$ and $T_w(i,1)$ of the reference transmission path is determined. During the minimization, several individual reference transmission paths may be obtained that have gear ratios falling within the limiting values of $R_{max}(i)$ and $R_{min}(i)$. Hence, all these possibilities must be treated as acceptable designs. Each of these acceptable reference transmission path results in a group of fixed speed ratio $S(i,1)$ and center distance D_i as input parameters for the next step to subsequently design the other gear sets.

In addition, the iteration procedure requires knowledge of upper and lower bounds for the number of teeth on gears. The region of acceptable designs can be established as that the region bounded by (T^p_{min}, T^p_{max}) and (T^w_{min}, T^w_{max}), where the T^p_{max}, T^w_{max} are the upper bounds and the T^p_{min}, T^w_{min} are the lower bounds for pinion and wheel respectively.

3.3.2 Step 2: Minimization of gear ratio deviations

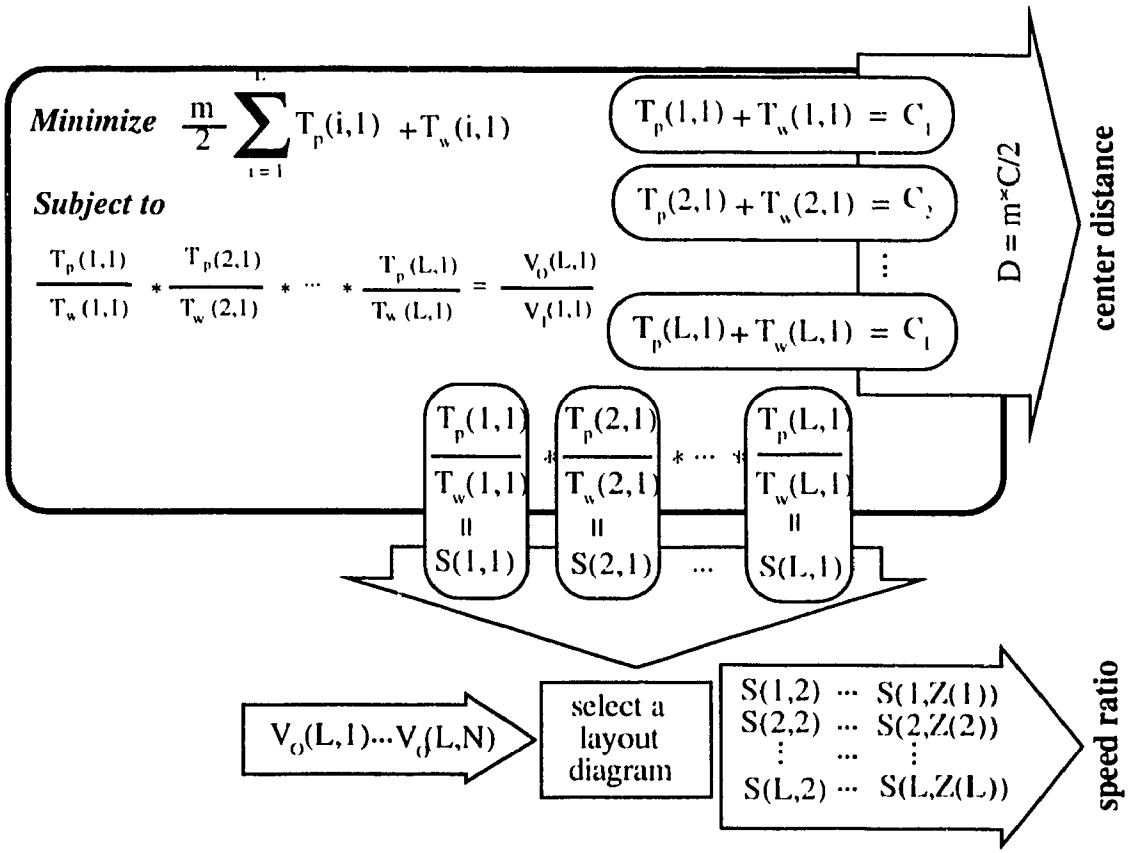

Figure 3.2 Obtaining the center distance and speed ratio

The step 2 is intended to determine the number of teeth in all gears other than in reference transmission path. Figure 3.2 shows, how the center distance and speed ratio are obtained for step 2, as a result of overall center distance minimization achieved in step 1. Referring to the method explained in Chapter 2, the speed ratios S(i,l), (where l = 2 to Z(i)) are obtained from the known values of S(i,1). For clarity, a layout diagram and its corresponding cluster/wheel mechanism for Z(i) = 3 is illustrated in Figure 3.3, where the input speed $V_I(i,k)$, output speeds $V_O(i,k)$ and speed ratios S(i,j), center distance D_i are also identified.

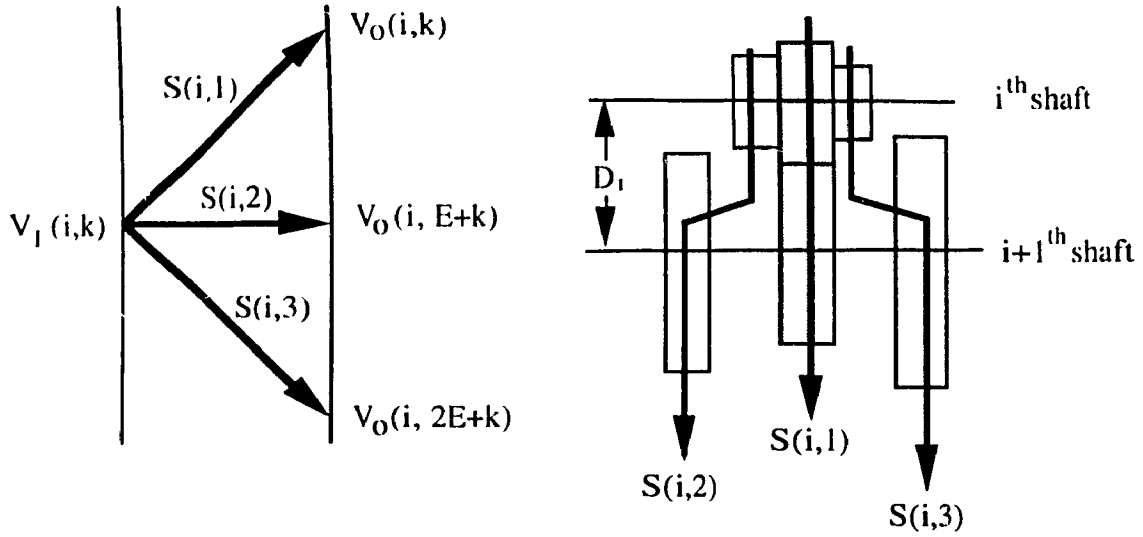

Figure 3.3 Layout diagram and its corresponding cluster/wheel mechanism for Z(i) = 3

The center distance D_i of the reference gear set, based on the assumption that the reference pinion and wheel have the same module value m, is given as:

$$D_i = \frac{m}{2} * [T_p(i,1) + T_w(i,1)] \tag{3.9}$$

As indicated in Figure 3.3, the same center distance D_i is maintained for 1^{th} gear set in i^{th} transmission stage for i = 1, 2,..., L and 1 = 2,..., Z(i).

$$D_1 = \frac{m}{2} * [T_p(i,1) + T_w(i,1)] \tag{3.10}$$

Now by defining the mesh condition for the 1^{th} gear set in the i^{th} transmission stage, the equation relating the number of teeth can be obtained. That is,

$$\frac{m}{2} * [T_p(i,1) + T_w(i,1)] - \frac{m}{2} * [T_p(i,1) + T_w(i,1)] = 0 \tag{3.11}$$

i.e. $$T_w(i,1) = [T_p(i,1) + T_w(i,1)] - T_p(i,1) \tag{3.12}$$

Theoretically, the 1^{th} gear set is to have the gear ratio $T_p(i,1) / T_w(i,1)$ equal to $S(i,1)$. But in actual design, conversion of the number of teeth into integer value produces a deviation on gear ratio.

The deviation on the gear ratio is expressed as a percentage of its ideal value:

$$\varepsilon = \frac{\text{actual gear ratio} - \text{ideal gear ratio}}{\text{ideal gear ratio}}$$

or
$$\varepsilon = \frac{\frac{T_p(i,1)}{T_w(i,1)} - S(i,1)}{S(i,1)} \qquad (3.13)$$

i.e.
$$\varepsilon = \frac{T_p(i,1)}{T_w(i,1) * S(i,1)} - 1 \qquad (3.14)$$

Substituting for $T_w(i,1)$, the gear ratio deviation is given by

$$\varepsilon = \frac{T_p(i,1)}{\left[T_p(i,1) + T_w(i,1) - T_p(i,1) \right] * S(i,1)} - 1 \qquad (3.15)$$

To facilitate computational advantage a tolerance value δ is introduced to be associated with this deviation and is defined by,

$$-\delta \leq \varepsilon \leq \delta \qquad (3.16)$$

or
$$|\varepsilon| \leq \delta \qquad (3.17)$$

The objective function

The objective function is written for the net gear ratio deviation of all gear sets other than the reference transmission path.

Minimize Φ (= Total of all gear ratio deviations)

where $$\Phi = \sum_{i=1}^{L} \sum_{1=2}^{Z(i)} \left| \frac{T_p(i,1)}{[T_p(i,1) + T_w(i,1) - T_p(i,1)] * S(i,1)} - 1 \right| \quad (3.17)$$

The number of teeth of the pinion is taken as the design variable. Substituting the design variable x, this objective function takes the form

$$\Phi(x) = \sum_{i=1}^{L} \sum_{1=2}^{Z(i)} \left| \frac{x(k)}{[T_p(i,1) + T_w(i,1) - x(k)] * S(i,1)} - 1 \right| \quad (3.18)$$

$$\text{where } k = 1,N \text{ and } NV = \sum_{i=1}^{L} Z(i) - L$$

The constraints

Optimization is performed keeping in view the limitations on the number of teeth values as laid by the codal provisions. Values for number of teeth $T_p(i,1)$ (where i = L; 1 = 2 to Z(i)) are found within the range from (Tmin, Tmax). Hence, 2*NV number of inequality constraints can be formulated considering each set of lower and upper bounds.

$$F_k(x) = T_{min} - x(k) \leq 0 \quad , \quad k = 1, NV \quad (3.19)$$

$$F_k(x) = x(k) - T_{max} \leq 0 \quad , \quad k = NV+1, 2*NV \quad (3.20)$$

When the diameter of the output gear in a transmission stage is made equal to that of the input gear in the next transmission stage, the design is said to be composite. Focusing on the composite arrangements, more equality constraints are adopted here at this stage. Constraints are derived by equating corresponding gear diameters according to the composite nature. The number of design variables may also be reduced when more equality constraints are considered in the optimization.

3.4 Optimal design procedure

The design synthesis of this chapter is based on a optimal design procedure that is followed in the two minimization steps of the previous sections. Required input to the procedure are the values of number of spindle speeds N, number of shafts required NSR, speed of the drive unit $V_I(1,1)$, spindle speeds $V_O(NSR-1,n)$ where n = 1 to N, and module m(i,j) where i = 1 to NSR-1 and j = 1 to Z(i). In the present procedure, a same module value is assigned for all gears i.e. value for the array m(i,j) is replaced by a single constant m.

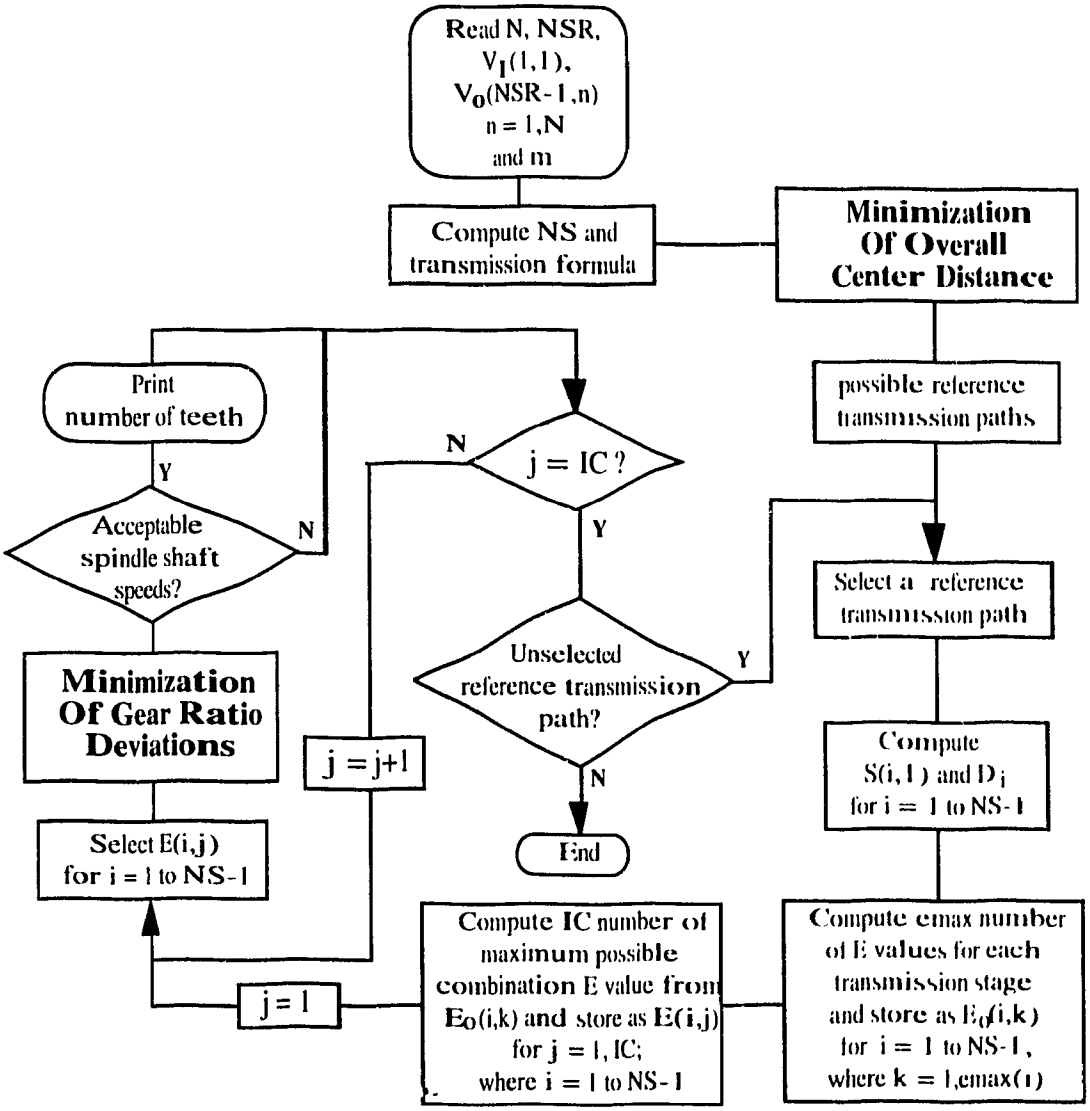

Figure 3.4 Flowchart for the kinematic design synthesis

The flowchart in Figure 3.4 illustrates an automated design procedure for obtaining all possible gear trains with minimum overall center distance. In the flowchart, both the minimization schemes that are presented as Step 1 and Step 2, are combined together with a procedure that finds all possible layout diagrams for a selected reference transmission path. Both the minimization schemes require that a global minimum be obtained for each of their multiple variable objective functions and constraints. Since, the present design procedure is capable of handling any number of N and NSR, the order of non linearity in the design procedure is not known. When the objective function and constraints are formulated with integer design variables for gear teeth, a powerful integer programming method is needed to solve this nonlinear problem. Most of available solution procedures are relatively inefficient dealing with heavily constrained problems with larger number of design variables. Knowing this, a Non Linear Integer Goal Programming approach NLIGP, details of which are presented in Appendix B, is selected as the solution algorithm for both minimizations in the present chapter. The algorithm of the selected NLIGP approach, is based on existing methods in non linear programming, integer programming and heuristics. The method deals with a model which uses goal programming with a pattern search algorithm, where all the constraints are converted as objectives and adopted in the set of objectives functions.

In the present optimization procedure, the initial values for design variables are randomly picked from the domain of integer numbers defined by the codal provisions that are particular to number of teeth for both the pinion and wheel. The optimum search is initiated to start with a random number generator to allow a complete examination within the feasible design region. The final results are printed out based on some criteria such as acceptable requirements on spindle or intermediate shaft speeds, gear ratios and composite arrangements. In the present design analysis, the spindle speeds are investigated to select the optimum design. The following FORTRAN statements are used to read the basic input data for the procedure:

```
Print*, 'Please type the number of spindle speeds'
      Read(6,*) N
Print*, 'Please type the number of shafts required'
      Read(6,*) NSR
Print*, 'Please type the speed of drive unit'
      Read(6,*) VI(1,1)
Print*, 'Please type the values for spindle speeds'
      DO n = 1, N
      Read(6,*) VO(NSR-1,n)
      end do
Print*, 'Please type the module'
      Read(6,*) modl
```

Gear train specification			Gear train information						
Number of spindle shaft speeds	Values of spindle shaft speeds (rpm)	Number of shafts required	Trans-mission stage	Number of gear sets	E	Number of teeth		Gear ratio	Module (cm)
						Pinion	Wheel		
18	1391.170	5	1	3	1	48	28	1.714286	0.305
	1220.588								
	1070.691					34	42	0.809524	
	939.2025								
	823.8618					20	56	0.307692	
	722.6857		2	3	1	35	33	1.060606	
	633.9349								
	556.0833					33	35	0.942857	
	487.7923								
	427.8880					31	37	0.837838	
	375.3403								
	329.2459		3	1	1	33	34	0.970588	
	288.8122								
	253.3440		4	2	3	27	49	0.551020	
	222.2316								
	194.9400								
	171.0000					20	56	0.357143	
	150.0000								

Table 3.1 Gear train details from Reference Rao et al [39]

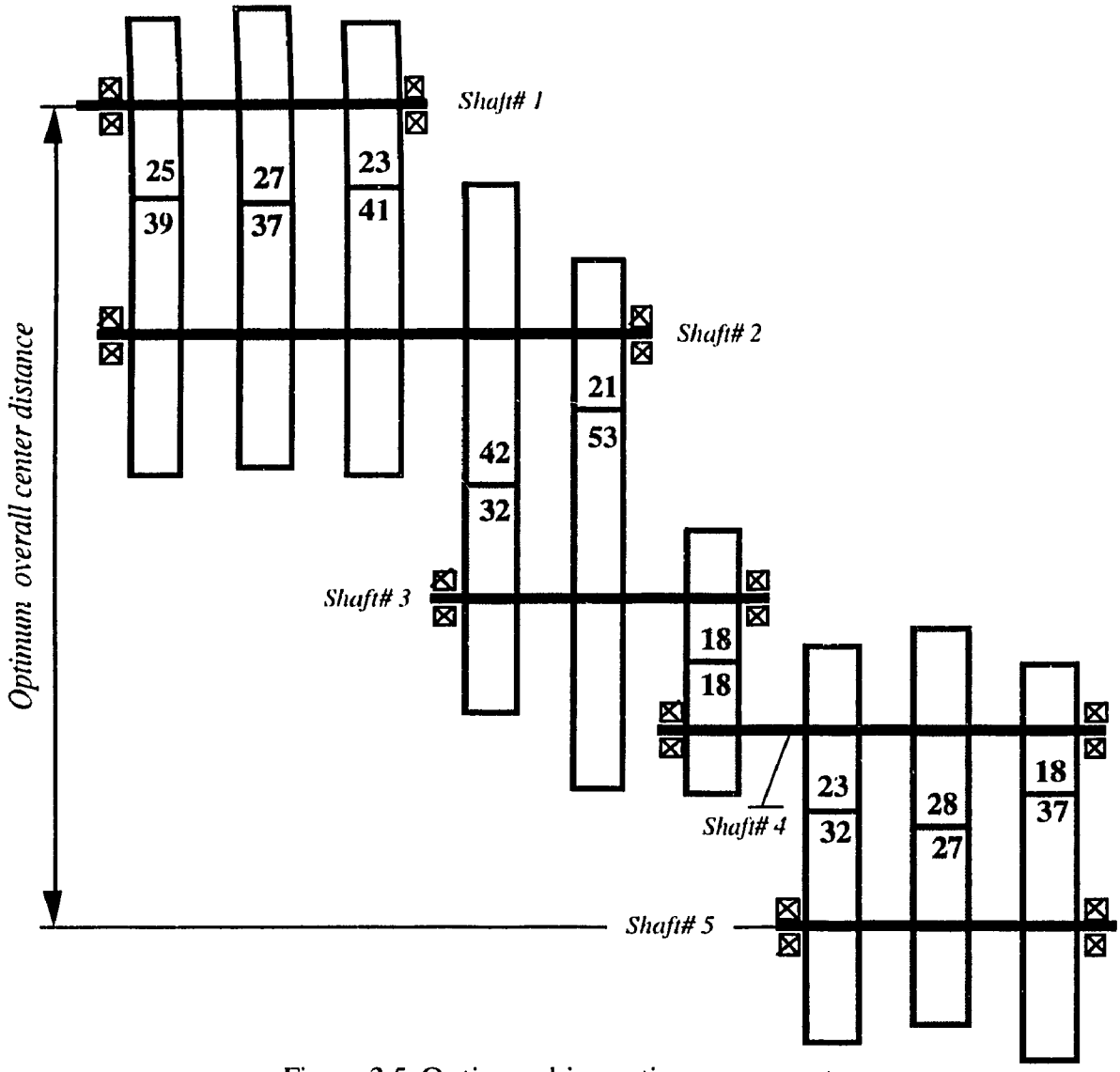

Figure 3.5 Optimum kinematic arrangement

3.5 Optimal design example

Based on the flowchart shown in Figure 3.4, numerical computations are carried out for a 18 speed gear train with module for all gears equal to 0.305 cm. In order to demonstrate the need for analyzing all possible layout diagrams, the gear train specifications are selected from an already optimized design that has been presented in Reference [39]. The drive unit speed of the selected gear train is 1400 rpm. All other details of the selected gear train are shown in the Table 3.1. The ideal speeds are calculated as 150 rpm to 1391.4697 rpm, using the equation (2.9) of Chapter 2 with the step ratio ϕ

equal to 1.14. From the gear ratios listed in Table 3.1, it can be noted that, the gear ratios fall between 0.307692 and 1.714286. The gear ratios 0.307692 and 0.357143 violate the standards defined in the Reference [54]. However, for the sake of demonstration an assumption is made to accept R_{min} equal to 0.30000 for the present optimization.

The reference transmission path is designed to produce the spindle speed of 1391.4697 rpm from the drive unit speed 1400. The total number of teeth is found to be equal to 287 on the above mentioned transmission path presented in Reference [39]. This value is inputed as the initial goal for the objective function. As the result, an alternate optimal reference transmission path is obtained with the total number of teeth equal to 229. This yields a 20.21% reduction of the center distance over the value presented as optimal design in Reference [39]. The gear ratios in the reference transmission path are also considerably optimized, yielding reduced largest speeds in the intermediate shafts, that are presented and compared with Reference [39] in Table 3.2.

i	Gear ratios in reference transmission path		Larger speeds in intermediate shafts	
	Rao et al [39]	Present	Rao et al [39]	Present
1	1.714286	0.7297297	2400.000	1021.622
2	1.060606	1.312500	2545.454	1340.878
3	0.9705882	1.000000	2470.588	1340.878
4	0.5510204	1.037037	1361.344	1390.540

Table 3.2 Results from the minimization of center distance

In completing the design synthesis, the new optimal design is obtained with transmission formula as 18 = 3 * 2 * 1 * 3. The optimum design is selected from a set of acceptable designs with different layout diagrams. This is done by a comparison of spindle speeds that are more closer to the ideal speeds required. The optimum number of teeth and

optimum gear ratios are provided in Table 3.3 and the layout of the optimum kinematic arrangement is shown in Figure 3.5.

specification		Gear train information						Actual spindle shaft speeds (rpm)
Number of spindle shaft speeds	Number of shafts required	Trans-mission stage	Number of gear sets	E	Number of teeth		Gear ratio	Module (cm)	
					Pinion	Wheel			
16	5	1	3	1	27	37	0.729780	0.305	1390.540
									1221.510
					25	39	0.641026		1068.970
									963.7563
					23	41	0.560976		846.6047
									740.8823
		2	2	3	42	32	1.312500		652.3192
									573.0250
					21	53	0.396226		501.4667
									419.7858
		3	1	1	18	18	1.000000		368.7577
									322.7080
		4	3	3	28	27	1.037037		290.9453
									255.5788
					23	32	0.718750		223.6626
									196.9265
					18	37	0.486487		172.9887
									151.3862

Table 3.3 Details of optimum kinematic design

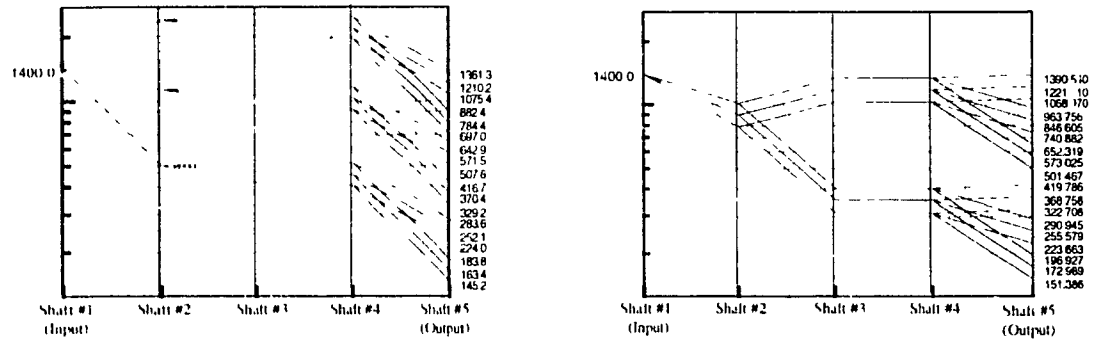

(A) Rao et al [39] (B) present design

Figure 3.6 Speed diagrams of (A) Reference Rao et al [39] and (B) optimal design

Transmission path index	Ideal speeds	Actual speeds		Deviation %	
		Rao et al [39]	Present	Rao et al [39]	Present
1	1391.170	1361.345	1390.540	2.143902	0.045233
2	1220.588	1210.208	1221.510	0.850421	-0.075577
3	1070.691	1075.410	1068.970	-0.440720	0.160687
4	939.2025	882.353	963.7563	6.052966	-2.614321
5	823.8618	784.394	846.6047	4.790611	-2.760519
6	722.6857	697.025	740.8823	3.550784	-2.517904
7	633.9349	642.857	652.3192	-1.407438	-2.900036
8	556.0833	571.487	573.0250	-2.769999	-3.046614
9	487.7923	507.832	501.4667	-4.108295	-2.803326
10	427.8880	416.667	419.7858	2.622496	1.893541
11	375.3403	370.408	368.7577	1.314050	1.753763
12	329.2459	329.151	322.7080	0.028965	1.985730
13	288.8122	283.614	290.9453	1.800049	-0.738572
14	253.3440	252.127	255.5788	0.480547	-0.882109
15	222.2316	224.044	223.6626	-0.815391	-0.643902
16	194.9400	183.824	196.9265	5.702509	-1.019053
17	171.0000	163.415	172.9887	4.435453	-1.162970
18	150.0000	145.214	151.3862	3.191010	-0.924113

Table 3.4 Comparison of spindle speeds and deviations

Transmission path index	Rotational speeds (rpm)				
	shaft # 1	shaft # 2	shaft # 3	shaft # 4	shaft # 5
1	1400.000	1021.622	1340.878	1340.878	1390.540
2	1400.000	897.4359	1177.885	1177.885	1221.510
3	1400.000	785.3658	1030.793	1030.793	1068.970
4	1400.000	1021.622	1340.878	1340.878	963.7563
5	1400.000	897.4359	1177.885	1177.885	846.6047
6	1400.000	785.3658	1030.793	1030.793	740.8823
7	1400.000	1021.622	1340.878	1340.878	652.3192
8	1400.000	897.4359	1177.885	1177.885	573.0250
9	1400.000	785.3658	1030.793	1030.793	501.4667
10	1400.000	1021.622	404.7934	404.7934	419.7858
11	1400.000	897.4359	355.5878	355.5878	368.7577
12	1400.000	785.3658	311.1827	311.1827	322.7080
13	1400.000	1021.622	404.7934	404.7934	290.9453
14	1400.000	897.4359	355.5878	355.5878	255.5788
15	1400.000	785.3658	311.1827	311.1827	223.6626
16	1400.000	1021.622	404.7934	404.7934	196.9265
17	1400.000	897.4359	355.5878	355.5878	172.9887
18	1400.000	785.3658	311.1827	311.1827	151.3862

Table 3.5 Rotational speeds of the optimal design

B

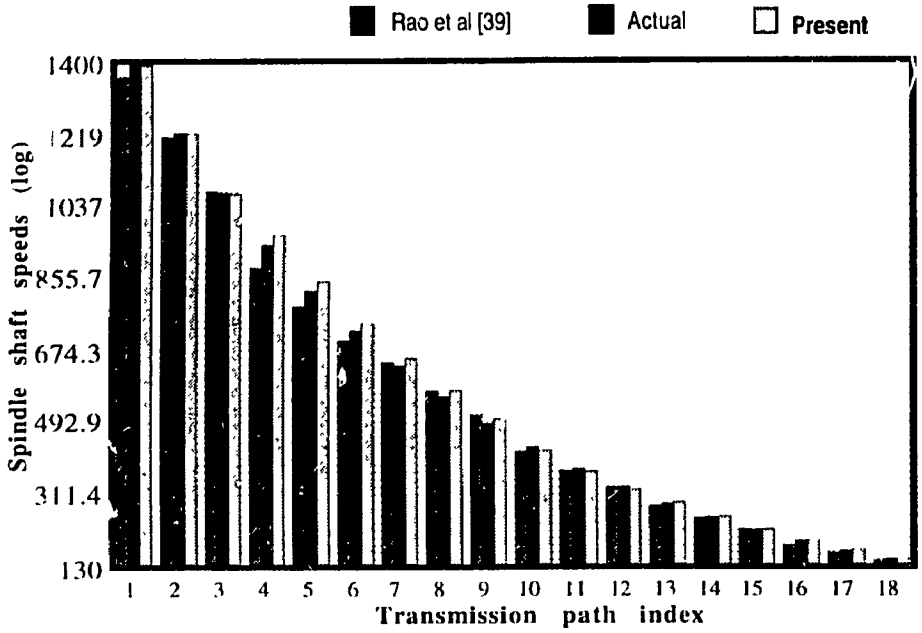

Figure 3.7 Spindle shaft speeds

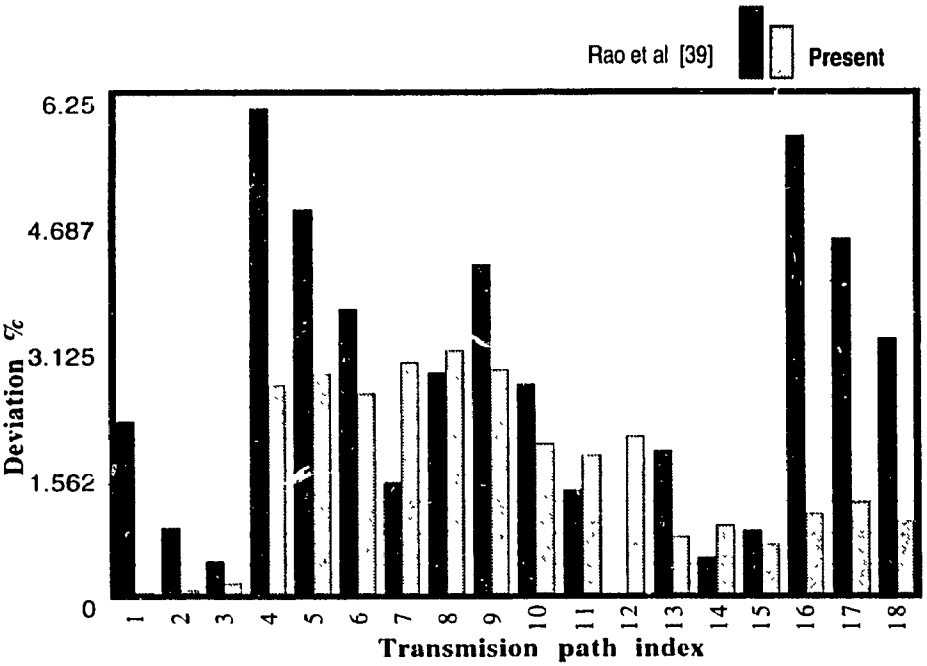

Figure 3.8 Speed deviations

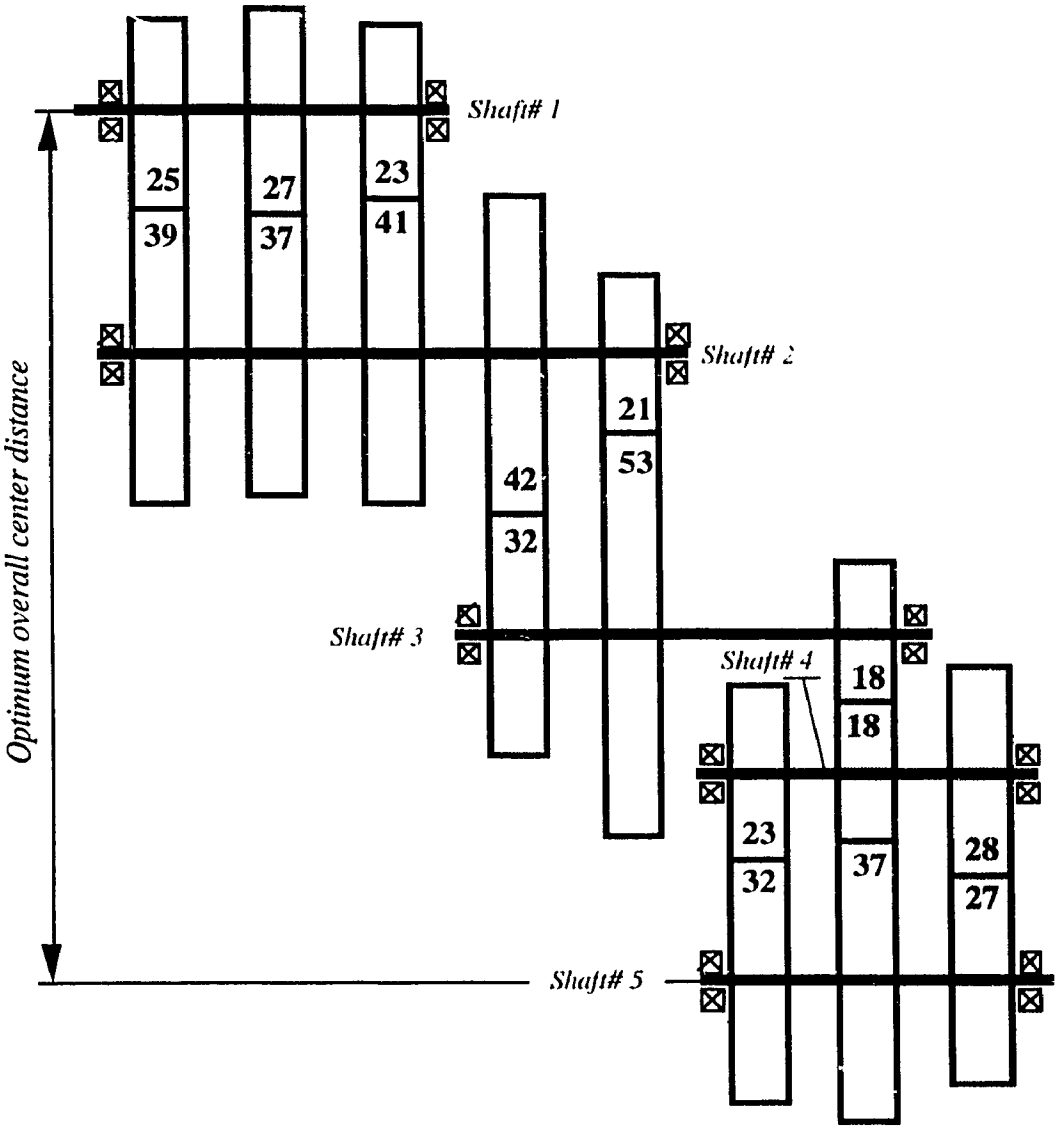

Figure 3.9 Composite arrangement

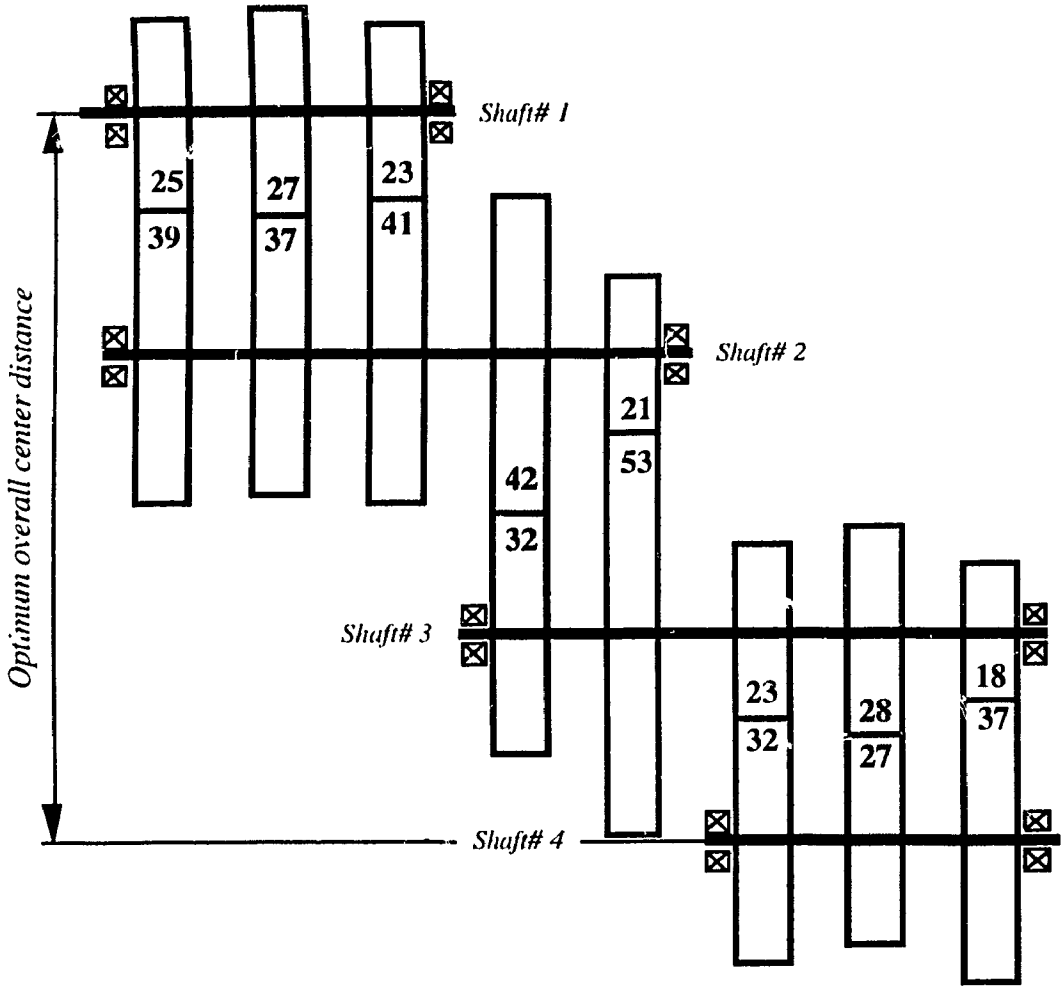

Figure 3.10 Optimal design with 4 shafts

The percentage of speed deviation for both drives, which is equal to (ideal speed - actual speed) / actual speed are shown in the Table 3.4. The results in Table 3.4, Figure 3.7 and Figure 3.8 show good improvement on the spindle speeds using the present optimum design compared to the optimum design given in Reference [39]. It can be noted that the overall center distance of the new design is 79.79% smaller and the spindle speeds are more closer to the ideal speeds required, where the percentage of new speed deviations are obtained between 0.045233 and 3.046614 as compared to 0.02895 and 6.052966. Also the largest speeds in the intermediate shafts of the optimal design are considerably

reduced and this can be noted by comparing the speed diagrams of both gear trains shown in Figure 3.6. The rotational speeds of the present optimal design is listed in the Table 3.5.

More improved features can also be noted in the selected optimum design presented here. A composite design can be created from this selected optimum design by completely eliminating the wheel in the 3rd transmission stage and allowing a particular pinion in the 4th transmission stage to be the composite. This reduces the number of gears in the gear train by one, that will further lower the weight and the manufacturing cost. The layout of the composite kinematic arrangement is shown in Figure 3.9.

Furthermore, 3rd transmission stage of the optimum design shown in Figure 3.5 contains a single gear set and the gear ratio of which is equal to 1.000. It is obvious that the absence of this transmission stage does not affect the required spindle speeds. Thus, an alternate gear train with reduced overall center distance can be designed by removing the above mentioned transmission stage. The new alternate design will have the transmission formula as 18 = 3 * 2 * 3, layout of which is shown in Figure 3.10. This yields the number of gears in the gear train to be 16 and the overall center distance of the new design to be 67.25% smaller than the value presented as optimal design in Reference [39].

3.6 Conclusion

An optimal design procedure is developed in this chapter and the kinematic parameters of gear train systems for (1) minimum of overall center distance with specified module for all gears and (ii) improved gear ratios with minimum deviations from the ideal spindle speeds that are required for the application are evaluated based on this design optimization approach. In the optimization process, the values for number of teeth are treated as integer variables and the module can assume only values from a given set. The numerical study shows the sensitivity of different kinematic layouts for a given set of drive unit speed, spindle speeds and the number of shafts required. The need for analyzing all possible kinematic layouts is systematically borough out through incorporating the

methodology developed in chapter 2. The results show the inadequacies of previously obtained optimal design by Rao et al in Reference [39]. The improved kinematic design parameters provides an alternate layout diagram. The improvement is noted by reducing the overall center distance and gear ratios with minimum deviations. The foregoing results illustrate the ways of effectively integrating the concept of optimization for designing real life mechanical systems that require designs with reduced number of shafts or composite designs. In this Chapter, it is shown that checking all possible layout diagrams are essential in finding an optimal kinematic design of gear trains.

CHAPTER 4

Probabilistic design of multi-speed gear trains

4.1 Introduction

In the field of optimal design of machine elements, two different approaches are usually followed namely deterministic and probabilistic depending on the magnitude of uncertainty of basic design variables. A detailed design synthesis of finding the optimal mass and the transmitted power for a multi-speed gear trains using both the deterministic and the probabilistic concepts is presented in this chapter. The resulting power transmitting capacity (rating) is used to select the drive unit that runs the gear train. Knowing the transmitted power and the minimum rotational speeds on the shafts, the module is estimated so that it will provide the value for the overall center distance and satisfy the strength conditions.

Considering the transmitted power of a gear train, the system environment depends on four major variables namely the kinematic design parameters, operating conditions, material properties and tooth geometry. The kinematic design parameters and operating conditions are determined by the appropriate selection of the speed diagram of the gear train. The material properties depend on the characteristics of the gear materials. For a safe design, as the size of gear is minimized, the quality of material is expected to increase, thereby increasing the cost. The tooth geometry of each gear need to be properly defined in order to produce a high power transmitting capacity without power losses. Usually tooth geometry is directly obtained from the standard gear cutter that has been used to generate the gear tooth. Changes in the cutter geometry obviously affect the power transmitting capacity and gear characteristics such as contact ratio and under cutting.

For the optimization of gear train based on the deterministic concept, system environment is assumed to be constant during the entire search process. But in reality the

system environment of gear trains contains many random parameters, which require that the optimization scheme is to be based on a probabilistic concept. The probability of no failure or reliability is employed for the synthesis of the design of gear trains.

Reliability of a mechanical system is defined as the probability of non-occurrence of unacceptable mulfunctions or complete failure wherein the failure occurs due to the random characteristics of the system environment. The reliability is iterative in nature, since the safety can be expressed as a function of component strength. On the other hand, a set of strength constraints is to be satisfied for optimal design. Thus, the minimization of the mass, based on deterministic safety concepts, may reduce the level of reliability of the system. This reduction is expected to be stemming from the improper material distribution in the design components. Taking this into account, the best design might be achieved when the optimum design scheme is adopted along with a consideration of reliability.

The reliability based optimization has been proposed at the beginning of the sixties and is a developing area in machine tool design. Using a probabilistic analysis, the optimal design is achieved by satisfying all pre-selected constraints in addition to one given by the reliability criteria. As it is well known, two types of reliability are used in optimization, namely element reliability and system reliability. In the former type, the objective for minimization is formed considering the reliability of the individual members of the system. In the latter type, the optimum design is to satisfy the condition for the overall no-failure of the system, using the concepts of system reliability. The reliability-based optimization is more tedious than the deterministic optimization mainly due to two reasons [35]. First, the complexity involved in the reliability approach is amplified in proportion to the number of iterations required. Second, the reliability design requires many more variables than that of the deterministic design because of the additional parameters that describe the variations in loads and strengths.

The selected literature reveals how reliability based optimization is applied in various structural design problems. In general, different objectives such as minimum

mass, minimum cost and minimum probability of failure are proposed to achieve an optimal design. An analytical study of structures with respect to the optimal criteria of cost minimization has been presented in the works by Parimi and Cohn [35], wherein the estimation of reliability is discussed through the cost of failure. Jendo [21] obtained optimal solution of plastic frames based on the system reliability. Another scheme of cost minimization is reported in the work of Moses [30], incorporating failure cost in the objective function itself and both element and system reliabilities are discussed as case studies. Hsu [20] demonstrated the minimum mass criteria for a structure by considering the reliability constraints of both the elements and the overall system and a numerical study has also been included. In real life systems, many of the design parameters need to be considered as random quantities, so that the response also become random. The optimal mass of a structure is obtained in the work of Davidson et al [16] assuming that the random parameters are present in the system environment. For each element, the mean response, such as stress in all elements is made as a constraint. A framed structure is analyzed by Mahadevan [25], based on both element and system reliabilies. Here the element reliabilies are modeled through reliability indices and the sum of them is defined as the objective function for minimization. The reliability index of each element is constrained by a minimum value required. Moreover, some elements are constrained with respect to their performance limitations such as strength and geometrical shapes. The prescribed system reliability is achieved through an additional constraint that states the overall failure probability of system. The drawback of the work, however, is that the performance limitations are not treated as probabilistic parameters.

Numerous articles are available in the published literature that concern with the reliability analysis in machine tool design. As such example, the work by Sankar [41] can be cited, wherein the reliability based design is attempted for machine tool spindles that are subject to randomly varying cutting forces. Not many articles are available in the literature on the probability based optimum design in the area of machine tool design, particularly on

the design of gears or gear trains. It is further observed that many of the past investigations employ only the concept of factor of safety for obtaining reliable gear performance, which is a crude way of handling the inherent uncertainty. Safer designs can be achieved by an approach where the probability of failure of each gear pair in the gear train is considered separately, for different failure modes. Further, optimal design of gear trains should be performed through the simultaneous incorporation of kinematic requirements as well as component strength requirements based on an appropriate probabilistic setting.

The work by Rao [37], that deals with a design of a nine speed gear train can be sighted as the first of the few papers published on the probability based design of gear trains. The dimensions of gear pairs in the gear train are obtained such that the probabilities of failure due bending and wear stresses are made equal to some allowable values. The entire gear train is idealized as a weakest link kinematic chain, such that the failure of any mesh constitutes the failure of the whole system. Equations are derived for the mean and standard deviations of induced stresses. The face widths are treated as design variables. The approach is more realistic but it does not include any of the optimization procedures.

Rao et al presented another work [40] for a 9 speed gear train which is an extension of Reference [39]. In this work, they have included an optimization procedure along with a reliability constraint. The linear combination of the mean and standard deviation of gear mass is minimized satisfying the wear and bending strength constraints. The results are compared with that of the deterministic procedure. The mass that is obtained using the probabilistic approach is found to be higher than that of the deterministic approach. The results also indicate that introducing the standard deviation of gear mass into the objective function does not yield any improvement in the optimum design. However, these observations are based only on the minimization of gear mass. The drawback of this work is that it does not consider the transmitted power rating which is an important design factor of the gear train. Such a study has not yet been available in the present literature and is the subject of this chapter.

4.2 Stresses in gears

A gear train is intended to transmit power continuously at a steady speed and is also subjected to variable load conditions such as high initial torque or shock loads. The power is mainly transmitted through engaged gear teeth, where the repetitive engagement causes different modes of failure. Each mode is viewed as an unique failure with its own descriptive identification. Also the interactions of different forms of failure are let play a passive role consistent with analysis procedures. Operational safety of power transmission against any mode of failure requires that the stresses in all gears should not lead to stress related failures. Most commonly high amplitude tensile and compressive stresses are observed from measurements in power transmitting gears resulting in plastic and elastic deformations. Concentration of the induced stresses over an infinitely small area leads to a change in the microstructure of gears, which produces the metal rupture. Well known gear failures are classified into three major groups [54]. They are (i) failure due to fatigue, (ii) failure due to impact and (iii) excessive wear. The fatigue failure is characterized by the onset of cracking which occurs under stress reversals with amplitudes much lower than the ultimate tensile strength. Some modes of fatigue failure are bending fatigue, pitting and spalling. The impact failure usually occurs in the case of sudden over - load of mating gears. The impact makes the actual stresses to exceed the threshold value of the rupture stress, thus resulting in tooth failure. Some modes of impact failure are bending impact, tooth shear and tooth chipping. The wear failure is the surface deterioration of the actual profile of gear teeth. Two types of wear failures are most commonly encountered, namely abrasive wear and adhesive wear. The abrasive wear is prone to occur when the active profile of gear teeth is cut by small particles of abrasive material. The lubricant is mostly the source which carries the contaminated abrasive particles. Adhesive wear is the other type of wear which is initiated by the metal-to-metal contact of tooth surfaces. The transmitted load breaks down the overheated lubricant and permits the ends of teeth to undergo the plastic deformation and adhesion.

Certain modes of gear failures, such as tooth bending fatigue, tooth bending impact and abrasive wear are observed more often than others. A study reported in the Reference [2] shows that 32% of failures occur due to tooth bending fatigue, 12.5% occur due to tooth bending impact and 10% due to abrasive tooth wear. The description of different failures has been documented in detail by gear researchers and manufactures. Many international and industrial codal provisions, such as American Gear Manufactures Association (AGMA) International Standard Organization (ISO), DIN, Comecon standards and American Petroleum Standard (APS) also describe these gear failures. The AGMA, ISO, DIN and Comecon are compared to each other in Reference [48]. The AGMA 218 that classifies the gear failures as bending and wear failures in accordance with the induced stresses is used in this chapter.

During the power transmission using gearing, the high concentration of compressive stress is found over the contact area and at or near the pitch line of mating gears. This area is critical for the modes of failures due to wear. At the same time the tensile stress is concentrated at the root radius of the loaded side, and compressive stress at the root radius of the unloaded side. The bending fatigue can be expected on the loaded side of the root radius. In order to ensure that the amount of power being transmitted does not cause any stress related failures, two forms of failures, namely bending and wear failures, are considered in design. The maximum induced stresses are checked relative to the allowable values defined by standards. The maximum stresses are calculated using the theory of elasticity.

4.2.1 Bending stress

Bending stress due to tooth loads are estimated using Lewis equation which is based on the cantilever beam theory . In the case of two mating gears in action, as the load is applied at the top of a tooth, maximum bending stress is induced, where the repetitive application of these loads results in fatigue cracks.

In order to calculate the bending stress, a gear set with gear ratio T_p / T_w, module m, face width FW and transmitting torque M_t is considered. The maximum torque is obtained when the wheel of the corresponding gear set reaches to the lowest possible speed V_L. The induced bending stress s_B, is given by the following formula [39], that uses Lewis factor y

$$s_B = \frac{\beta' * M_t}{m^2 * FW} \qquad (4.1)$$

where $$M_t = \frac{97500 * P}{V_L}$$

$$\beta' = \frac{2 * K_C * K_D}{T_w * y * \cos \alpha} \quad , \quad \frac{T_p}{T_w} < 1$$

$$= \frac{2 * K_C * K_D}{T_p * y * \cos \alpha} \quad , \quad \frac{T_p}{T_w} \geq 1$$

$$y = 0.52\left(1 + \frac{20}{T_w}\right)$$

$$K_C = 1.5; \; K_D = 1.1$$

Hence,

$$s_B = \frac{\beta' * 97500 * P}{m^2 * FW * V_L} \qquad (4.2)$$

or

$$s_B = K_B * \frac{P}{m^2 * V_L * FW} \qquad (4.3)$$

where $$K_B = \frac{195000 * K_C * K_D}{T_w * y * \cos \alpha} \quad , \quad \frac{T_p}{T_w} < 1$$

$$K_B = \frac{195000 * K_C * K_D}{T_p * y * \cos\alpha} \quad , \quad \frac{T_p}{T_w} \geq 1$$

It can be seen that the bending stress is directly proportional to the transmitted power and is inversely proportional to the square of module, wheel speed and the face width of the mating gear set. A safe design implies that,

$$s_B = K_B * \frac{P}{m^2 * V_L * FW} \leq S_B \qquad (4.4)$$

Where S_B is the bending strength*.

4.2.2 Wear stress

Wear stress s_W, induced in a gear set is calculated as follows [39]:

$$s_W = \frac{\gamma'}{m} * \sqrt{\frac{M_t}{FW}} \qquad (4.5)$$

$$\gamma' = \frac{1.18}{T_w} * \sqrt{\left|\frac{T_w}{T_p} + 1\right| * \frac{E * K_C * K_D}{\sin 2\alpha}} \quad , \quad \frac{T_p}{T_w} < 1$$

$$= \frac{1.18}{T_p} * \sqrt{\left|\frac{T_p}{T_w} + 1\right| * \frac{E * K_C * K_D}{\sin 2\alpha}} \quad , \quad \frac{T_p}{T_w} \geq 1$$

hence, $$s_W = \frac{K_W}{m} * \sqrt{\frac{P}{FW * V_L}} \qquad (4.6)$$

where,

$$K_W = \frac{1.18}{T_w} * \sqrt{97500 * \left|\frac{T_w}{T_p} + 1\right| * \frac{E * K_C * K_D}{\sin 2\alpha}} \quad , \quad \frac{T_p}{T_w} < 1$$

$$= \frac{1.18}{T_p} * \sqrt{97500 * \left|\frac{T_p}{T_w} + 1\right| * \frac{E * K_C * K_D}{\sin 2\alpha}} \quad , \quad \frac{T_p}{T_w} \geq 1$$

* The word 'strength' has been used instead of 'allowable stress' from here onwards as per the recommendation of Dr. V.N. Latinovic.

It may be noted that, the wear stress is directly proportional to the square root of the transmitted power and is inversely proportional both to the module and to the square root of wheel speed and also to the face width. For a safe design,

$$s_W = \frac{K_W}{m} * \sqrt{\frac{P}{FW * V_L}} \leq S_W \qquad (4.7)$$

where S_W is the wear strength.

4.3 Basic equations

The magnitude of stresses induced in gears can vary over a considerable range due to the random nature of system environment. It is desirable to evaluate the variations using statistical methods, since the variations are assumed to obey distribution laws. Moreover the parameters that cause the variations are continuous, independent of one another and follows normal distributions. This results in a normally distributed stresses in gears, which determines the need for a probabilistic approach in design synthesis. The variability of the component stresses and strength can be seen through their distributions in many of the design text books. It can be stated that both the induced stress and strength are normally distributed. Thus, the mean values of stress and strength are denoted by $\bar{s}$ and $\bar{S}$ respectively. The density functions g(s) and g(S) are given as,

$$g(s) = \frac{1}{\sigma_s * \sqrt{2\pi}} \exp\left[-\frac{1}{2}\left(\frac{s-\bar{s}}{\sigma_s}\right)^2 \right] \qquad (4.8)$$

$$g(S) = \frac{1}{\sigma_S * \sqrt{2\pi}} \exp\left[-\frac{1}{2}\left(\frac{S-\bar{S}}{\sigma_S}\right)^2 \right] \qquad (4.9)$$

The design is said to be reliable when all values of induced stresses fall below the strength.

$$S > s \qquad (4.10)$$

i.e. $$S = s + \xi \qquad \text{where } \xi > 0 \qquad (4.11)$$

The excess value ξ is also a normally distributed variable for the difference of two independent normally distributed variables s and S, i.e.

$$\xi = S - s \qquad (4.12)$$

and as such is a linear transformation.

Further, $$\sigma_\xi = \sqrt{\sigma_S^2 + \sigma_\xi^2} \qquad \text{since Cov(s,S)} = 0 \qquad (4.13)$$

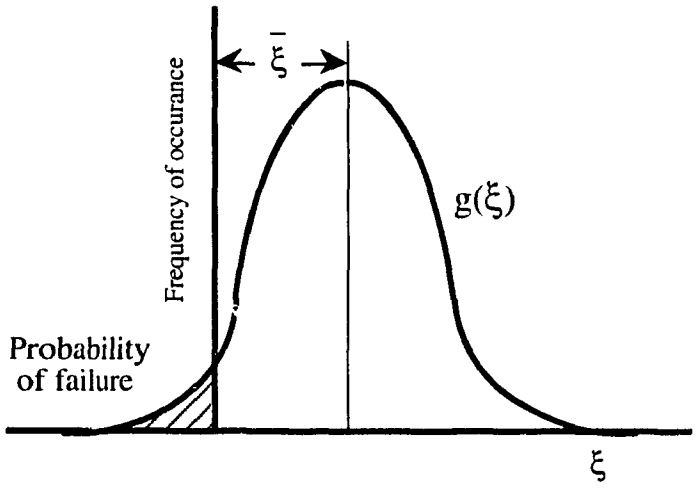

Figure 4.1 Density function of excess stress ξ

The density function of ξ is given by

$$g(\xi) = \frac{1}{\sigma_\xi * \sqrt{2\pi}} \exp\left[- \frac{1}{2}\left(\frac{\xi-\bar{\xi}}{\sigma_\xi}\right)^2 \right] \qquad (4.14)$$

Referring to the equation (4.11) the failure is said to occur when ξ is negative. As is shown in Figure 4.1, the reliable design can be seen to fall in the positive region. The probability of the event $\xi > 0$ is the reliability R, which is expressed as,

$$R = p(\xi>0) = \int_0^\infty g(\xi)\, d\xi \qquad (4.15)$$

i.e.,

$$R = \frac{1}{\sigma_\xi * \sqrt{2\pi}} \int_0^\infty \exp\left[- \frac{1}{2}\left(\frac{\xi-\bar{\xi}}{\sigma_\xi}\right)^2 \right] d\xi \qquad (4.16)$$

The transformation which relates ξ and a standard normalized variable z is given as

$$z = \frac{\xi-\bar{\xi}}{\sigma_\xi} \qquad (4.17)$$

The new limits now can be set for the standard normalized variable z as follows:

for $\xi = \infty$, $z = \frac{\infty-\bar{\xi}}{\sigma_\xi} = \infty$

for $\xi = 0$, $z = \frac{0-\bar{\xi}}{\sigma_\xi} = -\left(\frac{\bar{\xi}}{\sigma_\xi}\right)$

Using equation (4.17), $\frac{dz}{d\xi} = \frac{1}{\sigma_\xi}$

Substituting z and $d\xi$ in the equation (4.16), one gets

$$R = \frac{1}{\sqrt{2\pi}} * \int_{-\left(\frac{\bar{\xi}}{\sigma_\xi}\right)}^{\infty} \exp\frac{z^2}{2}\, dz \qquad (4.18)$$

The lower limit of integration is denoted by z_1.

$$-\frac{\bar{\xi}}{\sigma_\xi} = z_1 \qquad (4.19)$$

$$R = \frac{1}{\sqrt{2\pi}} * \int_{z_1}^{\infty} \exp\frac{z^2}{2}\, dz \qquad (4.20)$$

The value of standardized variable z_1 for a given reliability is obtained from the standard tables [19].

$$z_1 = \frac{|\bar{S} - \bar{s}|}{\sqrt{\sigma_S^2 + \sigma_s^2}} \qquad (4.21)$$

The equation (4.21) probabilistically relates the induced stress and the strength. This relationship may now be applied to establish constraints for the optimization procedure based on reliability approach.

4.3.1 Derivation of the additional constraint

A gear train is assembled using various individual elements, such as gear shafts, bearings, clutches, etc. Thus, the reliability of the assembly or system is seen as a function of individual reliabilities of its corresponding elements. According to the nature of assembly, the system reliability can be viewed as three major groups. They are parallel, serial and the combination of both.

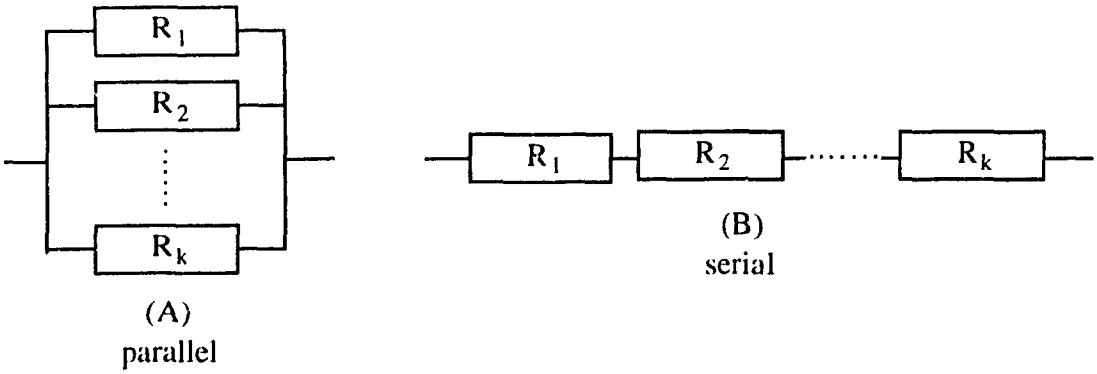

Figure 4.2 Parallel and serial combination

Figure 4.2 (A) shows the parallel combination, where only one element has to function to maintain system performance. Failure of any single element redistributes the load to the remaining elements so that it does not cause total system failure. The safety level of parallel combination is increased by the independent strength of its individual elements. The system reliability R_{sys} for the parallel combination is thus given as,

$$R_{sys} = 1 - \prod_{i=1}^{k} (1 - R_i) \tag{4.22}$$

where R_i is the reliability of i^{th} element.

The serial or weakest link reliability that is shown in Figure 4.2 (B), is the one where each individual element must contribute to system reliability. The failure of any single element will result in the total failure of the system. The serial system reliability R_{sys} is thus given as,

$$R_{sys} = \prod_{i=1}^{k} R_i \tag{4.23}$$

Most of the gear trains are modeled as serial combination of reliability and parallel systems are limited to some special cases such as multiple planet gears in epicyclic trains. The gear trains in machine tools are idealized as kinematic chains with serial combination

for each of the spindle speed. Thus, for each output speed, (NS - 1) number of gear pairs will be engaged consisting of 2*(NS - 1) elements in series. The system reliability R is given as,

$$R_{sys} = \prod_{i=1}^{NS-1} R_i \qquad (4.24)$$

With reference to the equations (4.20) and (4.24), the following expression can be formulated for the reliability of a gear train:

$$R_0^{\frac{1}{NS-1}} = \int_{z_{10}}^{\infty} \exp\left(-\frac{z^2}{2}\right) dz \qquad (4.25)$$

The standardized variable z_{10} is obtained from standard tables [19].

Comparing the above equation with equation (4.21), the following inequality relationship is formulated.

$$z_1 \leq z_{10} \qquad (4.26)$$

4.4 Formulation of the optimal design

The optimal values of facewidths of mating gears and transmitted power are obtained by solving for the minimum mass and the maximum transmitted power that satisfy constraints of bending and wear stress equations. The objective for the minimization of mass, eventually searches for the magnitude of smaller face width. This trend is to be restricted by the requirement for the maximization of power, because the larger power transmitting capacity requires larger facewidths. This conflicting nature of both objectives renders the optimization to be a multi-objective problem.

4.4.1 Optimization based on deterministic concept

To accomplish the task of minimizing mass and maximizing transmitted power, corresponding two individual objective functions are combined together as one single function.

The objective function

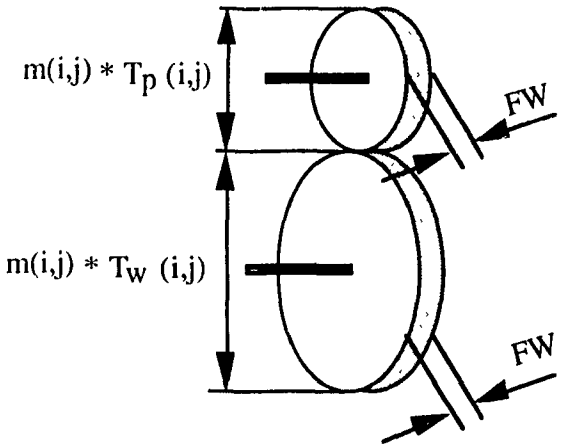

Figure 4.3. Pinion and wheel as cylindrical bodies

The first individual objective function is written for the total mass of the material used in the fabrication of gears. The Figure 4.3 shows j^{th} pinion and wheel of i^{th} transmission stage as two cylindrical bodies.

Minimize f_1 = The total mass of all gears

The total mass is the sum of the individual masses of all gears in the gear train. In order to calculate the total mass, each gear is modeled as a cylindrical body with the diameter equal to the pitch diameter of the corresponding gear. This leaves the first objective function as

$$\textit{Minimize} \quad f_1 = \sum_{i=1}^{NS-1} \sum_{j=1}^{Z(i)} \left[j^{th} \text{ pinion mass of } i^{th} \text{ transmission stage} \right] + \left[j^{th} \text{ wheel mass of } i^{th} \text{ transmission stage} \right]$$

That is to *Minimize*

$$f_1 = \sum_{i=1}^{NS-1} \sum_{j=1}^{Z(i)} \left[\rho * \pi * \left(\frac{m(i,j) * T_p(i,j)}{2} \right)^2 * FW(i,j) \right] + \left[\rho * \pi * \left(\frac{m(i,j) * T_w(i,j)}{2} \right)^2 * FW(i,j) \right] \quad (4.27)$$

$$\text{or} \qquad f_1 = \sum_{i=1}^{NS-1} \sum_{j=1}^{Z(i)} \frac{\rho * \pi * m(i,j)^2 * \left[T_p(i,j)^2 + T_w(i,j)^2\right]}{4} * FW(i,j) \qquad (4.28)$$

The second objective is written to maximize transmitted power.

$$\textit{Maximize} \quad f_2 = \text{Transmitted power}$$

As stated earlier, these two objective functions f_1 and f_2 are of conflicting nature. In order to combine both objectives, the second objective function is transformed into an alternate form. The inverse power is minimized so that the power will be maximized.

$$\textit{Minimize} \qquad f_2 = 1 / P$$

where P designates transmitted power

The multi-objective formulation results in

$$\textit{Minimize} \qquad f = f_1 + f_2$$

Minimize

$$f = \sum_{i=1}^{NS-1} \sum_{j=1}^{Z(i)} \frac{\rho * \pi * m(i,j)^2 * \left[T_p(i,j)^2 + T_w(i,j)^2\right]}{4} * FW(i,j) + \frac{1}{P} \qquad (4.29)$$

Upon substituting the design variables into the objective function, NG number of design variables are selected for facewidths. For a conventional gear train arrangement, NG is given as

$$NG = \sum_{i=1}^{NS-1} Z(i)$$

The transmitted power is treated as an independent design variable. Thus, an additional variable x is introduced for the transmitted power. This will increase the number of design variables to (NG + 1).

The objective function with (NG+1) design variables can be expressed using the following equation:

$$f(x) = \sum_{i=1}^{NS-1} \sum_{j=1}^{Z(i)} \frac{\rho * \pi * m(i,j)^2 * \left[T_p(i,j)^2 + T_w(i,j)^2\right]}{4} * x(k) + \frac{1}{x(NG+1)} \qquad (4.30)$$

where k is assigned values from 1 to NG in accordance with i and j.

If all gears are assumed with same module m, then the objective function based on deterministic framework is given by the following form of f(x)

$$f(x) = \frac{\rho * \pi * m^2}{4} * k_1 * \sum_{i=1}^{NS-1} \sum_{j=1}^{Z(i)} \left[T_p(i,j)^2 + T_w(i,j)^2\right] * x(k) + k_2 * \frac{1}{x(NG+1)} \quad (4.31)$$

where k_1 and k_2 are weighting factors.

The constraints

A set of inequality (bending and wear stress) constraints is derived for each gear set in the gear train. The conditions are written such that the maximum induced stresses in all gears shall not exceed their respective allowable values. This is expressed in the generalized form of F as

$$F = s - S \leq 0 \quad (4.32)$$

The inequality constraints imply the safety thresholds for bending and wear stresses s_B and s_W, and thus involve their respective strength. This results in NG number of constraints for each stress conditions.

The bending stress constraints are stated as,

$$F_k^B = s_B - S_B \leq 0 \qquad k = 1, NG \quad (4.33)$$

Substituting equation (4.19) in the above inequality condition yields,

$$F_k^B = K_B * \frac{P}{m^2(i,j) * V_L(i,j) * FW(i,j)} - S_B \leq 0 \quad (4.34)$$

which may be converted into the form of normalized constraints as

$$F_k^B = \frac{K_B}{S_B} * \frac{P}{m^2(i,j) * V_L(i,j) * FW(i,j)} - 1 \leq 0 \quad (4.35)$$

Assigning design variables to FW(i,j) and P, it can be shown that

$$F_k^B = \frac{K_B}{S_B} * \frac{x(NG+1)}{m^2(i,j) * V_L(i,j) * x(k)} - 1 \leq 0 \qquad (4.36)$$

With regard to wear stress conditions, a set of another NG number of constraints is formulated as

$$F_k^W(x) = s_W - S_W \leq 0 \qquad (4.37)$$

Substituting equation (4.23), this becomes

$$F_k^W = \frac{K_W}{m(i,j)} * \sqrt{\frac{P}{FW(i,j) * V_L(i,j)}} - S_W \leq 0 \qquad (4.38)$$

which is rewritten in the form of normalized constraints as

$$F_k^W = \frac{K_W}{m(i,j) * S_W} * \sqrt{\frac{P}{FW(i,j) * V_L(i,j)}} - 1 \leq 0 \qquad (4.39)$$

This equation becomes, after incorporating design variables, as

$$F_k^W(x) = \frac{K_W}{m(i,j) * S_W} * \sqrt{\frac{x(NG+1)}{x(k) * V_L(i,j)}} - 1 \leq 0 \qquad (4.40)$$

The minimum and maximum limits FW_{min} and FW_{max}, are imposed on the face widths to account for manufacturing difficulties. As the result, x(k) is governed by the condition given by

$$FW_{min} \leq X(k) \leq FW_{max}$$

For a lower bound solution, a set of inequality constraints are formulated as

$$F_k = FW_{min} - x(k) \leq 0 \qquad (4.41)$$

and similarly a set of the upper bound constraints is given as

$$F_k = x(k) - FW_{max} \leq 0 \qquad (4.42)$$

The computational scheme requires these lower and upper bounds for iteration. Assigning FW_{min} and FW_{max} to the corresponding bounds, the constraints expressed by the equations (4.41) and (4.42) can implicitly be enforced. Thus only 2*NG number of constraints resulting from bending and wear thresholds need to be satisfied in the deterministic optimization procedure.

4.4.2 Reliability based optimization

The optimization procedure involving reliability is formulated assuming that the facewidths, transmitted power, module, material density and wheel speeds are normally distributed random parameters. The mean value of FW(i,j) and P are selected as the design variables for the optimization procedure.

In order to formulate the reliability based optimization problem, all constraints with random parameters are converted to equivalent deterministic nonlinear constraints using the partial derivative rule. Thus, a constraint function F(x) with random parameters can be obtained using the mean values of x, as a Taylor series expansion

$$F(x) = F(\bar{x}) + \sum_{l=1}^{NV} \left(\frac{\partial F}{\partial x_l}\right)_{x=\bar{x}} * (x_l - \bar{x}_l) + \text{higher order derivative terms} \qquad (4.43)$$

If the standard deviations of x_l are small, the higher order derivatives can be neglected. Carrying out transformations as shown in Reference [38] the function F(x) can be approximated in the following form

$$\varphi^{-1}(R) * \sqrt{\sigma_F^2} - \bar{F}(x) \leq 0 \qquad (4.44)$$

where $\varphi^{-1}(R)$ is the normal variate corresponding to the reliability.

$$Z_l * \sqrt{\sigma_F^2} - \bar{F}(x) \leq 0 \qquad (4.45)$$

where Z_l is the variate corresponding to the reliability.

Further,

$$\bar{F}(x) = F(x)$$

$$\sigma_f = \left[\sum_{i=1}^{NV} \left(\frac{\partial f}{\partial x_i}\right)^2_{x=\bar{x}} \sigma^2_{x_i}\right]^{\frac{1}{2}} \tag{4.46}$$

The objective function

Similar transformations can now be applied to the deterministic objective function f and the new objective function is given as

Minimize $$\Phi(x) = k_1 \bar{f} + k_2 \sigma_f \tag{4.47}$$

where

$$\bar{f} = f(\bar{x})$$

$$\sigma_f = \left[\sum_{i=1}^{NV} \left(\frac{\partial f}{\partial x_i}\right)^2_{x=\bar{x}} \sigma^2_{x_i}\right]^{\frac{1}{2}}$$

$k_1 \geq 0$ and $k_2 \geq 0$ indicate the relative importance of mean f and the standard deviation σ_f for the minimization.

The design variables FW and P are assumed to be probabilistic. Material density ρ and module m are also of random nature. But all values of number of teeth are deterministic.

The mean value of objective function f is given by,

$$\bar{f} = \sum_{i=1}^{NS-1} \sum_{j=1}^{Z(i)} \frac{\pi * \bar{m}(i,j)^2 * \bar{\rho}}{4} * \left[T_p(i,j)^2 + T_w(i,j)^2\right] * FW(i,j) + \frac{1}{P} \tag{4.48}$$

As already noted, using partial derivative rule, the standard deviation σ_f is calculated as

$$\sigma_f = \left[\sum_{i=1}^{NV} \left[\frac{\partial \left(\sum_{i=1}^{NS-1} \sum_{j=1}^{Z(i)} \frac{\pi * m(i,j)^2 * \rho}{4} * \left[T_p(i,j)^2 + T_w(i,j)^2 \right] * FW(i,j) + \frac{1}{P} \right)}{\partial x_i} \right]^2_{x=\bar{x}} * \sigma_{x_i}^2 \right]^{\frac{1}{2}} \quad (4.49)$$

where NV is the total number of variables. The above expression can be rewritten as:

$$\sigma_f = \left\{ \sum_{i=1}^{NS-1} \sum_{j=1}^{Z(i)} \left[\left(\frac{\partial f}{\partial m(i,j)} \right)^2 * \sigma^2_{m(i,j)} \right] + \left[\left(\frac{\partial f}{\partial \rho} \right)^2 * \sigma_\rho^2 \right] + \sum_{i=1}^{NS-1} \sum_{j=1}^{Z(i)} \left[\left(\frac{\partial f}{\partial FW(i,j)} \right)^2 * \sigma^2_{FW(i,j)} \right] + \left[\left(\frac{\partial f}{\partial P} \right)^2 * \sigma_P^2 \right] \right\}^{\frac{1}{2}} \quad (4.50)$$

The following equations are formulated for each partial derivative term.

$$\sum_{i=1}^{NS-1} \sum_{j=1}^{Z(i)} \left[\left(\frac{\partial f}{\partial m(i,j)} \right)^2 * \sigma^2_{m(i,j)} \right] = \sum_{i=1}^{NS-1} \sum_{j=1}^{Z(i)} \left(\frac{\pi * \overline{m}(i,j) * \bar{\rho}}{2} * \left[T_p(i,j)^2 + T_w(i,j)^2 \right] * \overline{FW}(i,j) \right)^2 * \sigma^2_{m(i,j)}$$

$$\left[\left(\frac{\partial f}{\partial \rho} \right)^2 * \sigma_\rho^2 \right] = \left(\sum_{i=1}^{NS-1} \sum_{j=1}^{Z(i)} \frac{\pi * \overline{m}(i,j)^2}{4} * \left[T_p(i,j)^2 + T_w(i,j)^2 \right] * \overline{FW}(i,j) \right)^2 * \sigma_\rho^2$$

$$\sum_{i=1}^{NS-1} \sum_{j=1}^{Z(i)} \left[\left(\frac{\partial f}{\partial FW(i,j)} \right)^2 * \sigma^2_{FW(i,j)} \right] = \sum_{i=1}^{NS-1} \sum_{j=1}^{Z(i)} \left(\frac{\pi * \overline{m}(i,j)^2 * \bar{\rho}}{4} * \left[T_p(i,j)^2 + T_w(i,j)^2 \right] \right)^2 * \sigma^2_{FW(i,j)}$$

$$\left(\frac{\partial f}{\partial P} \right)^2 * \sigma_P^2 = \left(-\frac{1}{P^2} \right)^2 * \sigma_P^2$$

The probabilistic optimization of the present problem also contains a multi-objective nature where in two separate conflicting objective functions are involved. The minimum value of the linear combination that consists of the mean value and standard deviation is now sought:

minimize $\Phi(x) = k_1 * \bar{f} + k_2 * \sigma_f$ where k_1 and k_2 are weighting factors.

or equivalently

minimize $\Phi(x) = k_1 * \Phi_1(x) + k_2 * \Phi_2(x)$ (4.51)

The first objective function $\Phi_1(x)$ is written for the minimization of the mean value of the objective function f.

i.e. $$\Phi_1(x) = \bar{f}(x) \quad (4.52)$$

Substituting design vectors, $\Phi_1(x)$ becomes

$$\Phi_1(x) = \frac{\pi * \bar{m}(i,j)^2 * \bar{\rho}}{4} * \left[T_p(i,j)^2 + T_w(i,j)^2\right] * x(k) + \frac{1}{x(NG+1)} \quad (4.53)$$

The second objective function $\Phi_2(x)$ is written for the standard deviation of the deterministic objective function f. The function $\Phi_2(x)$ is obtained as the sum of four functions as shown below:

$$\Phi_2(x) = \Phi_2^{m(i,j)} + \Phi_2^{\rho} + \Phi_2^{FW(i,j)} + \Phi_2^{P} \quad (4.54)$$

where the superscripts denote respective independent variables.

Thus, $$\Phi_2^{m(i,j)} = \sum_{i=1}^{NS-1} \sum_{j=1}^{Z(i)} \left| \frac{\pi * \bar{m}(i,j) * \bar{\rho}}{2} * \left[T_p(i,j)^2 + T_w(i,j)^2\right] * x(k) \right|^2 * \sigma^2_{m(i,j)}$$

$$\Phi_2^{\rho} = \left(\sum_{i=1}^{NS-1} \sum_{j=1}^{Z(i)} \frac{\pi * \bar{m}(i,j)^2}{4} * \left[T_p(i,j)^2 + T_w(i,j)^2\right] * x(k) \right)^2 * \sigma^2_{\rho}$$

$$\Phi_2^{FW(i,j)} = \sum_{i=1}^{NS-1} \sum_{j=1}^{Z(i)} \left| \frac{\pi * \bar{m}(i,j)^2 * \bar{\rho}}{4} * \left[T_p(i,j)^2 + T_w(i,j)^2\right] \right|^2 * \sigma^2_{x(k)}$$

$$\Phi_2^{P} = \frac{1}{x(NG+1)^4} * \sigma^2_P$$

The probabilistic objective function now takes the following form:

$$\Phi(x) = k_1 * \Phi_1(x) + k_2 * \left(\Phi_2^{m(i,j)}(x) + \Phi_2^{\rho}(x) + \Phi_2^{FW(i,j)}(x) + \Phi_2^{P}(x) \right) \quad (4.55)$$

The constraints

For each spindle speed NG number of gear sets are engaged and so NG number of reliability constraints take the following form,

From equation (4.15), it can be shown that,

$$F_k = (Z_1)_k - Z_{10} \leq 0 \quad (4.56)$$

where F_k is the k^{th} inequality constraint. This general form is used to formulate the bending and wear stress constraints. Thus, NG number of bending stress constraints are formulated as shown below:

$$F_k^B = \frac{|\bar{S}_B - \bar{s}_{Bk}|}{\sqrt{\sigma_{S_B}^2 + \sigma_{s_{Bk}}^2}} - Z_{10} \leq 0 \quad k = 1 \cdots NG \qquad (4.57)$$

where $\bar{s}_{Bk}$ is the mean value for the bending stress of k^{th} constraint. From equation (4.19) the mean value of bending stress $\bar{s}_{Bk}$ is obtained as

$$\bar{s}_{Bk} = K_B * \frac{x(NG+1)}{\bar{m}^2(i,j) * \bar{V}_L(i,j) * x(k)} \qquad (4.58)$$

The standard deviation for the bending stress s_{BK} is calculated using partial derivative rule as,

$$\sigma_{s_{Bk}} = \left(\sigma_{s_{Bk}}^P + \sigma_{s_{Bk}}^{m(i,j)} + \sigma_{s_{Bk}}^{V_L(i,j)} + \sigma_{s_{Bk}}^{FW(i,j)}\right)^{\frac{1}{2}} \qquad (4.59)$$

where

$$\sigma_{s_{Bk}}^P = \left(\frac{\partial s_{Bk}}{\partial P}\right)^2 * \sigma_P^2 = \left(K_B^2 * \frac{1}{\bar{m}^4(i,j) * \bar{V}_L(i,j)^2 * x(k)^2}\right) * \sigma_{x(NG+1)}^2$$

$$\sigma_{s_{Bk}}^{m(i,j)} = \left(\frac{\partial s_{Bk}}{\partial m(i,j)}\right)^2 * \sigma_{m(i,j)}^2 = \left(4 * K_B^2 * \frac{x(NG+1)^2}{\bar{m}^6(i,j) * \bar{V}_L(i,j)^2 * x(k)^2}\right) * \sigma_{\bar{m}(i,j)}^2$$

$$\sigma_{s_{Bk}}^{V_L(i,j)} = \left(\frac{\partial s_{Bk}}{\partial V_L(i,j)}\right)^2 * \sigma_{V_L(i,j)}^2 = \left(K_B^2 * \frac{x(NG+1)^2}{\bar{m}^4(i,j) * \bar{V}_L(i,j)^4 * x(k)^2}\right) * \sigma_{\bar{V}_L(i,j)}^2$$

$$\sigma_{s_{Bk}}^{FW(i,j)} = \left(\frac{\partial s_{Bk}}{\partial FW(i,j)}\right)^2 * \sigma_{FW(i,j)}^2 = \left(K_B^2 * \frac{x(NG+1)^2}{\bar{m}^4(i,j) * \bar{V}_L(i,j)^2 * x(k)^4}\right) * \sigma_{x(k)}^2$$

Similarly, from equation (4.21), another set of NG number of inequality constrains for wear stress are obtained such as,

$$F_k^W = \frac{|\bar{S}_W - \bar{s}_{Wk}|}{\sqrt{\sigma_{W_B}^2 + \sigma_{s_{Wk}}^2}} - Z_{10} \leq 0 \qquad (4.60)$$

where F_k^W is the k^{th} inequality constraint. The mean value for the wear stress of k^{th} constraint is denoted by $\bar{s}_{Bk}$.

$$\bar{s}_{Wk} = \frac{K_W}{\bar{m}(i,j)} * \sqrt{\frac{x(\bar{NG}+1)}{x(k) * \bar{V}_L(i,j)}} \qquad (4.61)$$

The standard deviation for the wear stress s_{wK} is calculated using partial derivative rule, as

$$\sigma_{s_{Wk}} = \left(\sigma_{s_{Wk}}^{m(i,j)} + \sigma_{s_{Wk}}^{FW(i,j)} + \sigma_{s_{Wk}}^{P} + \sigma_{s_{Wk}}^{V_L(i,j)}\right)^{\frac{1}{2}} \qquad (4.62)$$

where

$$\sigma_{s_{Wk}}^{m(i,j)} = \left(\frac{\partial s_{Wk}}{\partial m(i,j)}\right)^2 * \sigma_{m(i,j)}^2 = \left(\frac{K_W^2}{\bar{m}(i,j)^4} * \frac{x(NG+1)}{x(k) * \bar{V}_L(i,j)}\right) * \sigma_{m(i,j}^2$$

$$\sigma_{s_{Wk}}^{FW(i,j)} = \left(\frac{\partial s_{Wk}}{\partial FW(i,j)}\right)^2 * \sigma_{FW(i,j)}^2 = \left(\frac{K_W^2}{4 * \bar{m}(i,j)^2} * \frac{x(NG+1)}{x(k)^3 * \bar{V}_L(i,j)}\right) * \sigma_{x(k)}^2$$

$$\sigma_{s_{Wk}}^{P} = \left(\frac{\partial s_{Wk}}{\partial P}\right)^2 * \sigma_P^2 = \left(\frac{K_W^2}{4 * \bar{m}(i,j)^2} * \frac{1}{x(NG+1) * x(k) * \bar{V}_L(i,j)}\right) * \sigma_{x(NG+1)}^2$$

$$\sigma_{s_{Wk}}^{V_L(i,j)} = \left(\frac{\partial s_{Wk}}{\partial V_L(i,j)}\right)^2 * \sigma_{V_L(i,j)}^2 = \left(\frac{K_W^2}{4 * \bar{m}(i,j)^2} * \frac{x(NG+1)}{x(k) * \bar{V}_L^3(i,j)}\right) * \sigma_{V_L(i,j}^2$$

4.5 Optimal design procedure

The optimal design space developed in this chapter uses a minimization procedure for both deterministic and probabilistic design that is shown in the previous sections. The kinematic parameters such as number of shafts NS, number of gears on each shafts, number of teeth on each gear and module are inputed. The bending and wear strength, allowable reliabiiity and the factors involved in various equations are assumed to be known data. The lower limit of integration in equation (4.19) is obtained from standard normal Table [19]. In the present computational scheme a separate subroutine is written for finding the Z_1. The generalized flowchart for both optimization procedures is shown in Figure 4.4. By assigning the objective function value at the local point as the goal for the next iteration, the global optimum is achieved. The numerical solution for this nonlinear

problem is implemented using the Penalty function along with Hook and Jeeves pattern search method. The interior penalty function method and search algorithm using Hooke and Jeeves method are described in Appendix C and section B.3 of Appendix B respectively. The computer code is capable of handling the variables in double precision.

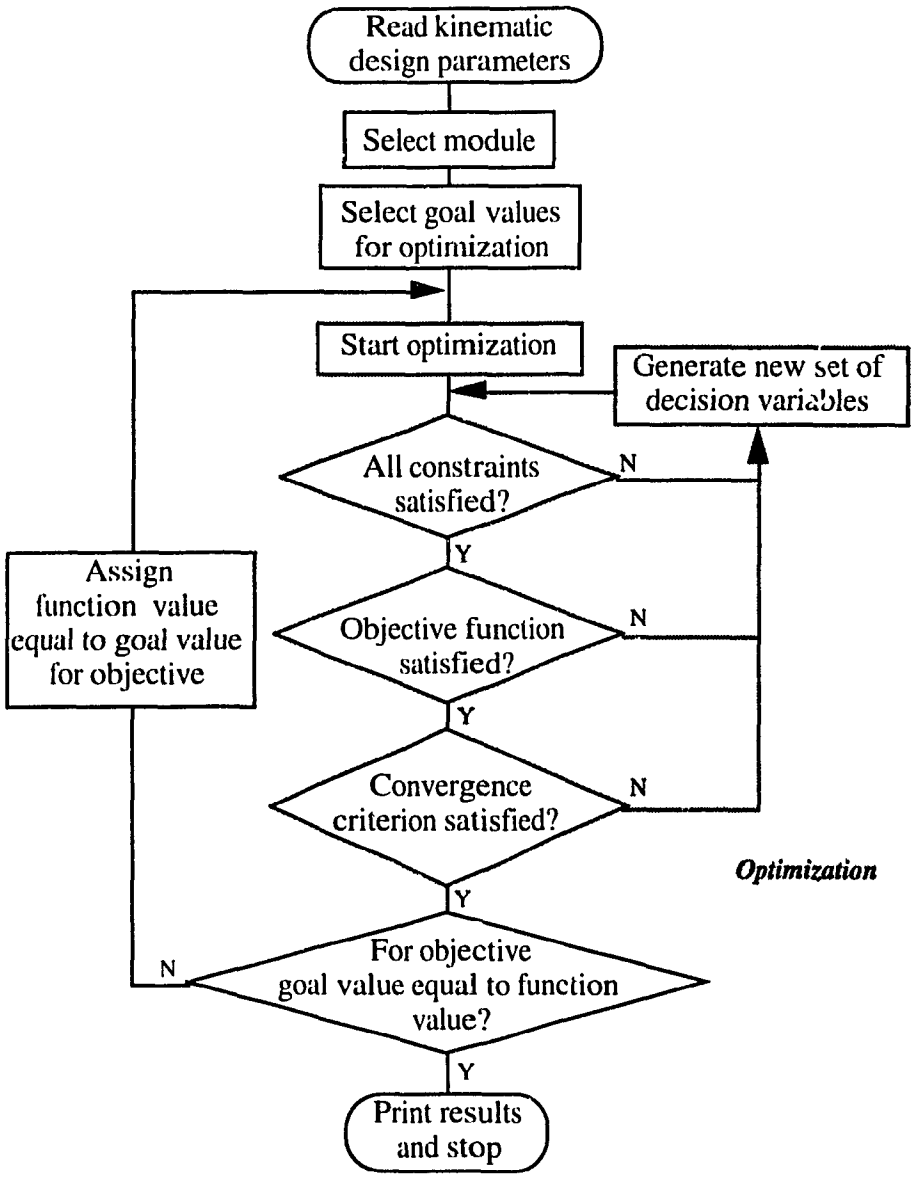

Figure 4.4 Flowchart for optimization procedure

4.6 Optimal design example

The kinematic design parameters from the optimal design of previous chapter is selected to demonstrate the effectiveness of the proposed method. In particular, the deterministic and probabilistic optimal designs are generated by using the optimal design procedure. The probabilistic study is conducted to find the effect of uncertainty of the selected module, that eventually can represent the variability on the random characteristics in the overall center distance. The mean module is taken as 0.305 cm as it is taken in previous chapter, yielding the mean of the overall center distance of the gear train equal to 34.9225 cm. Further more, the mean value of the rotational speed for each gear is calculated using the relevant gear ratios which are constant values. These values can be verified with Table 3.5 of the previous chapter. The mean of the input speed of the power source is 1400 rpm. The gear material with mean strength 25000 N/cm^2 for bending and 175000 N/cm^2 for wear is selected the density of which equal to 0.00775 kg/cm^3 [40]. Although the probabilistic characteristics of the random variables affecting the gear train performance need not to follow any particular rule, the coefficient of variation for transmitted power, facewidths, bending stress, wear stress, material density and rotational speeds are taken as 0.10, 0.01, 0.20, 0.20, 0.10 and 0.070 respectively.

C_m	Total mass (kg			Transmitted power (kw		
	Reliability					
	0.999	0.990	0.900	0.999	0.990	0.900
0.01	29.5855970	27.5019134	26.2813241	32.587109	36.297656	37.150391
0.02	29.5314187	27.2104898	26.0353371	32.748438	36.343750	37.334766
0.03	29.4032164	26.9604932	26.0558980	32.978906	36.735547	38.279688
0.04	29.5845000	26.6863878	25.3921200	33.716406	37.403906	38.602344
0.05	28.8969263	26.0756950	25.3261126	33.601172	37.910938	40.284766
0.06	28.9052415	25.6202884	24.6037499	34.453906	38.994141	41.414063
0.07	27.7196762	24.1250992	22.7635493	34.960938	40.054297	42.497266
0.08	27.6700750	24.1287483	22.6610269	35.099219	41.437109	44.433203
0.09	27.7593967	23.2910761	21.4785507	36.574219	43.096484	45.908203
0.10	25.9890698	21.3828154	19.7211958	36.942969	44.317969	47.751953

Table 4.1 Optimum total mass and transmitted power

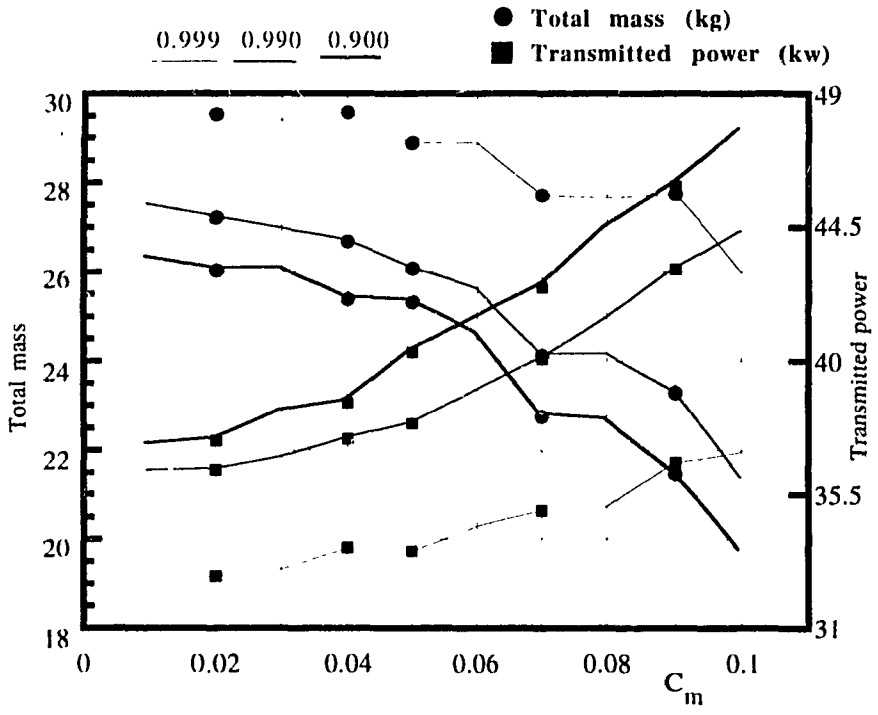

Figure 4.5 Optimum reliable region

Coefficient of variation for module = 0.10
Reliability = 0.900

Number of teeth		Face width (cm)	Center distance (cm)	Mass (kg)	
pinion	wheel			pinion	wheel
25	39	0.7078	9.7600	0.25058	0.60980
27	37	0.6437	9.7600	0.26583	0.49921
23	41	0.7820	9.7600	0.23432	7.4459
42	32	0.7695	11.2850	0.76887	0.44633
21	53	1.6495	11.2850	0.41205	2.62463
18	18	6.7579	5.4900	1.24028	1.24028
23	32	3.5571	8.3875	1.06591	2.06332
28	27	2.8450	8.3875	1.26346	1.17483
18	37	5.0228	8.3875	0.92184	3.89507
Total			34.9225	19.72120	
Transmitted power (kw) = 47.7520					

Table 4.2 The optimal values for the reliable design

Number of teeth		Face width (cm)	Mass (kg)	
pinion	wheel		pinion	wheel
25	30	0.8024	0.28409	0.69137
27	37	0.7295	0.30124	0.56570
23	41	0.8869	0.26577	0.84455
42	32	0.8727	0.87205	0.50622
21	53	1.8701	0.46716	2.97565
18	18	7.6453	1.40316	1.40316
23	32	4.0244	1.20594	2.33437
28	27	3.2185	1.42935	1.32907
18	37	5.6824	1.04290	4.40658
Total minimum mass			22.32834	
Transmitted power (kw)			15.0023	

Table 4.3 The optimal values for the deterministic design

The Table 4.1 lists the minimum total mass of gears and the maximum transmitted power obtained with reliabilities 0.900, 0.990 and 0.999 for different values of the coefficient of variation C_m with the selected module m equal to 0.305 mm. The results are plotted in Figure 4.5 clearly indicates the reliable region for the selection of the nominal transmitted power of the drive unit and the corresponding safer total mass of gears due to bending and wear. It also can be observed, that with increased reliability, the value for the minimized total mass of gears increases and the capability of maximum transmitted power decreases. It also confirms that as C_m decreases, the total mass of gears increases and the maximum transmitted power decreases. The results with 0.900 reliability and c_m equal to 0.10 are given as the optimal values for the selected gear train in Table 4.2. The optimal values that are obtained for the deterministic design for the same gear train are tabulated in Table 4..3.

4.7 Conclusion

A method has been developed and presented here for the synthesis of multi-speed gear trains using the probabilistic concept of reliability theory. The approach leads to the minimum mass and maximum transmitted power of the gear train and involves simultaneous incorporation of both kinematic requirements and component strength requirements. An output set of optimal values of gear train parameters like that of face width of all gears and transmitted power, has been obtained using an efficient problem reduction strategy. The kinematic design of a 18 speed gear train has been used to illustrate the full potentials of the present approach.

CHAPTER 5

Torsional vibration safety of gear trains

5.1 Introduction

The wider range of spindle speeds, that are to be provided as the output of a multi-speed gear train does necessitate the corresponding engagement patterns. As is known, the mesh position of the pinion and wheel dictates such engagement patterns. So, for particular spindle speed, a unique engagement pattern is to be realized through the mesh position of component gears. Figure 5.1 shows 18 different engagement patterns for a 18 speed 5 shaft gear train. It must be ensured in the design of any gear train that the required engagement patterns lead to safer operating conditions. Through the dependence of the natural frequency of the gear train, the distinct engagement patterns severely affect the dynamic behavior of the system. During start-up and shut-off operations of the motor, the gear train is subjected to accelerated and decelerated operating frequencies. Further, it is quite common and more advantageous to operate machine tool structures at frequencies well above the critical speeds. As the accelerated or decelerated frequencies determine the system natural frequencies, which in the present case is a spectrum of wide band, high amplitude vibrations. High stress levels develop due to buildup of oscillations. A potentially dangerous operating condition is made to occur. To avoid component failure in such circumstances, the design must provide not closely located sets of natural frequencies and operating speeds. However, it can easily be recognized that not all the kinematically distinct dynamic configurations that arise due to different engagement patterns, provide the same order of the natural frequency of the system. Identical dynamic configurations, identical with respect to the resulting natural frequency can always be seen as distinct pairs.

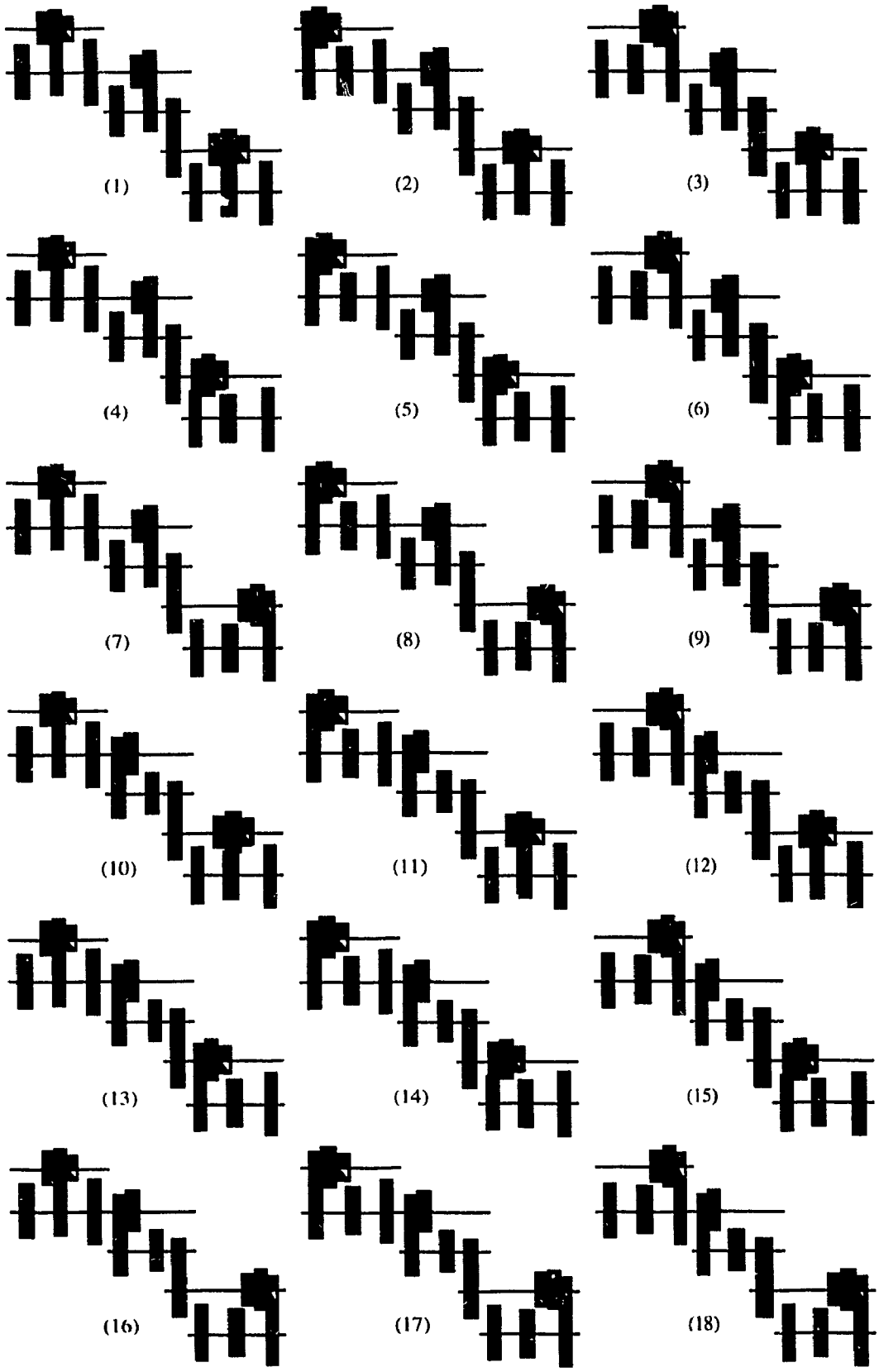

Figure 5.1 Engagement patterns of 18 = 3 * 2 * 1 * 3 gear train

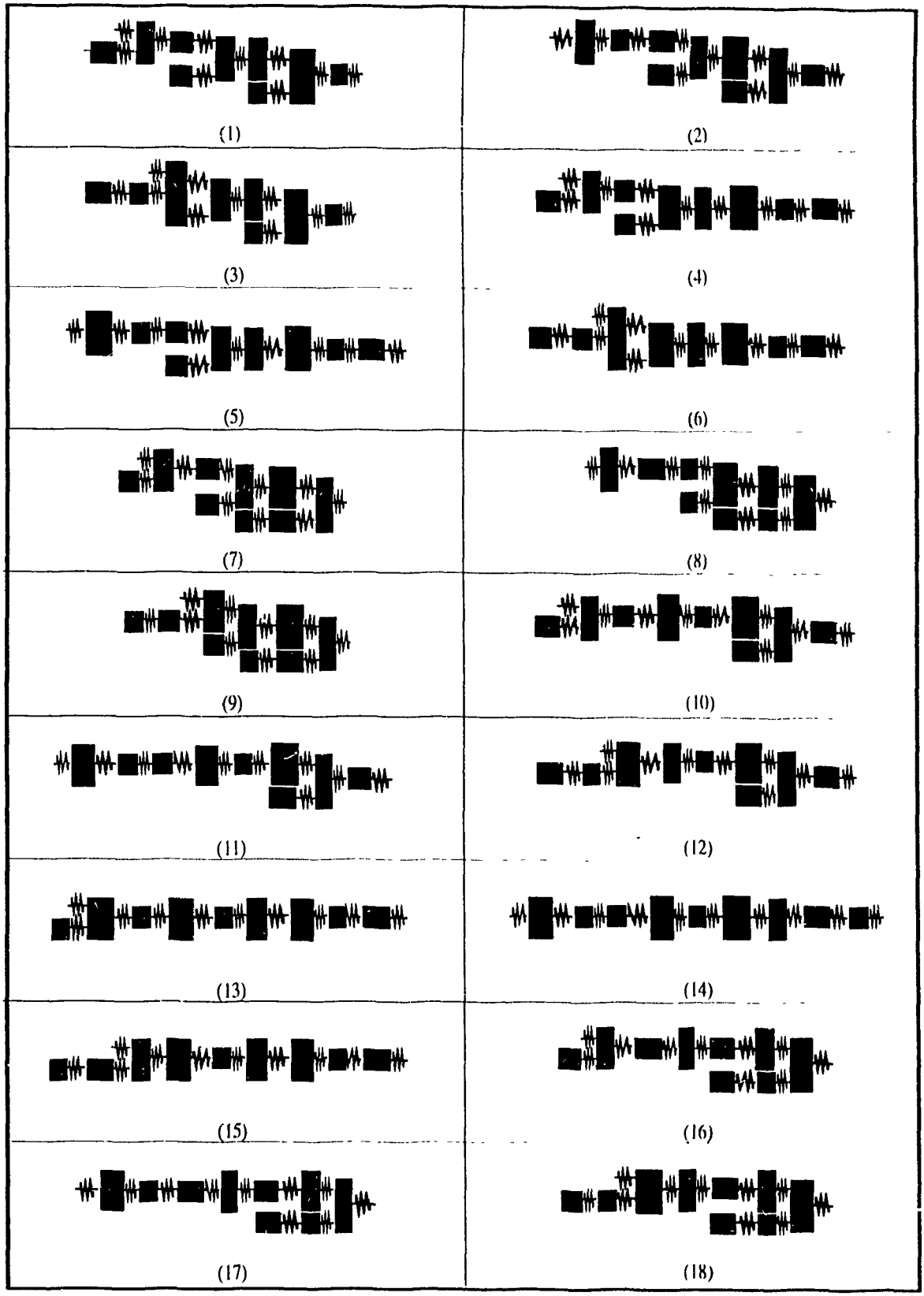

Figure 5.2 Dynamic configurations of 18 = 3 * 2 * 1 * 3 gear train

Available works on dynamic analysis and optimum design of gear trains deal with elementary case of multi-speed gear systems, wherein the consideration of one engagement pattern was involved [8, 9, 44]. The lateral vibration that stems from and within the system, is due to the excitation, of which is the dynamic load on gears. Such dynamic load is created by external factors like eccentric mounting of gears, the variation of tooth stiffness during engagement, changes in tooth profile due to elastic distortion under sustained loadings, errors in manufacture etc. [45]. Active control of lateral vibration can independently be achieved without a reanalysis. The torsional vibration is the most critical source of failure for a geared system. The characteristic of the inherent dynamic properties is seen from the entire torsional system of gear trains represented by the inertia, stiffness, and damping characteristics of the rotating components [18, 29, 36,47]. Massive multi-speed gear trains have not been analyzed in detail for their dynamic response in available literature. Moreover, the computational schemes that are currently in practice can be altered to take advantage of presence of identical dynamic configurations. So, when matrix methods are adopted to analyze the dynamic behavior of the system, this point can be exploited to provide computationally economical and faster methods of solutions. Such a computational scheme is developed in this chapter from first principles, and the optimum design based on torsional vibration aspects of multi-speed gear trains is carried out that essentially makes use of this computational scheme. The optimum design is to satisfy the condition of wider spacing between the operating speeds and the natural frequency of the overall gear train system. The design parameters of the 18 speed 5 shaft gear train obtained in the previous chapter, are considered herein for the optimal dynamic configuration. Keeping the mass of the gear train constant, this is achieved in principle, by minimizing the shaft stiffness. Each engagement pattern is represented by the transmission path index that takes on integer values between 1 and 18 in the computational scheme for the given gear train. Figure 5.2 shows all possible 18 distinct dynamic configurations corresponding to

Figure 5.1, along with their corresponding transmission path indices. All of these dynamic configurations are identified to formulate the design constraints.

5.2 Basic equations

5.2.1 Calculating the natural frequency

Gear train is seen as a complicated rotating system with many lumped parameters and torsional branches. With torques acting at different stations, the principle of super position can be applied to determine the angular displacements. In this respect matrix methods are ideally suited to express the system behavior. In most general form, matrix equations for a torsional vibratory system is expressed as:

$$[\mathcal{J}] * \{\ddot{\theta}\} + [C] * \{\dot{\theta}\} - [K] * \{\theta\} = \{T\} \qquad (5.1)$$

Where $[\mathcal{J}]$ - inertia matrix

$[K]$ - stiffness matrix

$[C]$ - damping matrix

θ - angular displacement

$\dot{\theta}$ - angular velocity

$\ddot{\theta}$ - angular acceleration

T - torque

Considering free undamped harmonic motions of frequency ω that are represented by the eigen problem obtained as follows:

$$[\mathcal{J}] * \{\ddot{\theta}\} - [K] * \{\theta\} = 0 \qquad (5.2)$$

$$[\mathcal{J}] * [K]^{-1} \{\ddot{\theta}\} - [I] * \{\theta\} = 0 \qquad [I] \text{ - unit matrix} \qquad (5.3)$$

$$[\mathcal{J}] * [\alpha] \{\ddot{\theta}\} - [I] * \{\theta\} = 0 \qquad [\alpha] = [K]^{-1} \qquad (5.4)$$

$$[\mathcal{A}] * \{\ddot{\theta}\} - [I] * \{\theta\} = 0 \qquad [\mathcal{A}] = [\mathcal{J}] * [\alpha] \qquad (5.5)$$

Assuming harmonic motion, the characteristic equation becomes

$$[\mathcal{A} - \lambda_i * I] * \{\theta\}_i = \{0\} \qquad (5.6)$$

where the eigen value λ_i is given by

$$\lambda_i = \frac{1}{\omega_i^2} \tag{5.7}$$

Thus, natural frequencies of the system is the square root of inverse of eigen value.

$$\omega_i = \sqrt{\frac{1}{\lambda_i}} \tag{5.8}$$

This term of standard eigen problem is computationally easier and more economical than the form of generalized eigen problem. It may be noted that, most of the numerical routines that operate on generalized eigen problems first convert them into the standard form to avoid numerical instability.

5.2.2 Branch geared system

The method of equivalent inertia and stiffness of branched torsional vibratory systems is followed to obtain time invariant magnitudes of dynamic parameters of linear lumped parameter system. The equations (5.1) to (5.6) are valid for single shaft system, where no speed changes are notified [52]. But in a multi-speed gear train the input speed is changed in various transmission stages. Hence, in writing equations of motion, the rotational speed changes are to be adopted in the equations. In order to do this, the concept of equivalent inertia and equivalent stiffness is introduced. The equivalent inertia and stiffness may replace the actual values in the equations (5.1) to (5.6) resulting a single shaft system.

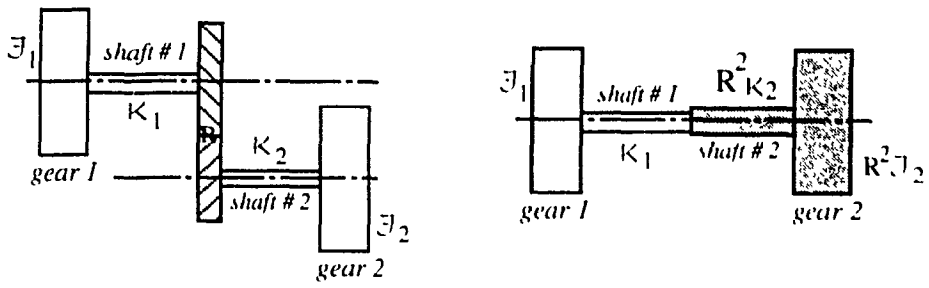

Figure 5.3 Branch and equivalent single shaft geared system

The Figure 5.3 illustrates a gear set, gear ratio of which is denoted by R. Consider that the gear 1 is rotated along with shaft #1 through an angle θ_1. This rotation θ_1 is changed by the gear ratio R which will make gear 2 and shaft # 2 to rotate through an angle θ_2. Thus, the angular speed $\dot{\theta}_2$ is given as:

$$\dot{\theta}_2 = R * \dot{\theta}_1 \tag{5.9}$$

Assume that inertia of the gear 1 and gear 2 are given as $\mathcal{J}_1$, $\mathcal{J}_2$ and stiffness of shaft #1 and shaft # 2 are given as K_1, K_2 respectively.

Kinetic energy KE of the system is given as:

$$KE = \frac{1}{2} * \mathcal{J}_1 * \dot{\theta}_1^2 + \frac{1}{2} * \mathcal{J}_2 * \dot{\theta}_2^2 \tag{5.10}$$

Using equation (5.9)

$$KE = \frac{1}{2} * \mathcal{J}_1 * \dot{\theta}_1^2 + \frac{1}{2} * \mathcal{J}_2 * R^2 * \dot{\theta}_1^2 \tag{5.11}$$

Thus,

$$KE = \frac{1}{2} * \mathcal{J}_1 * \dot{\theta}_1^2 + \frac{1}{2} * J_2 * \dot{\theta}_1^2 \tag{5.12}$$

The equivalent inertia J_2 for the gear 2 referred to shaft # 1 can be given as $R^2 * \mathcal{J}_2$. Knowing this, the rule for the equivalent inertia J can be set as multiplying all actual inertias $\mathcal{J}$ of gear system by the square value of corresponding gear ratio R.

$$J = R^2 * \mathcal{J} \tag{5.13}$$

In order to determine the equivalent stiffness of the geared system the potential energy PE can be considered.

$$PE = \frac{1}{2} * K_1 * \theta_1^2 + \frac{1}{2} * K_2 * \theta_2^2 \tag{5.14}$$

Using the equation (5.9),

$$PE = \frac{1}{2} * K_1 * \theta_1^2 + \frac{1}{2} * K_2 * R^2 * \theta_1^2 \tag{5.15}$$

Thus

$$PE = \frac{1}{2} * K_1 * \theta_1^2 + \frac{1}{2} * K_2 * \theta_1^2 \tag{5.16}$$

The value $R^2 * K_2$ can be viewed as equivalent stiffness K_2 for the shaft # 2 referred to shaft # 1. The rule for the equivalent stiffness K can also be set by multiplying all actual stiffness K of the system by the square value of corresponding gear ratio R.

$$K = R^2 * K \tag{5.17}$$

5.2.3 Dunkerley equation

Assume a gear train system is given by its equivalent inertia matrix [J] and equivalent stiffness matrix [K]. From the equation (5.6), the eigen solutions (λ_i, $\{\theta\}_i$), i = 1,2,.. r are orthonormal so that,

$$\{\theta_i\}^T * [J] * \{\theta_i\} = [I] \tag{5.18}$$

$$\{\theta_i\}^T * [K] * \{\theta_i\} = [\lambda_i] \tag{5.19}$$

where [λ_i] is the diagonal matrix with its leading diagonal elements (h,h) being a non-zero element and equal to λ_h.

Further, because of the orthonormal nature of eigenvectors, it can be shown that,

$$[A] = \sum_{h=1}^{r} \lambda_h * \{\theta\}_h * \{\theta\}_h^T \tag{5.20}$$

$$[A]^{-1} = \sum_{h=1}^{r} \frac{1}{\lambda_h} * \{\theta\}_h * \{\theta\}_h^T \tag{5.21}$$

Knowing equation (5.7),

$$[A]^{-1} = \sum_{h=1}^{r} \omega_h^2 * \{\theta\}_h * \{\theta\}_h^T \qquad (5.22)$$

The characteristic polynomial of degree r can now be generated from these equations as,

$$p(\lambda) = \det ([K] - \lambda * [J]) \qquad (5.23)$$

Now, the Dunkerley equation yields the lower bound to the fundamental frequency of the gear train system described by its characteristic equation as,

$$\begin{vmatrix} (a_{11}*J_1-\lambda) & a_{12}*J_1 & \cdots & a_{1\,r-1}*J_{r-1} & a_{1\,r}*J_r \\ a_{21}*J_1 & (a_{22}*J_2-\lambda) & \cdots & a_{2\,r-1}*J_{r-1} & a_{2\,r}*J_r \\ a_{31}*J_1 & a_{32}*J_3 & \cdots & a_{3\,r-1}*J_{r-1} & a_{3\,r}*J_r \\ \vdots & \vdots & & \vdots & \vdots \\ a_{r-2\,1}*J_1 & a_{r-2\,2}*J_2 & \cdots & a_{r-2\,r-1}*J_{r-1} & a_{r-2\,r}*J_r \\ a_{r-1\,1}*J_1 & a_{r-1\,2}*J_2 & \cdots & (a_{r-1\,r-1}*J_{r-1}-\lambda) & a_{r-1\,r}*J_r \\ a_{r\,1}*J_1 & a_{r\,2}*J_2 & \cdots & a_{r\,r-1}*J_{r-1} & (a_{r\,r}*J_r-\lambda) \end{vmatrix} = 0 \qquad (5.24)$$

Expanding this determinant equation it can be factored into the following form,

$$(\lambda - \lambda_1) * (\lambda - \lambda_2) * \ .... \ * (\lambda - \lambda_r) = 0 \qquad (5.25)$$

As is known in Algebraic theory, the coefficient of second highest power is equal to the sum of the roots of the characteristic equation. It is also equal to the trace of the matrix.

$$\lambda_1 + \lambda_2 + \cdots + \lambda_{r-1} + \lambda_r = a_{11} * J_1 + a_{22} * J_2 + \cdots a_{r-1\,r-1} * J_{r-1} + a_{r\,r} * J_r \qquad (5.26)$$

The above equation can be rewritten as:

$$\frac{1}{\omega_1^2} + \frac{1}{\omega_2^2} + \cdots + \frac{1}{\omega_{r-1}^2} + \frac{1}{\omega_r^2} = a_{11} * J_1 + a_{22} * J_2 + \cdots a_{r-1\,r-1} * J_{r-1} + a_{r\,r} * J_r \qquad (5.27)$$

If ω_1 is the fundamental frequency then,

$$\frac{1}{\omega_1^2} \leq a_{11} * J_1 + a_{22} * J_2 + \cdots a_{r-1\,r-1} * J_{r-1} + a_{r\,r} * J_r \qquad (5.28)$$

$$\omega_1 \geq \sqrt{\frac{1}{a_{11} * J_1 + a_{22} * J_2 + \cdots a_{r-1\,r-1} * J_{r-1} + a_{r\,r} * J_r}} \qquad (5.29)$$

t.c. $$\omega_1 \geq DV \qquad (5.30)$$

The value DV can be said as lower bound value for the fundamental frequency. The actual value of fundamental frequency is higher than the value DV.

5.3 Modeling

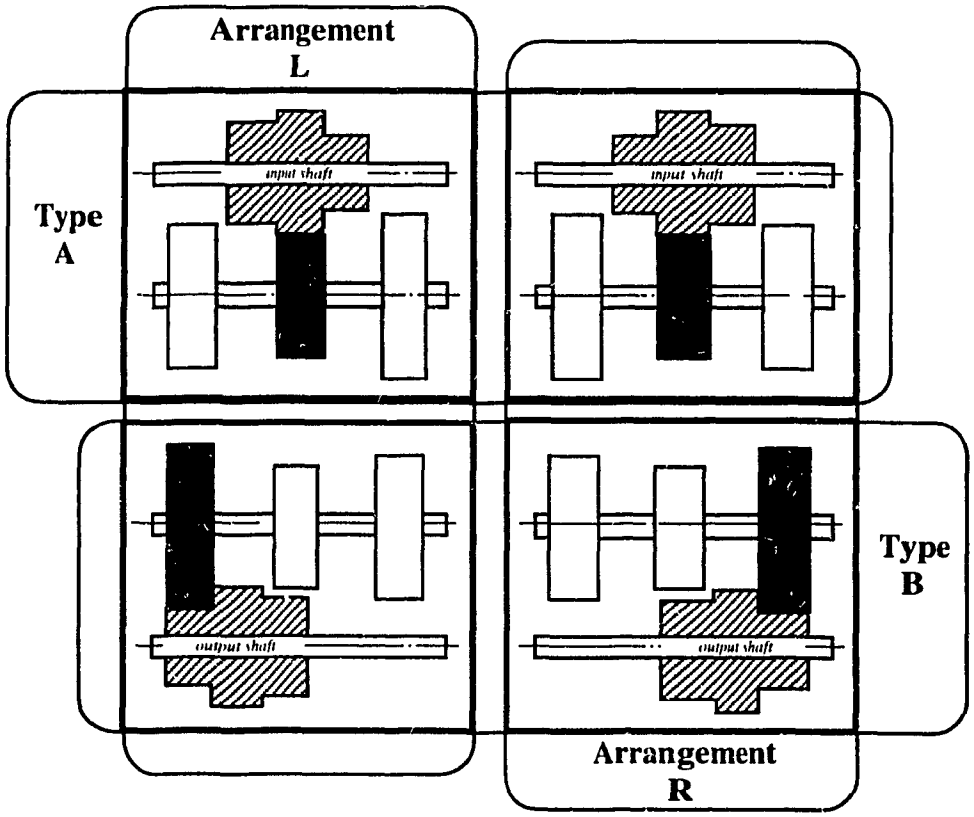

Figure 5.4 Possible ways for locating the gears and clusters

It is obvious that for any transmission path index, the dynamic configuration due to that particular engagement pattern decides the inertial distribution and the physical location of gears on the shafts for the same engagement pattern determines the compliance distribution. The way with which such influences take place is now described. The numerical encoding using alpha-numeric characters for a cluster mechanism contains three gear sets and the physical location of the gears are also thereby illustrated.

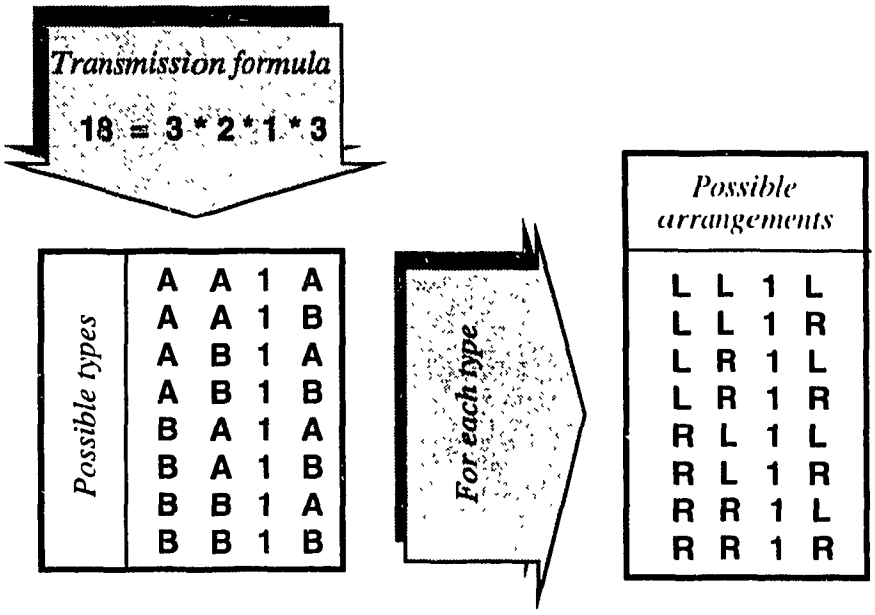

Figure 5.5 Alpha-numeric characters for locating gears and clusters

For a particular engagement pattern, different ways of locating the gears on the shafts are possible, which will not alter the spindle speed but are deemed to affect the inertial distribution of the overall gear train system. Four possible ways of locating the gears and clusters in a transmission stage are shown in Figure 5.4, viz. Type A, Type B, Arrangement R and Arrangement L. The arrangement arising, when the gear set with largest gear ratio is located on the left side of the gear set with lowest gear ratio is identified as 'Arrangement L' and that arising when the gear set with largest gear ratio is located on the right side of the gear set with lowest gear ratio is 'Arrangement R'. When the cluster is

located on the input shaft, 'Type A' results and 'Type B' results when it is on the output shaft. Figure 5.5 also gives all such combinations and corresponding representation within the computational scheme is also shown that is obtaining proper selection after permuting the alpha-numeric characters. Clubbing together all there with 18 such configurations that are shown as in Figure 5.2, 1152 possible dynamic configurations of the system are generated for a 18 = 3*2*1*3 gear train.

5.4 Calculation of system matrices

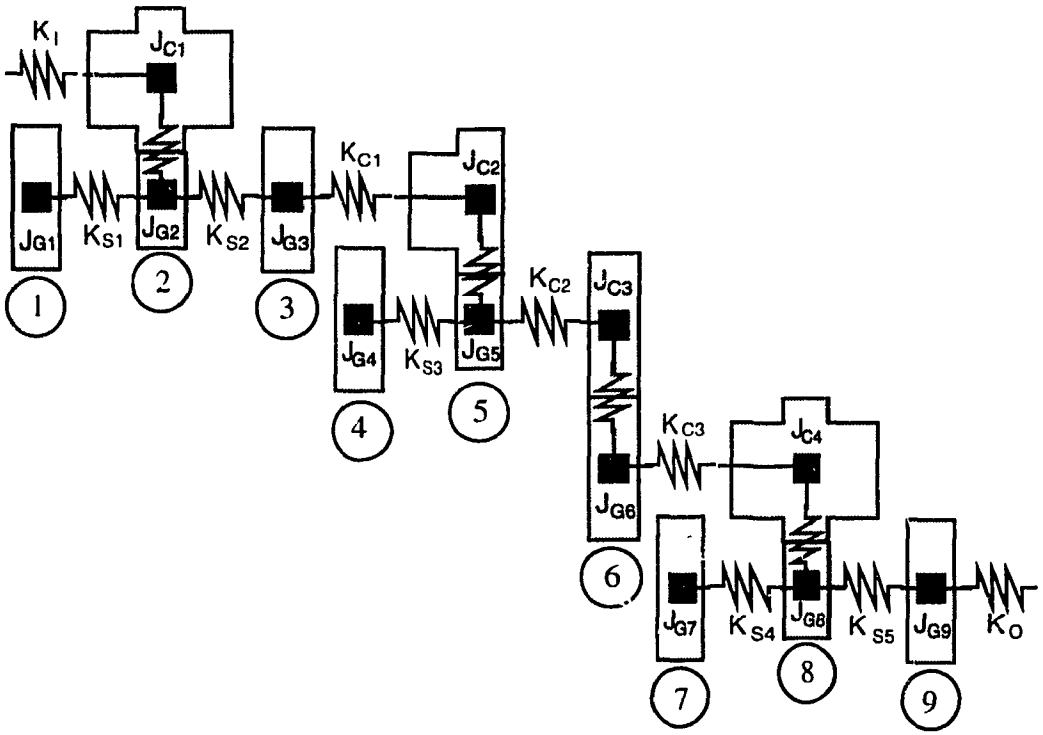

Figure 5.6 Lumped parameter model of a 18 = 3*2*1*3; type A A 1 A gear train

The mathematical model that eventually captures all the dynamic characteristics of this physical mechanical system is obtained following the scheme of lumped parameter modeling. The gear train is now represented as a torsional vibratory system with many nodal concentrations of lumped parameters. Inertial concentrations are treated to act in pre-

selected number of nodes and the compliance of the entire system is represented through the stiffness of the springs that couples the inertial concentrations.

The Figure 5.6 shows inertia / stiffness diagram for a 18 = 3*2*1*3 gear train where gear engagement pattern is to produce the largest spindle speed. For simplicity, all transmission stages are assumed to be 'Type A', where each cluster, as in the Figure 5.6, is a single unit with two or three component gears mounted in the input shaft of the corresponding transmission stage. The component gears in a cluster are fasten together as mechanically coupled rigid body. Since the stiffness between coupled gears are neglected and the gears have the same rotational axis, inertia of the cluster is equal to the sum of individual component gear inertias [45].

Consideration of single shaft dynamic equivalent system yields (i) equivalent torsional inertia of clusters and wheels and (ii) equivalent stiffness of shafts. The nodes for the proposed gear train are indexed from 1 to 9. The equivalent inertia for clusters in transmission stage 1, 2, 4 are denoted by J_{C1}, J_{C2} and J_{C4} respectively. The equivalent pinion inertia in the 3rd transmission stage is denoted as J_{C3}. The equivalent coupling stiffness K_{C1}, K_{C2} and K_{C3} are assumed between transmission stages. The equivalent stiffness of the input shaft in the 1st transmission stage and equivalent stiffness of the output shaft in the 4th transmission stage are given as K_I and K_O respectively. The equivalent stiffness between wheels mounted on output shafts K_{S1}, K_{S2}, K_{S3}, K_{S4} and K_{S5} are found accordingly. Considering the particular arrangement of location of gears, the equivalent inertia of any cluster and the equivalent stiffness of the elastic spring that couples this cluster with its neighbor cluster can be written in terms of R(i,j), which is the quotient obtained from $T_p(i,j)$ and $T_w(i,j)$. Here, $T_p(i,j)$ and $T_w(i,j)$ are number of pinion and wheel teeth corresponding to the i^{th} transmission stage of the j^{th} gear set and thus R(i,j) is the gear ratio.

Further, referring the equation (5.13) and equation (5.17):

(A) Equivalent inertia

1st transmission stage:

$$J_{G1} = J_{G1} * (R(1,1))^2$$

$$J_{G2} = J_{G2} * (R(1,1))^2$$

$$J_{G3} = J_{G3} * (R(1,1))^2$$

$$J_{C1} = J_{C1}$$

2nd transmission stage:

$$J_{G4} = J_{G4} * (R(1,1))^2 * (R(2,1))^2$$

$$J_{G5} = J_{G5} * (R(1,1))^2 * (R(2,1))^2$$

$$J_{C2} = J_{C2} * (R(1,1))^2$$

3rd transmission stage:

$$J_{G6} = J_{G6} * (R(1,1))^2 * (R(2,1))^2 * (R(3,1))^2$$

$$J_{C3} = J_{C3} * (R(1,1))^2 * (R(2,1))^2$$

4th transmission stage:

$$J_{G7} = J_{G7} * (R(1,1))^2 * (R(2,1))^2 * (R(3,1))^2 * (R(4,1))^2$$

$$J_{G8} = J_{G8} * (R(1,1))^2 * (R(2,1))^2 * (R(3,1))^2 * (R(4,1))^2$$

$$J_{G9} = J_{G9} * (R(1,1))^2 * (R(2,1))^2 * (R(3,1))^2 * (R(4,1))^2$$

$$J_{C4} = J_{C4} * (R(1,2))^2 * (R(2,1))^2 * (R(3,1))^2$$

(B) Equivalent stiffness

$$K_I = K_I$$

$$K_{S1} = K_{S1} * (R(1,1))^2$$

$$K_{S2} = K_{S2} * (R(1,1))^2$$

$$K_{C1} = K_{C1} * (R(1,1))^2$$

$$K_{S3} = K_{S3} * (R(1,1))^2 * (R(2,1))^2$$

$$K_{C2} = K_{C2} * (R(1,1))^2 * (R(2,1))^2$$

$$K_{C3} = K_{C3} * (R(1,1))^2 * (R(2,1))^2 * (R(3,1))^2$$

$$K_{S4} = K_{S4} * (R(1,1))^2 * (R(2,1))^2 * (R(3,1))^2 * (R(4,1))^2$$

$$K_{S5} = K_{S5} * (R(1,1))^2 * (R(2,1))^2 * (R(3,1))^2 * (R(4,1))^2$$

$$K_O = K_O * (R(1,1))^2 * (R(2,1))^2 * (R(3,1))^2 * (R(4,1))^2$$

Stiffness between two mating gear teeth is in nonlinear form and depends on various factors. To ease the modeling, it is treated as infinitely stiffness. When this assumption is made, inertia of two rotating elements - i.e. cluster and mating wheel - will act as one inertia element [28]. The equivalent dynamic system for the engagement pattern of the kinematic arrangement shown in Figure 5.6, is shown in Figure 5.7.

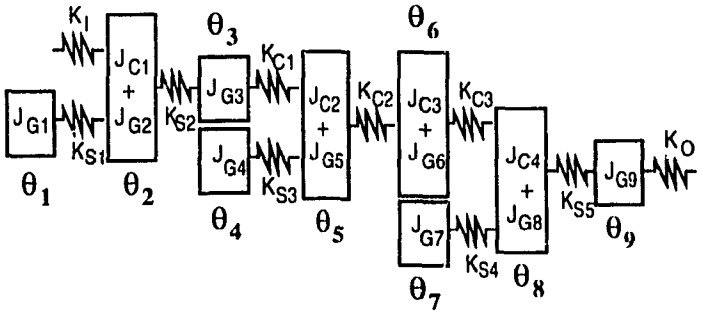

Figure 5.7 Equivalent dynamic system

Now, consideration of the dynamic equilibrium based on the energy balance of any rotational degree of freedom leads to the equation of motion of that corresponding node.

1. $J_{G1}*\ddot{\theta}_1^2 + K_{S1}*(\theta_1 - \theta_2) = 0$ (5.31)
2. $(J_{C1}+J_{G2})*\ddot{\theta}_2^2 + K_I*\theta_2 + K_{S1}*(\theta_2 - \theta_1) + K_{S2}*(\theta_2 - \theta_3) = 0$ (5.32)
3. $J_{G3}*\ddot{\theta}_3^2 + K_{S2}*(\theta_3 - \theta_2) + K_{C1}*(\theta_3 - \theta_5) = 0$ (5.33)
4. $J_{G4}*\ddot{\theta}_4^2 + K_{S3}*(\theta_4 - \theta_5) = 0$ (5.34)
5. $(J_{C2}+J_{G5})*\ddot{\theta}_5^2 + K_{S3}*(\theta_5 - \theta_4) + K_{C1}*(\theta_5 - \theta_3) + K_{C2}*(\theta_5 - \theta_6) = 0$ (5.35)

6. $J_{C3}*\ddot{\theta}_6^2 + K_{C2}*(\theta_6 - \theta_5) + K_{C3}*(\theta_6 - \theta_8) = 0$ (5.36)

7. $J_{G7}*\ddot{\theta}_7^2 + K_{S4}*(\theta_7 - \theta_8) = 0$ (5.37)

8. $(J_{C4}+J_{G8})*\ddot{\theta}_8^2 + K_{S4}*(\theta_8 - \theta_7) + K_{C3}*(\theta_8 - \theta_6) + K_{S5}*(\theta_8 - \theta_9) = 0$ (5.38)

9. $J_{G9}*\ddot{\theta}_9^2 + K_{S5}*(\theta_9 - \theta_8) + K_O*\theta_9 = 0$ (5.39)

A vector of all nodal torsional degree of freedom in sequence can be formed as the column vector $\{\theta\}$. Now, the equation of motion of the overall system for the selected transmission path is given by matrix equation shown as in equations (5.40) and (5.41).

$$|J|_n = \begin{bmatrix} J_{G1} & 0 & 0 & & & & & & \\ 0 & J_{C1}+J_{G2} & 0 & & & & & & \\ 0 & 0 & J_{G3} & & & & & & \\ & & & J_{G4} & 0 & & & & \\ & & & 0 & J_{C2}+J_{G5} & & & & \\ & & & & & J_{C3}+J_{G6} & & & \\ & & & & & & J_{G7} & 0 & 0 \\ & & & & & & 0 & J_{C4}+J_{G8} & 0 \\ & & & & & & 0 & 0 & J_{G9} \end{bmatrix}_N \quad (5.40)$$

$$|K|_n = \begin{bmatrix} K_{S1} & -K_{S1} & 0 & & & & & & \\ -K_{S1} & K_1+K_{S1}+K_{S2} & -K_{S2} & & & & & & \\ 0 & -K_{S2} & K_{S2}+K_{C1} & 0 & -K_{C1} & & & & \\ & & 0 & K_{S3} & -K_{S3} & & & & \\ & & -K_{C1} & -K_{S3} & K_{C1}+K_{S3}+K_{C2} & -K_{C2} & & & \\ & & & & -K_{C2} & K_{C2}+K_{C3} & 0 & -K_{C3} & \\ & & & & & 0 & K_{S4} & -K_{S4} & 0 \\ & & & & & -K_{C3} & -K_{S4} & K_{C3}+K_{S4}+K_{S5} & -K_{S5} \\ & & & & & & 0 & -K_{S5} & K_{S5}+K_O \end{bmatrix}_N \quad (5.41)$$

The $[\ J\ ]_n$ and $[\ K\ ]_n$ are the inertia and stiffness matrices of the dynamic configuration of the n^{th} engagement pattern, where the subscript 'n' denotes the transmission path index. There are N number of different dynamic configurations that are possible for a gear train with N spindle speeds. The inertia and stiffness matrices shown in equations (5.40) and (5.41) are derived only for the N^{th} transmission path, engagement pattern of which is shown in Figure 5.6. In order to obtain the matrices for other spindle speeds, as another set of engagement patterns, associated equations of motions are also to be evaluated.

The matrices$[\ J\ ]_n$ and $[\ K\ ]_n$ can be partitioned into L number of submatricess, where each submatrix may be associated with a transmission stage of the gear train. In other words, L number of submatricess may be formulated and assembled to create matrices$[\ J\ ]_n$ and $[\ K\ ]_n$. Each submatrix that essentially consists of (i) one cluster and (ii) two or three gears as the case may be, is viewed as an individual dynamic sub-system of overall system. The increased order of the diagonal terms are preferred to be assigned for increasing number of transmission stages. The last column and row of each submatrix, except for the L^{th} submatix, contain the coupling terms. For each spindle speed, resulted vibration system is established from coupled sub-systems. Changing to different spindle speeds is directly viewed as change in the sub-system according to the engagement position of the pinion and wheel.

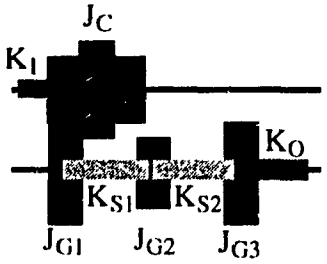

p(i) = 1

J_C+J_{G1}	0	0
0	J_{G2}	0
0	0	J_{G3}

$K_I + K_{S1}$	$-K_{S1}$	0
$-K_{S1}$	$K_{S1} + K_{S2}$	$-K_{S2}$
0	$-K_{S2}$	$K_{S2} + K_O$

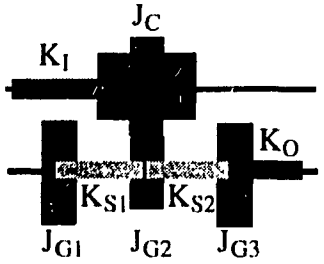

p(i) = 2

J_{G1}	0	0
0	J_C+J_{G2}	0
0	0	J_{G3}

K_{S1}	$-K_{S1}$	0
$-K_{S1}$	$K_I + K_{S1} + K_{S2}$	$-K_{S2}$
0	$-K_{S2}$	$K_{S2} + K_O$

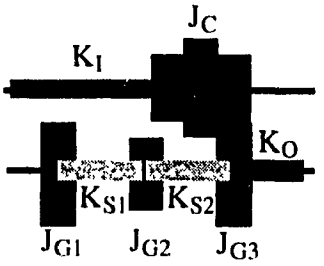

p(i) = 3

J_{G1}	0	0
0	J_{G2}	0
0	0	J_C+J_{G3}

K_{S1}	$-K_{S1}$	0
$-K_{S1}$	$K_{S1} + K_{S2}$	$-K_{S2}$
0	$-K_{S2}$	$K_I + K_{S2} + K_O$

Z(i) = 3

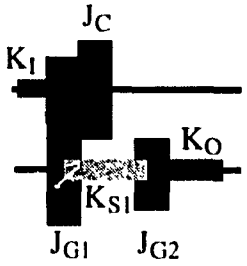

p(i) = 1

J_C+J_{G1}	0
0	J_{G2}

$K_I + K_{S1}$	$-K_{S1}$
$-K_{S1}$	$K_{S1} + K_O$

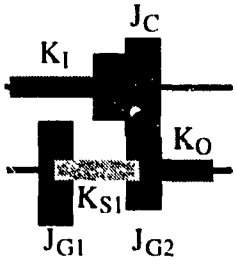

p(i) = 2

J_{G1}	0
0	J_C+J_{G2}

K_{S1}	$-K_{S1}$
$-K_{S1}$	$K_I + K_{S1} + K_O$

Z(i) = 2

Figure 5.8 The pinion/gear engagement positions and their submatrices for Z(i) = 3

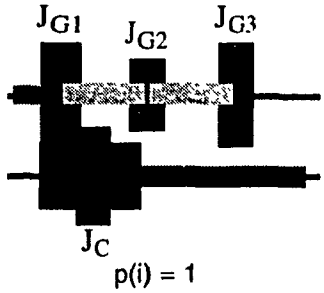

p(i) = 1

J_C+J_{G1}	0	0
0	J_{G2}	0
0	0	J_{G3}

$K_I + K_{S1} + K_O$	$-K_{S1}$	0
$-K_{S1}$	$K_{S1} + K_{S2}$	$-K_{S2}$
0	$-K_{S2}$	K_{S2}

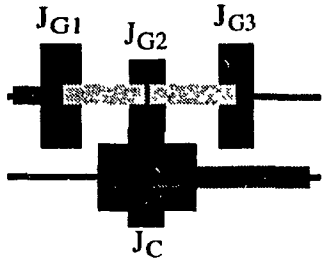

p(i) = 2

J_{G1}	0	0
0	J_C+J_{G2}	0
0	0	J_{G3}

$K_I + K_{S1}$	$-K_{S1}$	0
$-K_{S1}$	$K_{S1} + K_{S2} + K_O$	$-K_{S1}$
0	$-K_{S2}$	K_{S2}

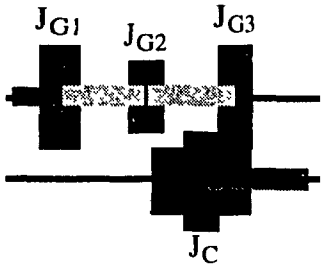

p(i) = 3

J_{G1}	0	0
0	J_{G2}	0
0	0	J_C+J_{G3}

$K_I + K_{S1}$	$-K_{S1}$	0
$-K_{S1}$	$K_{S1} + K_{S2}$	$-K_{S2}$
0	$-K_{S2}$	$K_{S2} + K_O$

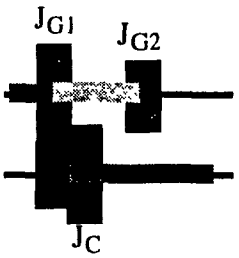

p(i) = 1

J_C+J_{G1}	0
0	J_{G2}

$K_I + K_{S1} + K_O$	$-K_{S1}$
$-K_{S1}$	K_{S1}

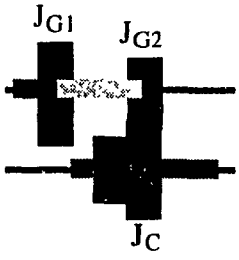

p(i) = 2

J_{G1}	0
0	J_C+J_{G2}

$K_I + K_{S1}$	$-K_{S1}$
$-K_{S1}$	$K_{S1} + K_O$

Figure 5.9 The pinion/gear engagement positions and their submatrices for $Z(i) = 2$

Following the scheme detailed in the previous paragraphs, the submatrices of inertia and stiffness that correspond to the vector of torsional d.o.f. pertinent to each sub-system are identical as shown in Figures 5.8 and 5.9. Each is thus a open loop configuration. The corresponding matrices of particular gear set are identified by the parameter set (Z(i), p(i)) where Z(i) is the number of gears of the i^{th} transmission stage, and 'p' is the index assigned to identify the location of mating gear sets ($1 \leq p \leq 3$). The overall inertia and stiffness matrices are first formed as square matrices of order equal to the unrestrained torsional d.o.f. of the entire gear train. They are initialized using zero elements. Then, each sub-system is considered in sequence and the following rule is used to post the corresponding submatrices into their overall system counterparts. For i^{th} transmission stage with Z(i) gear set,

(i) Submatrices are square matrices of order Z(i) * Z(i)

(ii) Sub matrices are arranged to be posted diagonally along the leading diagonal.

(iii) Off-diagonal terms that arise due to coupling stiffnesses are posted as follows; depending on the arrangement patterns:

$(i+1)^{th}$ transmission state of Type A:

(b + Z(i) - 1 + p(i+1) th row, (a + Z(i)-1) th column

(b + Z(i)-1) th row, (a + Z(i) - 1 + p(i+1) th column

$(i+1)^{th}$ transmission state of Type B:

(b + Z(i)) th row, (a + Z(i) - 1) th column

(b + Z(i) - 1) th row, (a + Z(i)) th column

where b = Z(1) + Z(2) + ... + Z(i-1)

5.5 Formulation of the optimal design

A torsional dynamic system with smaller inertia or larger stiffness will have larger natural frequency. For a specified inertial distribution of a gear train system, the shaft stiffness may be increased theoretically upto infinity for dynamically safer design. Since

the upper bound values for shaft stiffness are set to infinity, the lower bound values may be obtained by optimizing the stiffness distribution. The NV number of design variables, which are denoted by x(k) where k is 1 to NV, are assigned to each stiffness between two lumped inertias.

The problem for the optimal design of a gear train is thus stated as follows:

(1) Given inertia of the lumped parameters

(2) find lower bound for shaft stiffness in the design region

(3) satisfy the condition that the fundamental natural frequency of the torsional system is driven away from any of its operating speeds.

The objective function

The objective function is now formulated taking into account the net value of the individual shaft stiffnesses. The objective function is expected to take the following mathematical form:

$$\Phi(x) = \sum_{k=1}^{NV} x(k) - K_{int} \qquad (5.42)$$

Where the K_{int} is a maximum permissible value for the net value of the shaft stiffness specified by the designer. The net value of the optimized shaft stiffness will be smaller than K_{int}.

The constraints

Two types of constraints, one to take into account the resonance and another to take into account the realizability of the shafts that yield the optimized stiffness are possible. The first type is applied for all N number of Dunkerley values. The Dunkerley values are to be kept larger than maximum rotational speed frequency encountered anywhere in the corresponding transmission path.

$$F_n(x) = SF(n) - DV(n) \leq 0 \qquad n = 1,2,..., N \qquad (5.43)$$

The DV(k) is the Dunkerley value which corresponds to the n^{th} spindle speed. The SF(n) is the largest speed frequency obtained anywhere along the n^{th} transmission path that produces the n^{th} spindle speed. The largest speed frequency is not necessarily be obtained from the spindle speeds. Depending on the layout diagram, it may be possible to select the largest speed frequency value from the intermediate shaft speeds.

Other type of the constraints is derived to include the upper and lower limits of the shaft stiffnesses. If NV number of design variables are selected, then 2*NV number of inequality constraints are to be implemented to find the design variables within the realizable range.

Constraints for the minimum and maximum stiffness values are given as

$$F_k(x) = K_{min}(k) - x(k) \leq 0 \qquad k = 1 \text{ to NV} \qquad (5.44)$$

$$F_k(x) = x(k) - K_{max}(k) \leq 0 \qquad k = 1 \text{ to NV} \qquad (5.45)$$

where the $K_{min}(k)$ and $K_{max}(k)$ are the minimum and maximum bounding stiffness values for k^{th} design variable respectively.

5.6 Optimal design procedure

Depending upon the case of transmission formula, the number of design variables and size of each submatrices are decided. Since NG number of pinion/wheel engagements are noted in the gear train, total NG number of equivalent inertia submatrices and NG number of equivalent stiffness submatrices are being created. The optimization procedure requires N number of constrains for Dunkerley values. To perform this task, each time a set of L number of relevant submatrices are selected from the NG number of submatrices, based on the engagement pattern of the required n^{th} transmission path. Then, the computational scheme automatically places the selected L number of submatrices diagonally and couples with K_C in order to form the equivalent stiffness $[K]_n$ matrix. Similarly

equivalent inertia [J]$_n$ is also created. Using these system matrices, all Dunkerley values, which are the constraints for the entire optimization procedure are established.

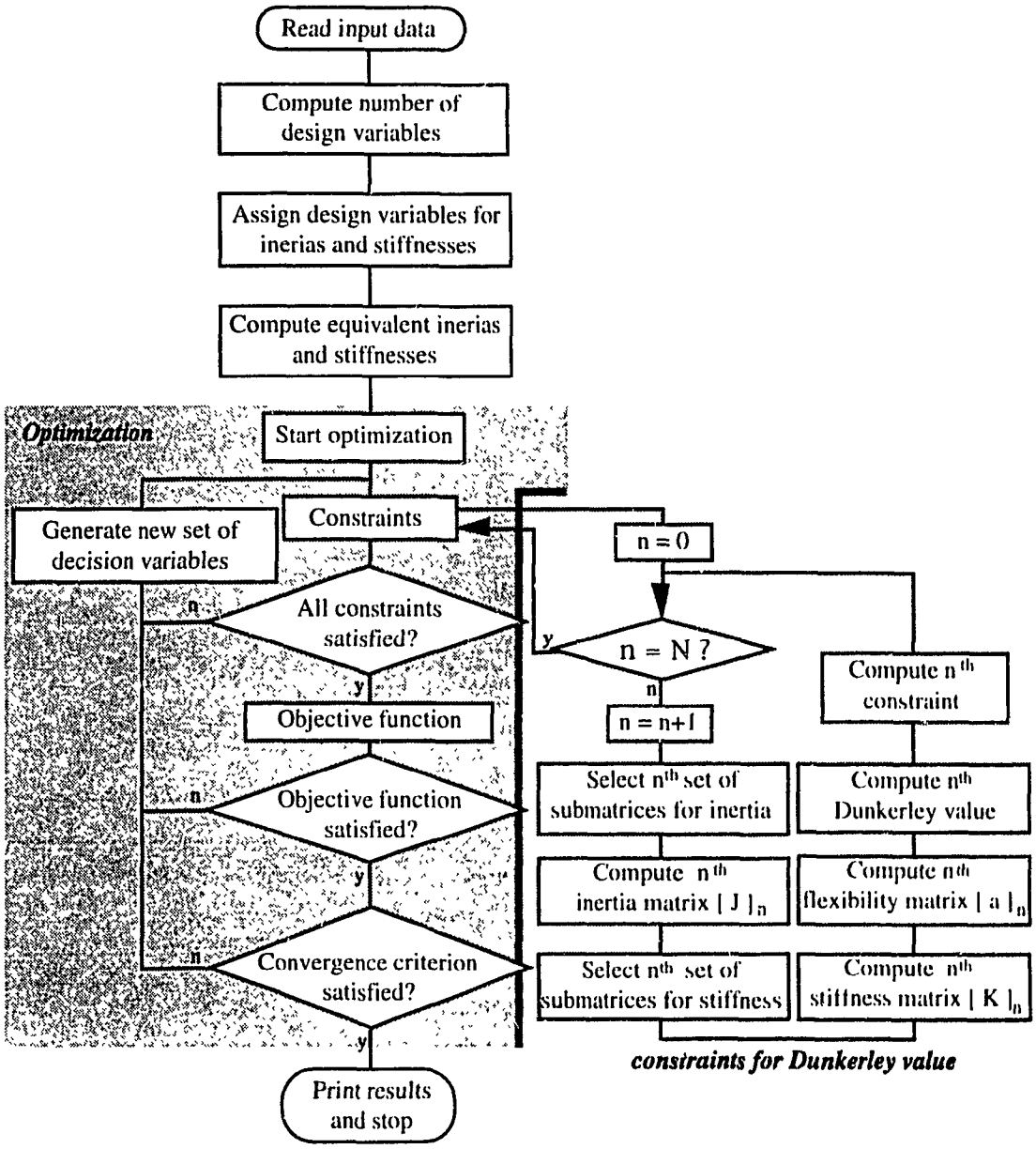

Figure 5.10 Flowchart for satisfying Dunkerley values

The computational scheme makes use of the submatrices that are generated for each transmission stage individually. This leads to avoiding the repeated storage and numerical

instability that arise during computation. So when a particular transmission stage is considered, its sub-system matrices are generated and immediately posted as nonzero elements of already initialized overall system matrices. Then the same memory locations used for these overall system matrices are used for the next set of sub-systems by overwriting.

5.6.1 Number of design variables

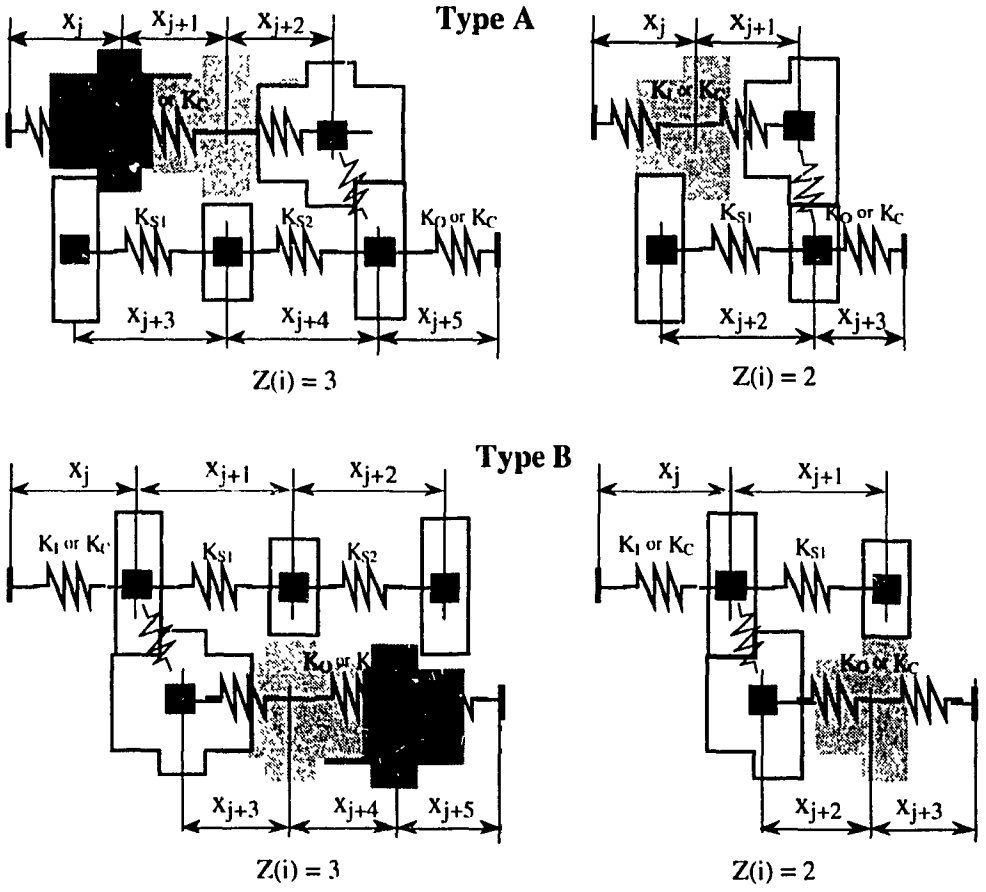

Figure 5.11 Assigning the design variables

If K is sum of l number of individual stiffness x_1, x_2 ...x_{j-1}, x_j... x_{l-1} and x_l connected in series, then the K is calculated as

$$\frac{1}{K} = \sum_{j=1}^{l} \frac{1}{x_j} \qquad (5.46)$$

The rule for assigning the design variables is shown Figure 5.11. The number of design variables depend on the transmission formula and the type of consecutive transmission stages. Total number of design variables NV is the sum of the individual number of design variables for K_I, K_S, K_C, and K_O.

(i) Number of design variables for the input shaft stiffness K_I

Although, each submatrix contains its input shaft stiffness, the computational scheme assigns K_I to the 1st transmission stage. For all other transmission stages, the K_I is changed to coupling stiffness K_C. The number of design variables for K_I is given as:

Type A and Z(i) = 2 ... Number of design variables for $K_I = 2$

Type B and Z(i) = 2 ... Number of design variables for $K_I = 1$

Type A and Z(i) = 3 ... Number of design variables for $K_I = 3$

Type B and Z(i) = 3 ... Number of design variables for $K_I = 1$

(ii) Number of design variables for the output shaft stiffness K_O

Although each submatix is derived to have output shaft stiffness, K_O is assigned only to the L^{th} transmission stage. In all other transmission stages K_O is changed to coupling stiffness K_C. The number of design variables for K_O is given as:

Type A and Z(i) = 2 ... Number of design variables for $K_O = 1$

Type B and Z(i) = 2 ... Number of design variables for $K_O = 2$

Type A and Z(i) = 3 ... Number of design variables for $K_O = 1$

Type B and Z(i) = 3 ... Number of design variables for $K_O = 3$

(iii) Number of design variables for the shaft stiffness K_S

The values for shaft stiffness K_S are fixed quantities seen in relevant transmission stages. They do not change with the engagement pattern.

$$\text{Number of design variables for } K_S = \sum_{i=1}^{L} (Z(i) - 1)$$

(iv) Number of design variables for the coupling stiffness K_C

In order to assemble the [K] matrix, all of the submatrices are coupled by the coupling stiffness K_C. The K_I and K_O in submatrices are converted into K_C, where it is necessary. The number of design variables for coupling stiffness is determined by two consecutive transmission stages. The Table 5.1 shows the number of design variables for K_C of i^{th} transmission stage.

			i^{th} Transmission stage			
			Type A		Type B	
			Z(i) = 2	Z(i) = 3	Z(i) = 2	Z(i) = 3
$i+1^{th}$ Transmission stage	Type A	Z(i) = 2	2	3	1	1
		Z(i) = 3	2	3	1	1
	Type B	Z(i) = 2	4	6	2	2
		Z(i) = 3	6	9	3	3

Table 5.1 Number of design variables for the coupling stiffness K_C

5.6.2 Description of subroutines

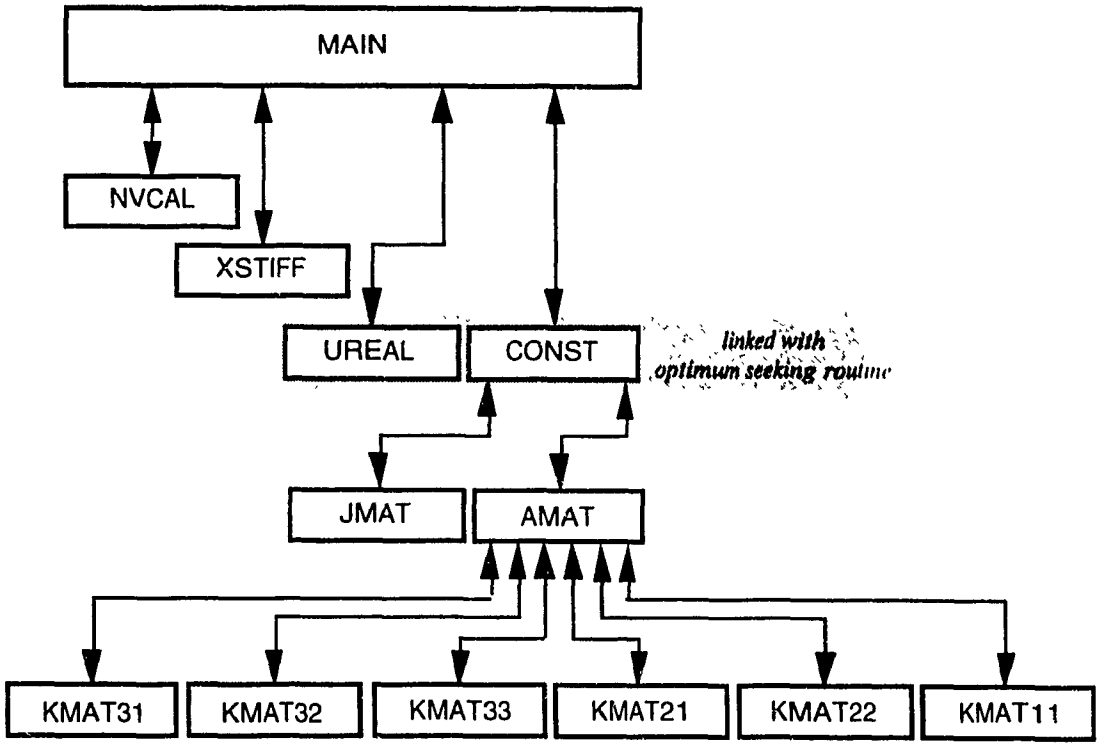

Figure 5.12 Organization of subroutines

Totally there are 12 subroutines written to perform the optimization. The Figure 5.12 shows the sequential order of the subroutines that are called by the main program. The main program calls 4 major subroutines NVCAL, XSTIFF, UREAL and CONST. The input data for the design is first studied in subroutine NVCAL, where the number of variables are then calculated. The sequential call for subroutine XSTIFF assigns the design variables to all stiffnesses of involved shaft portions. The subroutine UREAL and CONST are written as the part for the optimum seeking routine. Subroutine UREAL computes the objective function. The subroutine CONST is written to define all constraints for the procedure. In order to calculate the constraints for Dunkerley values, the subroutine CONST calls N times the subroutines JMAT and AMAT. The subroutine JMAT computes the equivalent inertias for the corresponding n^{th} transmission path. In accordance with the

Z(i) and p(i), the subroutine AMAT calls subroutines KMAT31, KMAT32, KMAT33, KMAT21, KMAT22 and KMAT11 to construct the stiffness matrix $[K]_n$. Using the relevant gear ratios, the equivalent stiffness are also simultaneously computed in these subroutines. Finally, the subroutine AMAT calculates the flexibility matrix $[a]_n$ which is the inverse of stiffness matrix $[K]_n$. After calling the JMAT and AMAT, the subroutine CONST computes Dunkerley value to define the corresponding inequality constraint. The main program is linked with the optimum seeking routine that uses the subroutines UREAL and CONST. The problem defined in this chapter is seen as a highly non linear problem. Thus, an interior penalty function approach with Hooke and Jeeve pattern search method is implemented here to solve the problem. The interior penalty function method and search algorithm using Hooke and Jeeve method are described in Appendix C and section B.3 of Appendix B respectively.

5.7 Demonstration results

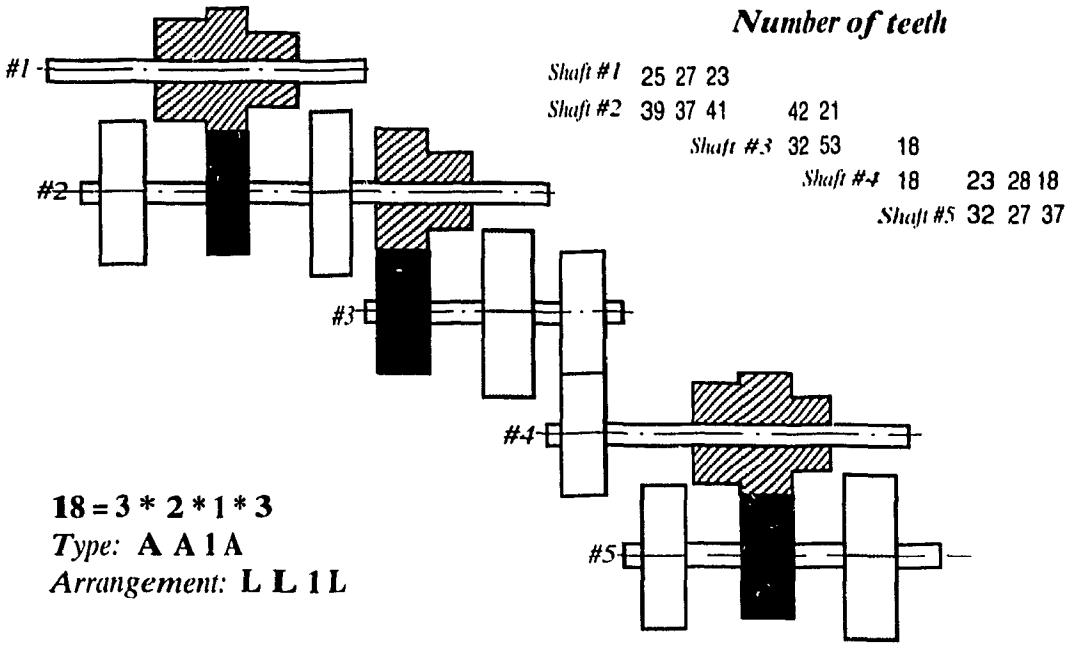

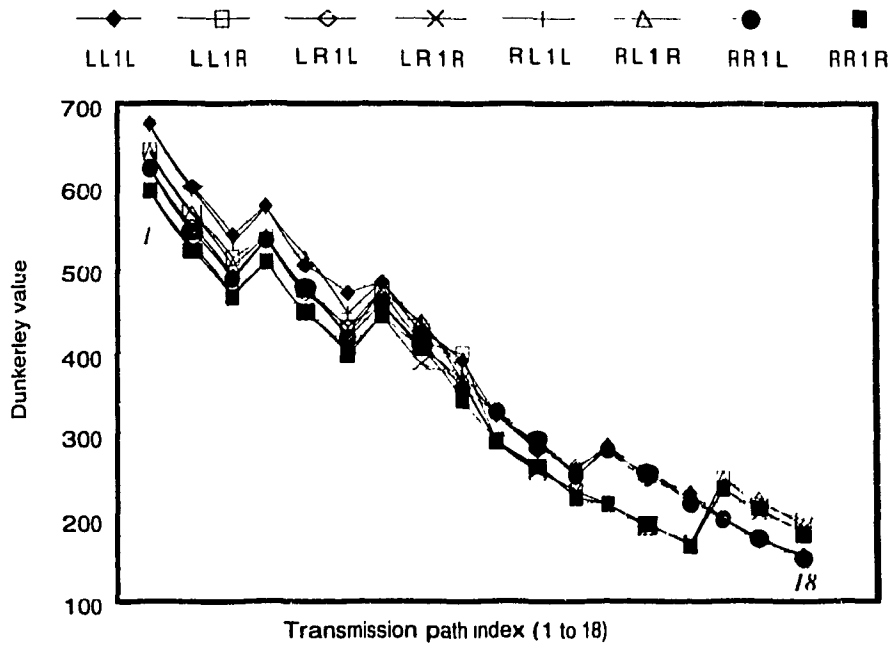

Figure 5.13 Dunkerley value vs transmission path for type A A 1 A

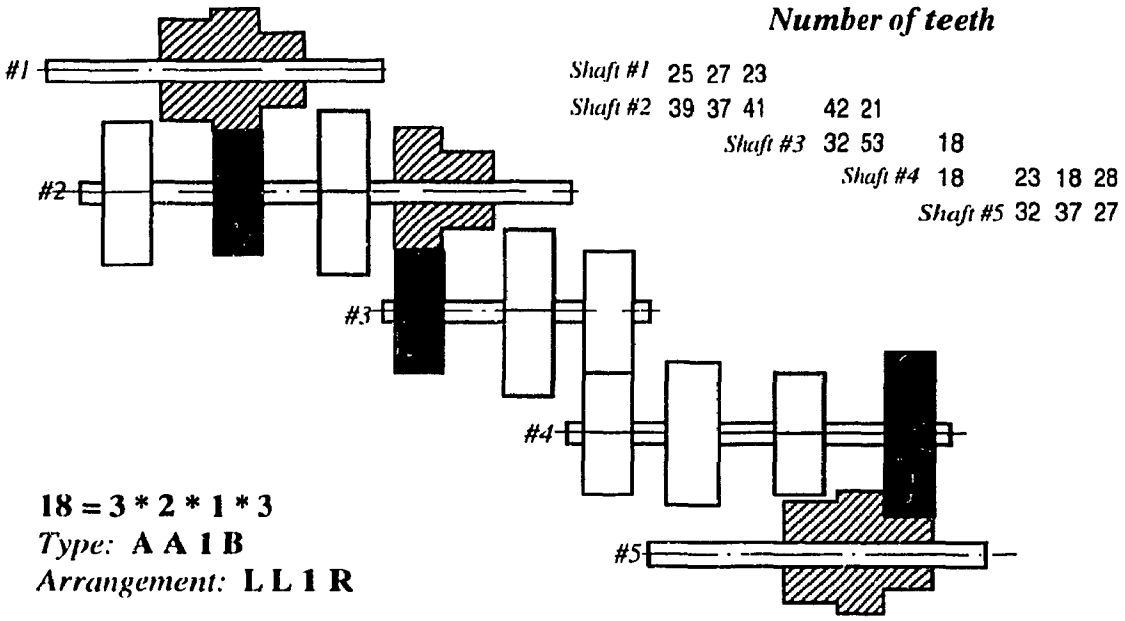

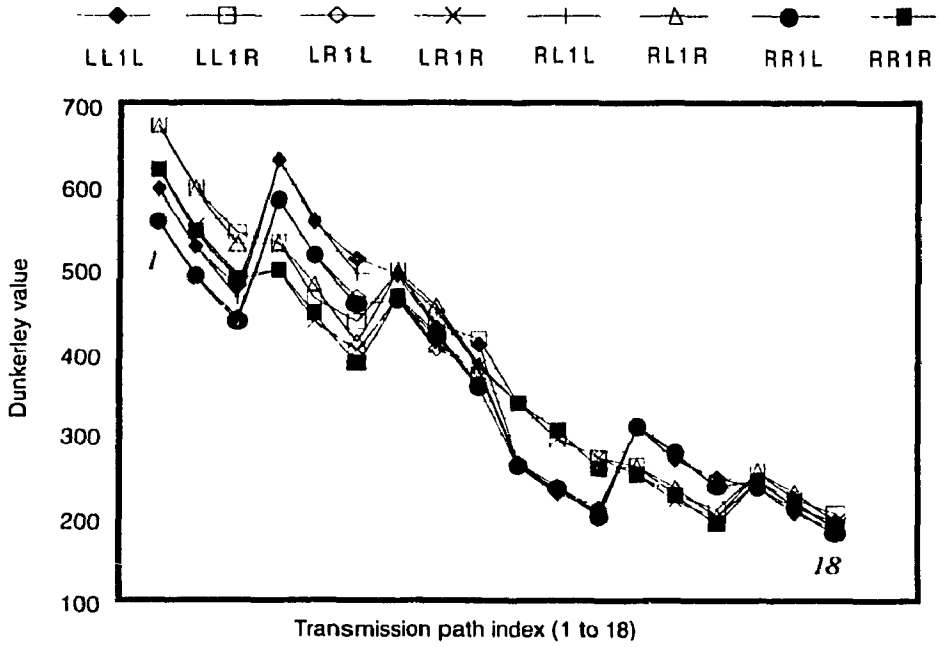

Figure 5.14 Dunkerley value vs transmission path for type A A 1 B

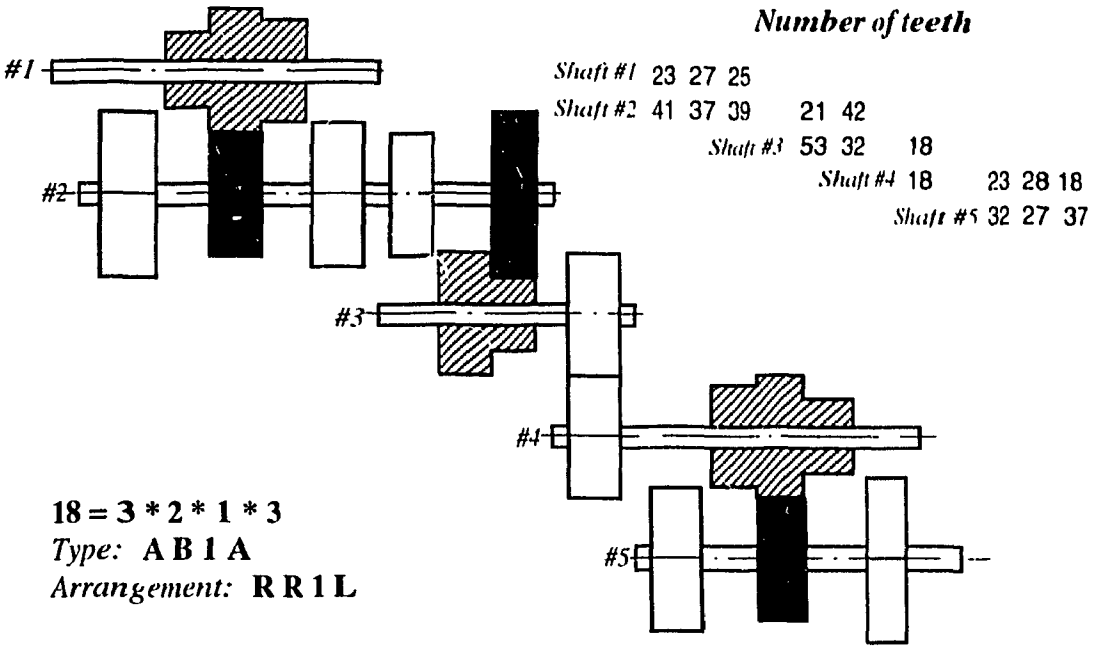

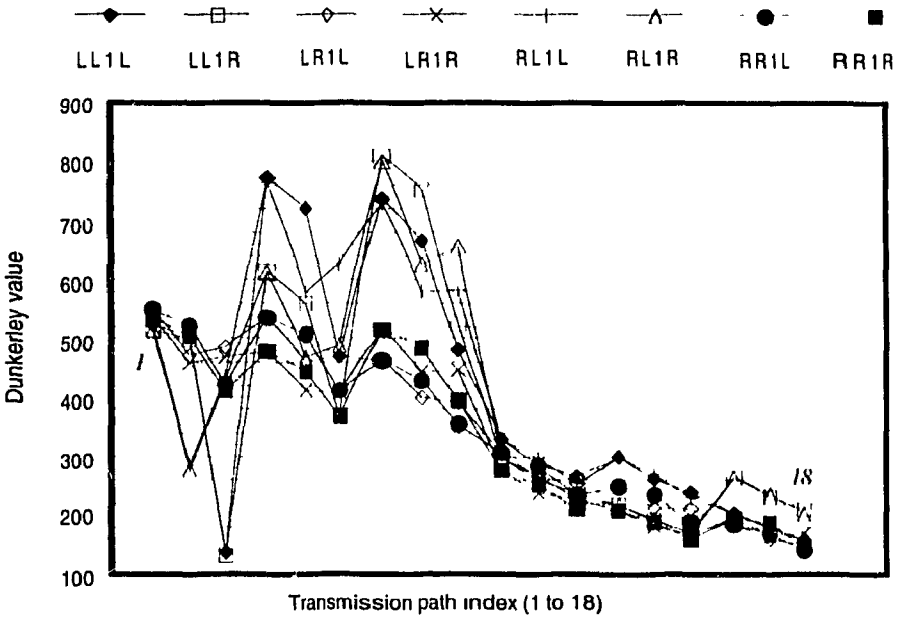

Figure 5.15 Dunkerley value vs transmission path for type A B 1 A

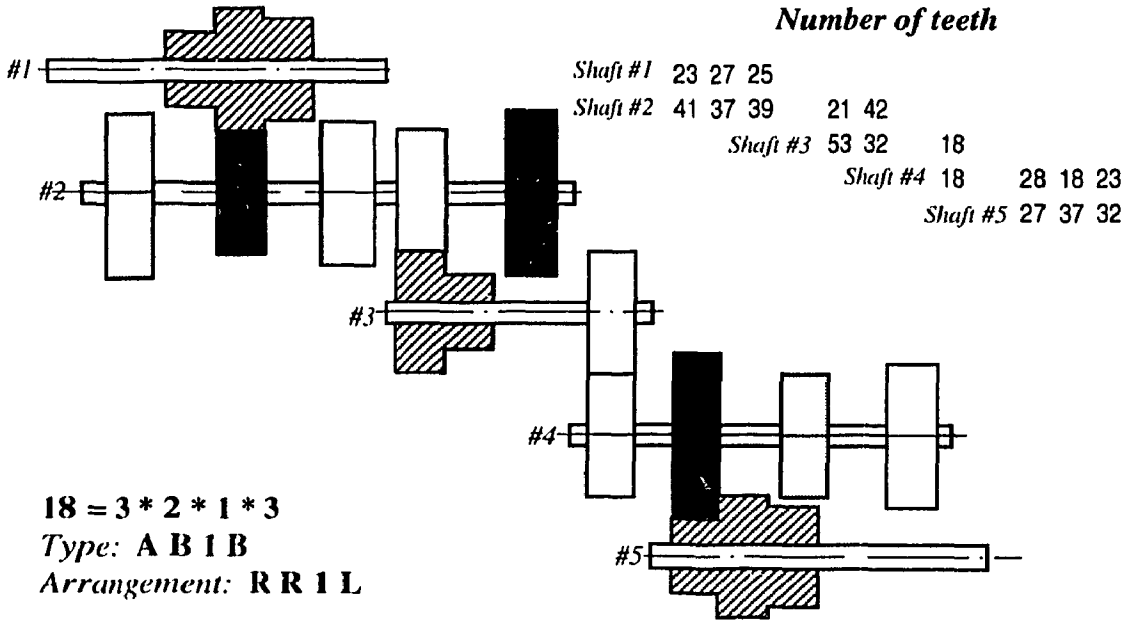

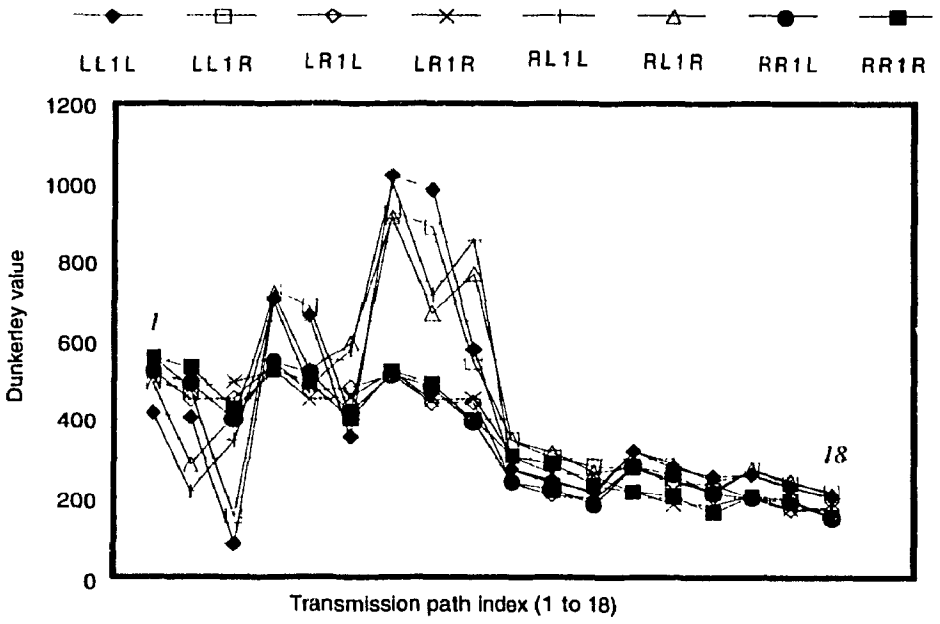

Figure 5.16 Dunkerley value vs transmission path for type A B 1 B

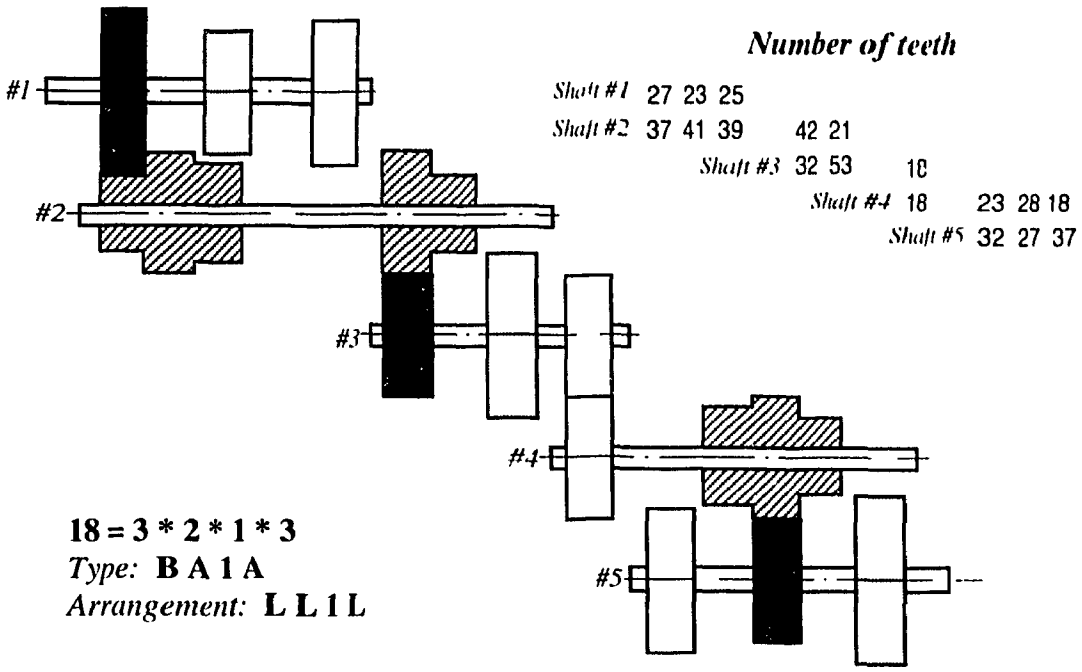

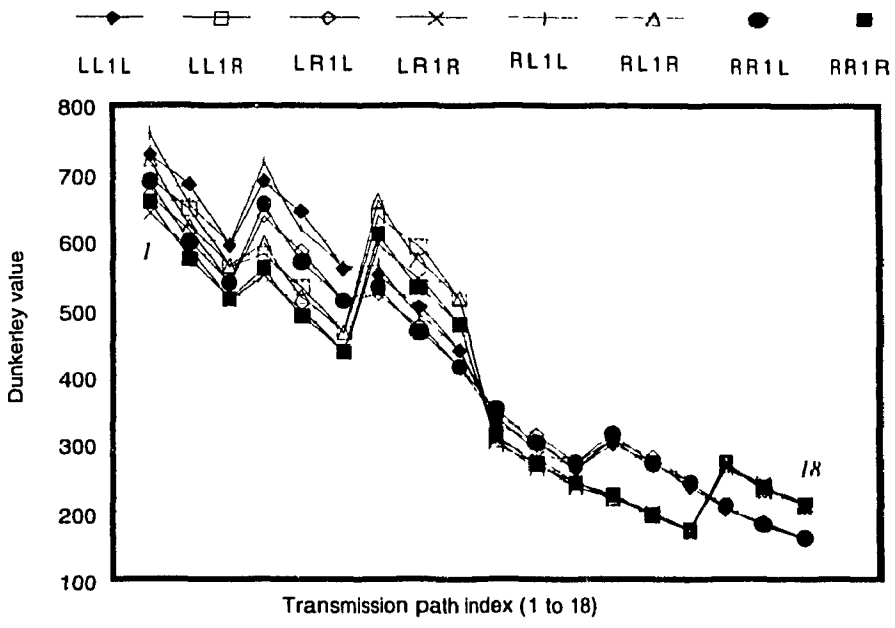

Figure 5.17 Dunkerley value vs transmission path for type B A 1 A

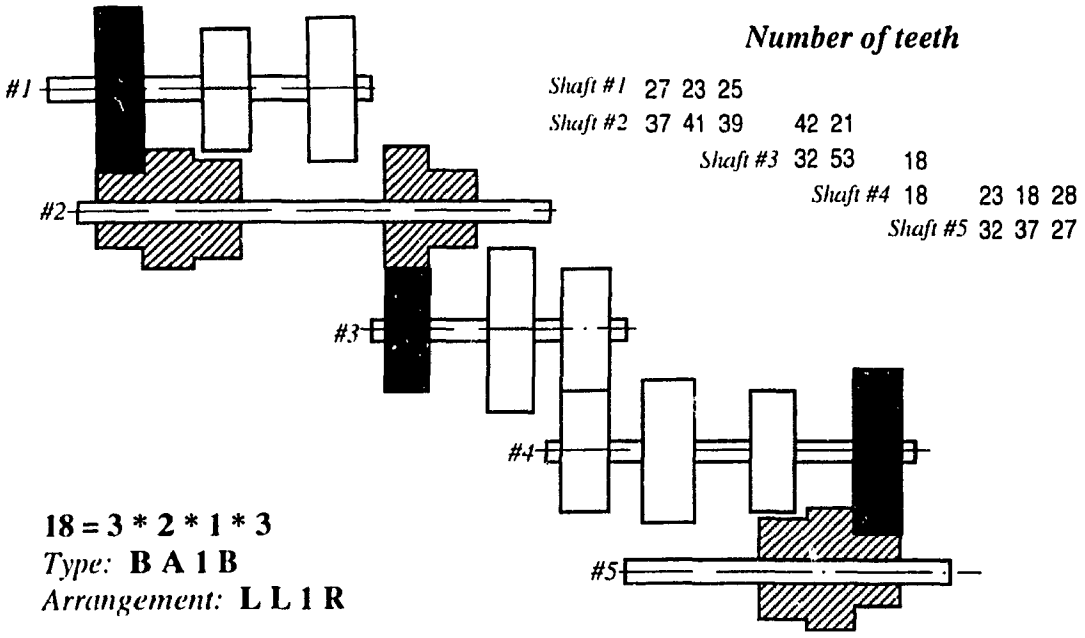

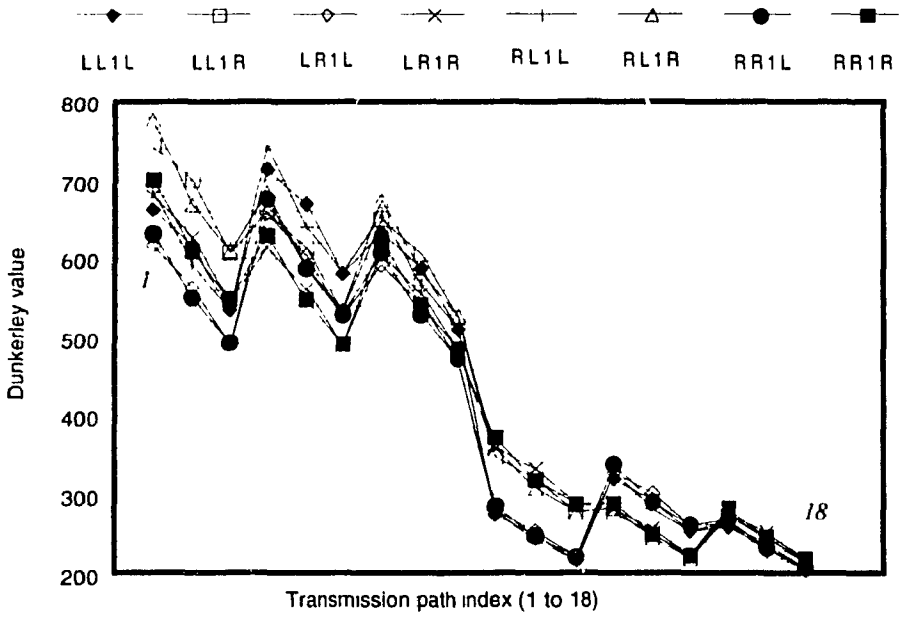

Figure 5.18 Dunkerley value vs transmission path for type B A 1 B

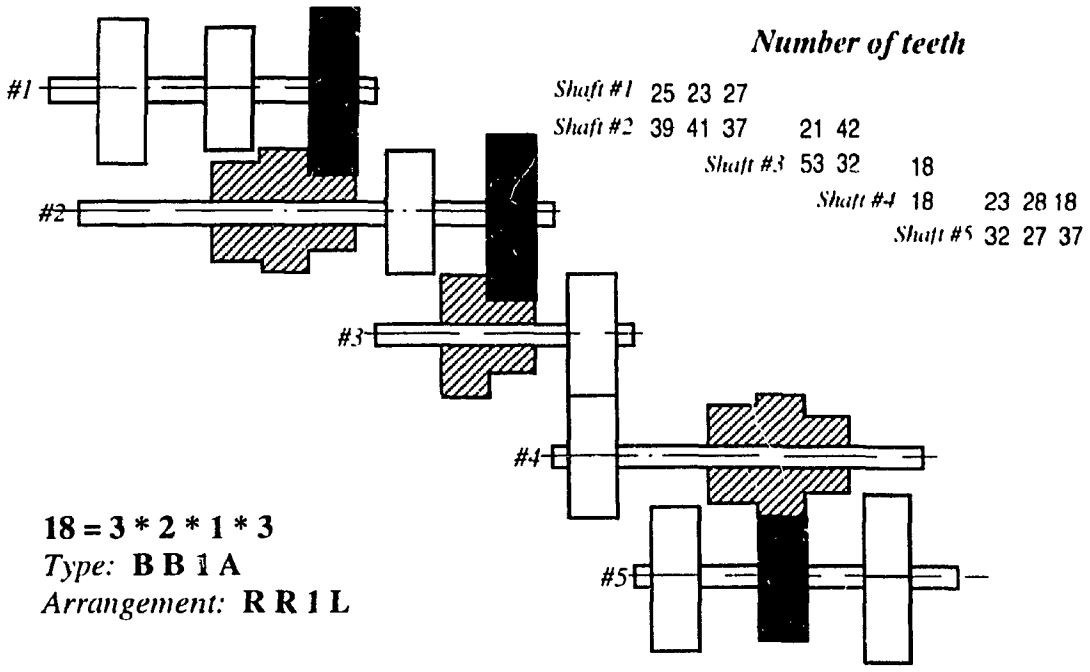

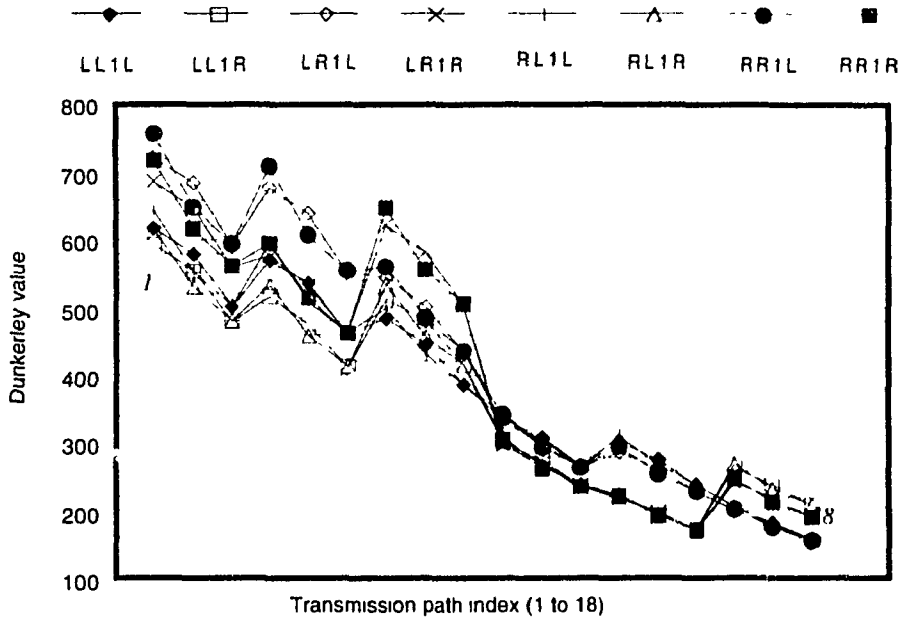

Figure 5.19 Dunkerley value vs transmission path for type B B 1 A

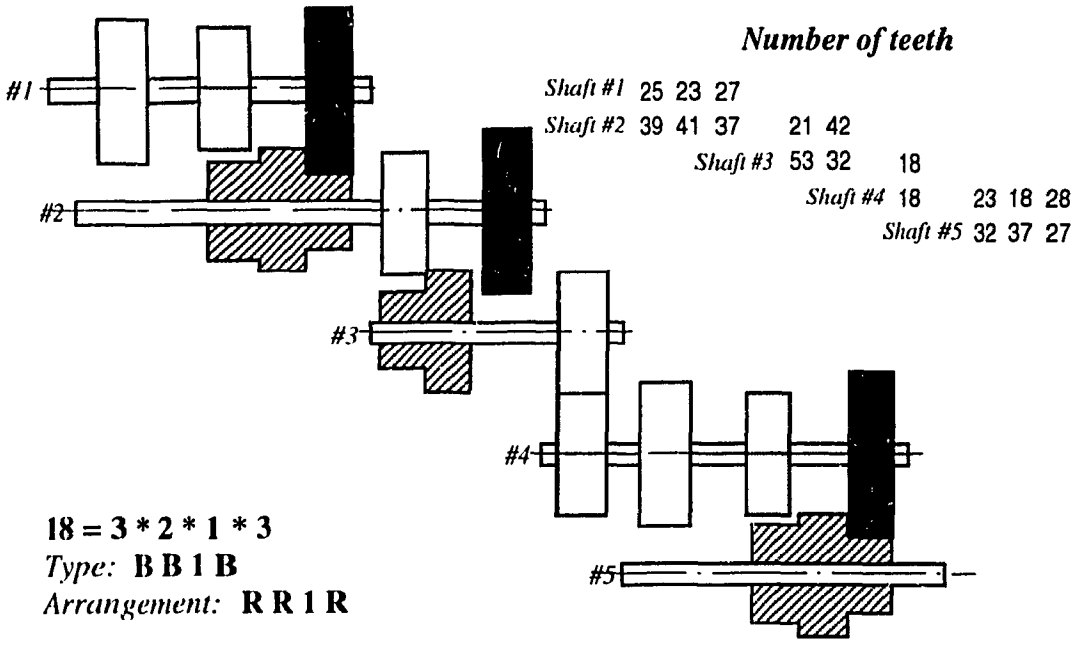

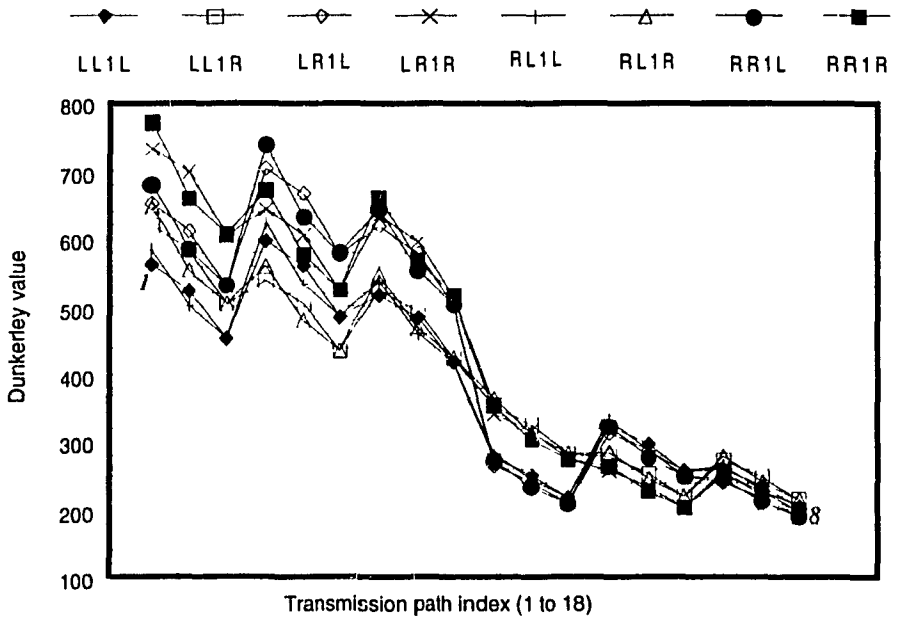

Figure 5.20 Dunkerley value vs transmission path for type B B 1 B

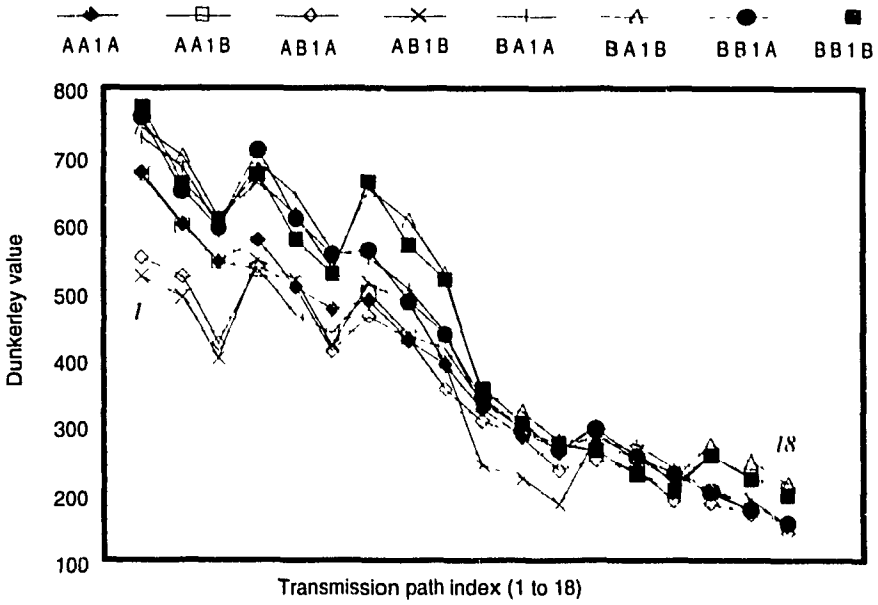

Figure 5.21 Dunkerley value vs optimum type

Spindle shaft speed (rpm)	Largerst speed frequency (Hz`)	Dunkerley value	Dunkerley value / Largerst speed frequency
1390.540	23.333	772.152	33.092
1221.510	23.333	660.437	28.304
1068.970	23.333	606.147	25.978
963.756	23.333	672.375	28.816
846.605	23.333	577.303	24.742
740.882	23.333	525.184	22.508
652.319	23.333	661.706	28.359
573.025	23.333	568.058	24.345
501.467	23.333	516.640	22.142
419.786	23.333	354.608	15.197
368.758	23.333	303.236	12.996
322.708	23.333	274.263	11.754
290.945	23.333	263.425	11.290
255.579	23.333	227.325	9.742
223.663	23.333	203.167	8.707
196.927	23.333	256.255	10.982
172.989	23.333	221.181	9.479
151.386	23.333	197.601	8.469

Table 5.2 Dunkerley value obtained from optimum design

5.8 Optimal design example

The following listing is the final form of the results using the present design synthesis. The sequential implementation of the optimization procedures presented in Chapter 3, Chapter 4 and Chapter 5 will yield the optimal kinematic design and the shaft stiffnesses. The design requirements for the entire procedure are given only through 5 lines of FORTRAN read statements as it is shown in page 60.

```
-----------------------------------------------------------

OPTIMIZATION RESULTS

-----------------------------------------------------------

Transmission formula:    3 * 2 * 1 * 3

Type of gear train:  B    B    1    B

Arrangement of gears:  R    R    1    R

Module:  0.305

-----------------------------------------------------------

Transmission stage = 1; CLUSTER IS ON OUTPUT SHAFT
Number of pinion teeth (Input shaft)  25   23   27
Number of wheel teeth (Output shaft)  39   41   37
Face widths:    0.7078000; 0.7820000 and 0.6437000

Transmission stage = 2; CLUSTER IS ON OUTPUT SHAFT
Number of pinion teeth (Input shaft)  21   42
Number of wheel teeth (Output shaft)  53   32
Face widths:    1.649500 and 0.7695000

Transmission stage = 3; NO CLUSTER (Z(i) = 1)
Number of pinion teeth (Input shaft)  18
Number of wheel teeth (Output shaft)  18
Face width:    6.757900

Transmission stage = 4; CLUSTER IS ON OUTPUT SHAFT
Number of pinion teeth (Input shaft)  23   18   28
Number of wheel teeth (Output shaft)  32   37   27
Face widths:    3.557100, 5.022800 and 2.845000
```

```
-----------------------------------------------------------

OPTIMAL STIFFNESSES:

* EQUIVALENT STIFFNESS

Transmission stage = 1
     Input shaft stiffness  = 107638.0
     Shaft stiffness = 107638.0 and 107638.0
     Coupling stiffness = 107638.0; 107638.0  and 107638.0

Transmission stage = 2
     Shaft stiffness = 107638.0
     Coupling stiffness = 107638.0 and 107638.0

Transmission stage = 3
     Shaft stiffness      NO (Z(i) = 1)
     Coupling stiffness = 107638.0

Transmission stage = 4
     Shaft stiffness = 107638.0 and 107638.0
     Output shaft stiffness = 107638.0; 107638.0 and 107638.0

-----------------------------------------------------------

* ACTUAL STIFFNESS

Transmission stage = 1
     Input shaft stiffness = 107638.0
     Shaft stiffness = 107638.0 and 107638.0
     Coupling stiffness = 35879.34; 53819.00 and 107638.0

Transmission stage = 2
     Shaft stiffness = 107638.0
     Coupling stiffness = 53819.00 and 107638.0

Transmission stage = 3
     Shaft stiffness      NO (Z(i) = 1)
     Coupling stiffness = 107638.0

Transmission stage = 4
     Shaft stiffness = 107638.0 and 107638.0

     Output shaft stiffness = 35879.34; 53819.00 and 107638.0
```

5.9 Conclusion

An efficient way of integrating the concepts of optimization, discrete system modeling of machine tool gear trains and matrix analysis is studied to obtain practically useful solution algorithms. A reduced set of number of distinguished torsional vibration constraints are evaluated via the resulting Dunkerley values. Also, various physical configurations are represented in a more straightforward manner, into the equations of motion via reformulating the coefficients of characteristic matrices. The problem of a single optimization with added number of constraints due to different dynamic configurations is solved. Dynamically stable layouts are generated by the pure imaginary torsional vibration frequencies. Ready for inclusion of dissipative forces straightforwardly. Optimal system offering a wider spacing of excitory and inherent frequencies of oscillations for any dynamically admissible kinematic configuration of any engagement pattern is evaluated.

CHAPTER 6

Concluding remarks and future work

The design procedure presented in this thesis provides an improved methodology for optimal design of industrial multi-speed gear trains, specifically, with spur gear, parallel shaft arrangements. The methodology is able to handle any number of spindle speeds as well as any number of shafts. The optimal design is carried out for minimum volume, minimum mass, maximum power transmitted, minimum error in gear ratios and maximum torsional vibrational safety. The final results are obtained through different stages considering all possible gear train configurations. Furthermore, the reliability of the component gears along with the system is increased by introducing probabilistic variables. The vibrational safety is ensured by analyzing various locations of the component gears on shafts. The methodology presented in this thesis has more advantages over many works of the past, which are listed in the literature survey. Comparison of results with other published works for identical initial design requirements reveals the superiority of the present methodology.

In gear industry, variety of tooth properties are possible to manufacture. Because of this fact, it has been found desirable to standardize some gear parameters. The standards on gear parameters provide a means of achieving increased manufacturability and interchangeability. These standards specify various relationships among the number of teeth, tooth thickness, addendum and pressure angle of gears. However, these standards are not intended to be absolutely rigid, designers are at liberty to modify the gear parameters within limitations. For example, values for number of teeth are restricted by many existing standards to provide specific gear ratios and interchangeability. These restrictions are useful to some extent, but they do not facilitate the development in the ever increasing demand for machine tool applications. The procedure provided in Chapter 3

offers the means of satisfying the designers' expectations and the standards. The procedure is formulated in such a way, that the industrial standards can also be specified as constraints. The procedure examines all possible kinematic arrangements and all possible speed diagrams. Given the design requirements as it is given by Rao et al [39], the procedure examines 12 different possibilities of kinematic arrangements and 72 possible speed diagrams for a gear train with 18 spindle speeds and 5 shafts. The results successfully show that the spindle speeds are achieved much closer to the proposed ideal speeds and the overall center distance of the new design is reduced to 79.79% as compared to the optimum design given in Reference by Rao et al [39]. The results in Table 3.4, Figure 3.7 and Figure 3.8 show the improvements on the spindle speeds using the proposed design procedure. Also the higher speeds in the intermediate shafts of the optimal design are considerably reduced and this can be seen by comparing the speed diagrams of both gear trains shown in Figure 3.6.

Eventhough industrial standards are maintained in the design synthesis, appropriate considerations are to be taken in performing the optimal design synthesis of multi-speed gear trains. For instance, pinion of a mating gear set in machine tool applications is allowed to have minimum number of teeth, that is 18, according to AGMA. This number can not be applied as an absolute rule to gear trains consisting of all component gears with the same module . In such type of design synthesis, the pinion which belongs to the set of smallest gear ratio in each transmission stage can only be allowed to have the minimum number of teeth given by standards. Otherwise the design procedure may face a serious feasibility problem. This observation is notified in Chapter 3 and it is useful to know before starting any design synthesis of multi-speed gear trains.

In gear industry, the single and double composite gear trains offer attractive design features. However, design of such composite gear trains is known to be a tedious process according to gear researchers [33]. The optimization procedure presented in Chapter 3 offers an alternate design method and the advantage of having composite designs by simply

initiating several sets of component gears to have equal size in the form of constraints. A composite design is created from the optimum design by completely eliminating one wheel from a selected transmission stage and allowing a particular pinion in next transmission stage to be the composite. This reduces the number of gears in the gear train by one, that will further lower the weight and the manufacturing cost. The layout of the composite kinematic arrangement is shown in Figure 3.9.

One of the important problems arising in machine tool industry is the alteration of existing design of gear trains. In many cases, some parameters may be required to take values that have been previously set. Obviously, it is very difficult to predict the effect of change in any of the preset values. With the integration of the optimization methods into design synthesis, most of these type of problems can be successfully solved. For example, eliminating one shaft from an existing design without affecting the spindle speeds is demonstrated in Chapter 3. Since the existing design is observed to contain a transmission stage with a single gear set, that particular set is forced to have the gear ratio equal to 1.000 using appropriate constraints. It is obvious that the absence of this transmission stage does not affect the required spindle speeds. Thus, an alternate gear train is designed by removing the above mentioned transmission stage. The new alternate design will continue to serve the same spindle speeds but with number of shafts reduced by one and number of gears reduced by two. This yields the overall center distance of the new design to be 67.25% of the original value.

The dynamic characteristics of the gear train system are sensitive to the inertial distribution due to the location of component gears on shafts, where the different locations are achieved by initiating different engagement patterns. The mounting of component gears on shafts can play an important role in the inertial distribution of the dynamic system. In contrast to the progress made in analysis of gear trains with different engagement patterns, a systematic analysis for identifying proper position of mounting of component gears on shafts is not available. Knowing this, a technique by rearranging the locations of the

component gears to avoid the resonance is used in Chapter 5 of this thesis. The minimum compliance is added at efficient gear locations to shift the natural frequency in all engagement patterns. Although, estimation of the exact natural frequency of the torsional system could be effective in the classical dynamic analysis, it is not used in this thesis. The objective in Chapter 5 is to shift the natural frequency away from the larger operational frequency observed in the transmission path of the current engagement pattern. From this view point, the Dunkerley method, which estimates the lower bound for the natural frequency, is proposed. The optimization problem is solved to ensure the torsional vibrational safety for each set of engagement patterns for all possible gear mountings.

The actual center distance in which the gear will perform in service, will have larger influence on the service life of gear trains. In any critical evaluation of a gear train, particularly in determining its reliable performance, the actual center distance should be used in the equations governing facewidths, backlash, contact ratio, tooth tip clearance etc. The actual center distance is determined by the factors such as the nominal center distance, manufacturing tolerances, differential expansion between gears on their mountings and the deflection in mountings due to service loads. The design aspects that should be considered when the nominal center distance is obtained are discussed in detail in Chapter 3. All other factors listed above are random in nature. It is known that nominal center distance has a linear relationship with gear module. In this case, variations in the actual center distance that results from the buildup of all randomness that influences the gear module are considered in Chapter 4. A new probabilistic design method for increased power transmitting capacity, minimum weight and the reliability of the components as well as the system is described in this chapter. The parameters that affect the gear train performance such as transmitted power, facewidth, bending stress, wear stress, material density and rotational speeds are also treated for uncertainty. The method improves optimization accuracy over the deterministic optimization with only a slight increase in computer time.

A new graphical procedure for identifying all possible speed diagrams has been developed and presented in Chapter 2. The method is based on the creation of graphical representation for combined results of layout diagrams with the values of rotational speeds. The procedure enables the designer to know the effect of speed ratio changes for the same initial requirements that are the number of spindle speeds, number of shafts required, speeds of the spindle and speed of the drive unit. This procedure was successfully adopted in the analysis of Chapter 3 to identify the optimal design parameters of the kinematic design.

Based on the new approaches presented in this thesis, an efficient procedure for the design synthesis of multi-speed gear trains for industrial applications is developed. The design procedure presented in the thesis can be benefitally applied to non metallic gear trains. However, the design synthesis employed herein is limited. During the entire study, spur gears with same module are only considered. It is also possible to design gear trains with different modules with proper profile modifications. The methodology used for spur gears can be extended to other types of gears where applicable. The tooth geometry is not considered in this thesis. Since the vibrational energy is transmitted to the housing through the shafts and bearings, more study is desired in the design of bearings, shafts and housing. Study on other vibrational problems, such as noise that is influenced by manufacturing precision of tooth profile and the error in them, is also to be focused for better design. Furthermore, the operating conditions such as temperature and lubrication of gears are not well studied in the area of gear trains. It is possible that some new techniques based on tribological aspects can be implemented as to further improve the service life of gear trains. Therefore, a further study may focus on these issues for developing the design synthesis of the real world machine tool multi-speed gear train systems.

REFERENCES

1. Acherkan, N, S., *Machine tool design*, Moscow, Mir Publishers, 1968.

2. Alban L., E., *Systematic analysis of gear failures*, Ohio, American society for metals, 1985.

3. Alvord, C., H., Large-scale systems optimization using nonlinear integer goal programming methods, *Thesis (Ph.D.)*, Pennsylvania state University, 1981.

4. Amirouche, F., M., L., Shareef, N., H. and Xie, M. "Dynamic analysis of flexible gear trains / transmissions: an automated approach", *Transactions of ASME*, Vol. 59, December 1992, pp. 976-982.

5. Arabyan A., and Shiflett G., R., "A method for determining all gear trains that provide a specific velocity ratio", ASME paper 86-DET-92.

6. Arabyan, A., and Shiflett G., R., "A method for determining the various gear trains that provide a specific velocity ratio" *Journal of mechanisms, transmissions and automation in design*, Vol. 109, December, 1987, pp. 475-480.

7. Arabyan A., and Shiflett G., R., "A method for determining all gear pairs which satisfy velocity ratio and / or center distance specifications", ASME paper 86-DET-190.

8. Bush, G. S., Computer aided synthesis of optimal multi-speed gear drive designs using problem reduction strategy , *Thesis (Ph.D.)*, Concordia University, 1987.

9. Bush, G., S., Osman M., O., M., and Sankar, S., "On the optimal design of multi-speed gear trains", *Mechanism and machine theory*, Vol. 19, 1984, pp. 183-194.

10. Carrol, R., K. and Johnson, G., E., "Optimal design of compact spur gear sets", *ASME Journal of mechanisms, transmissions and automation in design*, Vol. 106, No. 1, March 1984, pp. 95-101.

11. Carroll, R., K. and Johnson G., E., "Dimensionless solution to the optimal design of spur gear set", *ASME Journal of mechanisms, transmissions and automation in design*, Vol. 111, June 1989, pp. 290-296.

12. Chapman, W. "Analytical optimization of compound gear boxes", *Proceedings of 2nd international computer engineering conference*, August, 1982, San Diago, pp. 135-141.

13. Chiennann, A., H. and Shijun, M., "Discrepancy of gear tooth allowable bending stress using the extreme value distribution from different test methods", *Proceeding of 9th biennial conference on reliability, stress analysis and failure prevention*, Miami, Vol. 30, September, 1991, pp. 1-4.

14. Cornell, R.W., "Compliance and stress sensitivity of spur gear teeth", *ASME Journal of mechanical design*, Vol. 103, April 1981, pp. 447-459.

15. Dande, S. G. and Gupta , A., "Computer aided interactive graphical design of multi-speed gearboxes", *ASME Journal of mechanisms, transmissions and automation in design*, Vol. 106, 1984, pp. 163-170.

16. Davidson, J., W., Felton, L., P. and Hart, G., C., "Optimum design of structures with random parameters", *Computers and structures,* Vol. 7, 1977, pp. 481-486.

17. Dudley, D. W., *The evolution of the gear art,* Washington, American gear manufacturers association, 1969.

18. Gilbert, A., C., "A note on the calculation of torsional natural frequencies of branch systems", *Journal of engineering for industry*, Transactions of ASME, Series B, Vol. 94, No. 1, 1972, pp. 279-283.

19. Haugen, E., B. *Probabilistic approaches to design,* New York, John Wiley & sons inc., 1968.

20. Hsu, D., S., "Reliability constraint on optimum design", *Recent developments in structural optimization,* Proceedings of a session at structures congress'86, American society of civil engineers, 1986, pp. 72-85.

21. Jendo, S., "Multi-objective reliability based optimization of plastic frames", Descretization methods and structural optimization - Procedures and applications, Proceedings of GAMM-seminar, 1988, pp 171-177.

22. Jog, C.S. and Pande, S.S. "Computer-aided design of compact helical gear sets", *Journal of mechanisms, transmissions and automation in design,* Vol. 111, June 1989, pp. 285-289.

23. Koenisgsberger, F., *Design principles of metal cutting machine tools,* Oxfort, Pergamon press, 1964.

24. Lynwander, P., *Gear drive systems : design and application,* New York, M. Dekker, 1983.

25. Mahadevan, S., "Probabilistic optimum design of framed structures", *Computers and structures,* Vol. 42., No. 3, pp. 365-374.

26. Mahalingam, S., and Bishop, R., E., D., "Dynamic loading of gear teeth", *Journal of sound and vibration,* Vol. 36, No. 2, 1974, pp. 179-189.

27. Manjuntha Prasad, M., K., "Computer aided design of spur gears", *Journal of the institution of engineering (India),* Vol. 63, may, 1983, pp. 232-237.

28. Michalec, G.,W., *Precision gearing: Theory and practice,* New York, John wiley & sons, inc., 1966.

29. Mioduchowski, A., "On torsional waves and free vibrations of single gear transmissions", *Proceedings of 14th Canadian congress of applied mechanics,* Kingston, Vol. 2, June, 1993, pp. 753-754.

30. Moses F., "Structural system reliability and optimization", *Computers and structures,* Vol. 7, 1977, pp. 283-290.

31. Narayana Moorthy, M., Ganesan, R., Sankar, T.S., "Optimum gearbox systems subjected to torsional vibration constraints", *Proceedings of 14th Canadian congress of applied mechanics,* Kingston, Vol. 2, June, 1993, pp. 757-758.

32. Oda, S., Nagamura, K. and Aoki, K., "Stress analysis of thin rim spur gears by finite element method", *Bulletine JSME,* Vol. 42, Number 193, July, 1981, pp. 1273-1280.

33. Osman, M., O., M., Dukkipati, R., V., and Siva Prasad, V., "A new interactive algorithm for kinematic synthesis of gear drives for optimal speed ratio", *Mechanism and machine theory,* Vol. 28, 1993, pp. 729-740.

34. Osman, M.O.M., Sankar, S., and Dukkipati, R. V., "Design synthesis of a multi-speed machine gear transmission using multi-parameter optimization", *ASME Journal of machine theory,* Vol. 100, 1978, pp. 303 - 310.

35. Parimi S. R., and Cohn, M. Z., "Optimal criteria in probabilistic structural design", *Optimization in structural design,* International union of theoretical and applied mechanics symposium, Warsaw / Poland, August, 1973, pp. 278-291.

36. Rajendra Singh, Xie, H., and Comparin, R.J., "Vibro-impacts in a geared rotating system.", *Dynamics and design of rotating machinery,* Proceedings of second international symposium on transport phenomena, Dynamics and design of rotating machinery, part II, New York, 1990, pp. 241-255.

37. Rao, S., S., " A probabilistic approach to the design of gear trains", *International journal of machine tool design and research,* 1974, Vol. 14, pp. 267-278.

38. Rao, S. S., *Optimization : Theory and applications,* New Delhi : Wiley Eastern, 1984.

39. Rao, S. S. and Eslampour, H.R., "Multi-stage multi-objective optimization of gear boxes", *ASME Journal of mechanisms, transmissions and automation in design,* Volume 108, 1986, pp. 461- 467.

40. Rao, S.S. and Das, G., "Reliability based optimum design of gear trains", *ASME Journal of mechanisms, transmissions and automation in design,* Vol. 106, 1984, pp. 17-22.

41. Sankar, T., S., "A reliability estimate for machine tool spindles subjected to random forces" *Mechanism and machine theory,* Vol. 10, 1975, pp. 131-138.

42. Savage, M., Coy, J. and Townsend, D.P., "Optimal design of standard gear sets", *Advanced power transmission technology*, NASA conference publication 2210, 1983, pp.435-458.

43. Savage, M., Coy, J. and Townsend, D.P., "Optimal tooth numbers for compact standard spur gear sets", *ASME Journal of mechanical design,* Vol. 104, January, 1982, pp. 749-758.

44. Selfridge R., G., "Compound gear trains of minimum equivalent inertia", *Mechanism and machine theory,* Vol. 15, No. 4, 1980, pp. 287-294.

45. Smith, J., D., *Gears and their vibration : a basic approach to understanding gear noise,* New York, Macmillan Press, 1983.

46. Staph, P., H., "A parametric analysis of high contact ratio spur gears", *ASLE transactions,* Vol.19, No. 3, pp. 201-215.

47. Takuzo, I., Shirou, A. and Ryoji, K., "Coupled lateral-torsional vibration of rotor system trained by gears", *Bulletin of JSME,* Vol. 27, No. 224, February 1984, pp. 271-277.

48. Tanzer, J., H., *Gear design - manufacturing and inspection manual,* Warrendale, Society of automative engineers: Gear and spline technical committee, 1990.

49. Tavakoli, M., S. and Houser, D., R., "Optimum profile modifications for the minimization of static transmission errors of spur gears", *Transactions of ASME,* Vol. 108, March 1986, pp. 86-95.

50. Terauchi, Y. and Nagamura, K., "Study on deflection of spur gear teeth", *Bulletin of JSME,* Vol. 23, October 1980, Paper number 184-17.

51. Terauchi, Y., and Nagamura, K., "Study on deflection of spur gear teeth", *Bulletin of JSME,* Vol. 24, February 1981, Paper number 188-24.

52. Thomson, W., T., *Vibration theory and applications,* New Jersey, Prentice Hall, 1993.

53. Tobe, T. and Sato, K., " Statistical analysis of dynamic loads on spur gear teeth", *Bulletin of the JSME,* Vol.20, No. 145, July, 1977, pp. 882-889.

54. Townsend, D., P., *Dudley's gear handbook,* New York, McGraw-Hill, 1991.

55. Wallace, D., B. and Seireg, A., "Computer simulation of dynamic stress deformation and fracture of gear teeth", *Journal of engineering for industry*, Transactions of ASME, November 1973, pp. 1108-1114.

56. Watson, H., J., *Modern gear production*, New York, Pergamon press, 1970.

57. White, G., "Analysis of nine speed gear trains", *The Engineer*, Vol. 216, 1963, pp. 348-351.

58. White, G. and Sanger, D., J., " On the synthesis of gear trains of minimum size", *International journal of machine tool design and research*, Vol. 8, 1968, pp. 27-31.

59. Woodbury, R., S., *History of the gear cutting machines*, Massachusetts, The M. I. T. press, 1964.

60. Yang, D., C., H. and Lin, J.Y., "Hertzian damping, tooth friction and bearing elasticity in gear impact dynamics", *Journal of mechanisms, transmissions and automation in design*, Vol. 109, June 1987, pp. 189-196.

61. Yang, D., C., H. and Sun, Z., S., "A rotary model for spur gear dynamics", *Journal of mechanisms, transmissions and automation in design*, Vol. 107, December 1985, pp. 529-535.

APPENDIX A

OBTAINING E(i) VALUES FOR 18 SPEED GEAR TRAIN

A.1 Finding E(i) values for 18 speed 4 shaft gear train

Number of output shaft speeds N = 18

Number of shafts required NSR = 4

A.1-1 Kinematic arrangements

(i) Transmission formula :

$N = 18 = 3 * 3 * 2 = Z(1) * Z(2) * Z(3)$

$Z(1) = 3$ - *1st transmission stage has 3 gear sets*

$Z(2) = 2$ - *2nd transmission stage has 2 gear sets*

$Z(3) = 3$ - *3rd transmission stage has 3 gear sets*

$L = 3$

(ii) Possible kinematic arrangements:

$18 = 3 * 3 * 2$

$18 = 3 * 2 * 3$

$18 = 2 * 3 * 3$

A.1-2 Number of shafts:

$NS = L + 1 = 3 + 1 = NSR$

Number of shafts = 4

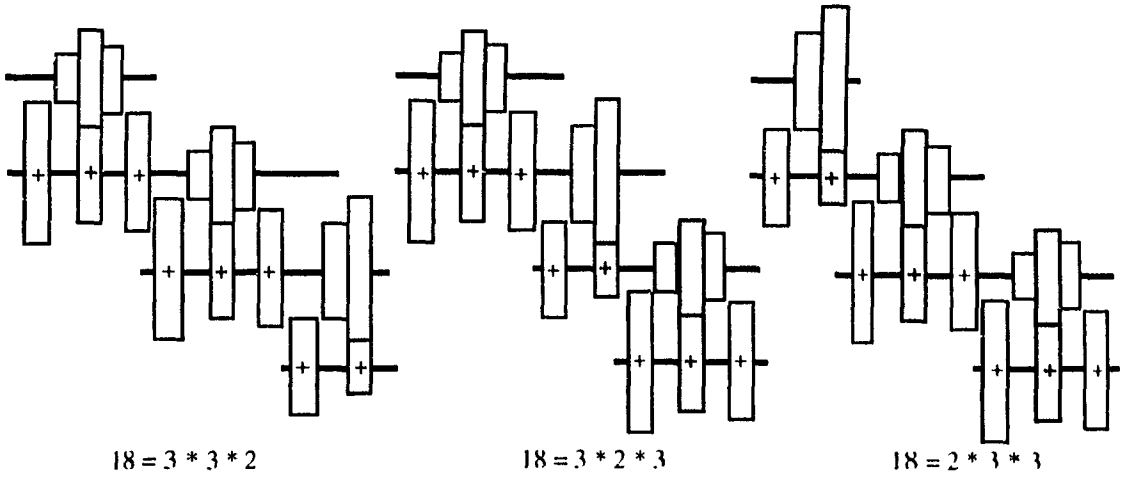

Figure A.1 Kinematic arrangements of 18 speed gear train

A.1-3 E(i) values

*(1) Select 18 = 3 * 3 * 2*

For transmission stage 3

number of output speeds $N_O(3) = 18$

number of input speeds $N_I(3) = N_O(3) / Z(3) = 18 / 2 = 9 = N_O(2)$

possible E(i) values:

$\frac{N_O(3)}{Z(1) * Z(2) * Z(3)}$	$\frac{N_O(3)}{Z(1) * Z(3)}$	$\frac{N_O(3)}{Z(2) * Z(3)}$	$\frac{N_O(3)}{Z(3)}$
$\frac{18}{3 * 3 * 2}$	$\frac{18}{3 * 2}$	$\frac{18}{3 * 2}$	$\frac{18}{2}$
1	3	3	9

For transmission stage 2

number of output speeds $N_O(2) = 9$

number of input speeds $N_I(2) = N_O(2) / Z(2) = 9 / 3 = 3 = N_O(1)$

possible E(i) values

$\frac{N_O(2)}{Z(1) * Z(2)}$	$\frac{N_O(2)}{Z(2)}$
$\frac{9}{3 * 3}$	$\frac{9}{3}$
1	3

For transmission stage 1

number of output speeds $N_O(1) = 3$

number of input speeds $N_I(1) = N_O(1) / Z(1) = 3 / 3 = 1$

possible E(i) value

$$\frac{N_O(1)}{Z(1)}$$

$$\frac{3}{3}$$

1

*(2) Select 18 = 3 * 2 * 3*

For transmission stage 3

number of output speeds $N_O(3) = 18$

number of input speeds $N_I(3) = N_O(3) / Z(3) = 18 / 3 = 6 = N_O(2)$

possible E(i) values:

$\frac{N_O(3)}{Z(1) * Z(2) * Z(3)}$	$\frac{N_O(3)}{Z(1) * Z(3)}$	$\frac{N_O(3)}{Z(2) * Z(3)}$	$\frac{N_O(3)}{Z(3)}$
$\frac{18}{3 * 2 * 3}$	$\frac{18}{3 * 3}$	$\frac{18}{2 * 3}$	$\frac{18}{3}$
1	2	3	6

For transmission stage 2

number of output speeds $N_O(2) = 6$

number of input speeds $N_I(2) = N_O(2) / Z(2) = 6 / 2 = 3 = N_O(1)$

possible E(i) values

$\frac{N_O(2)}{Z(1) * Z(2)}$	$\frac{N_O(2)}{Z(2)}$
$\frac{6}{3 * 2}$	$\frac{6}{2}$
1	3

For transmission stage 1

number of output speeds $N_O(1) = 3$

number of input speeds $N_I(1) = N_O(1) / Z(1) = 3 / 3 = 1$

possible E(i) value

$\frac{NOS(1)}{Z(1)}$
$\frac{3}{3}$
1

*(3) For 18 = 2 * 3 * 3*

For transmission stage 3

number of output speeds $N_O(3) = 18$

number of input speeds $N_I(3) = N_O(3) / Z(3) = 18 / 3 = 6 = N_O(2)$

possible E(i) values:

$\frac{N_O(3)}{Z(1) * Z(2) * Z(3)}$	$\frac{N_O(3)}{Z(1) * Z(3)}$	$\frac{N_O(3)}{Z(2) * Z(3)}$	$\frac{N_O(3)}{Z(3)}$
$\frac{18}{2 * 3 * 3}$	$\frac{18}{2 * 3}$	$\frac{18}{3 * 3}$	$\frac{18}{3}$
1	3	2	6

For transmission stage 2

number of output speeds $N_O(2) = 6$

number of input speeds $N_I(2) = N_O(2) / Z(2) = 6 / 3 = 2 = N_O(1)$

possible E(i) values

$$\frac{N_O(2)}{Z(1) * Z(2)} \qquad \frac{N_O(2)}{Z(2)}$$

$$\frac{6}{2 * 3} \qquad \frac{6}{3}$$

$$1 \qquad 2$$

For transmission stage 1

number of output speeds $N_O(1) = 2$

number of input speeds $N_I(1) = N_O(1) / Z(1) = 2 / 2 = 1$

possible E(i) value

$$\frac{N_O(1)}{Z(1)}$$

$$\frac{2}{2}$$

$$1$$

Kinematic arrangements	1 st Transmission stage	2 nd Transmission stage	3 rd Transmission stage
18 = 3 * 3 * 2	1	1 3	1 3 9
18 = 3 * 2 * 3	1	1 3	1 2 3 6
18 = 2 * 3 * 3	1	1 2	1 2 3 6

Table A.1 E(i) values for 18 speed 4 shaft gear train

Using the combination of values in Table A.1, all possible layout diagrams can be constructed for each kinematic arrangement of 18 speed 4 shaft gear train. In finding the speed diagrams, two of the possible 8 layout diagrams from 18 = 3 * 2 * 3 and 18 = 2 * 3 * 3 are rejected, because of non-symmetric speed ratios obtained.

A.2: Finding E(i) values for 18 speed 5 shaft gear train

For a 18 shaft train, if the number of shaft value is increased to 5, then an additional shaft with one gear set has to be added to satisfy the requirement. This may produce 12 different kinematic arrangement. For each kinematic arrangement possible E(i) values can be obtained which are shown in Table A.2. Using the combination of tabled values, 88 possible layout diagrams can be constructed for 18 speed 5 shaft drives. In finding the speed diagrams, 16 layout diagrams are rejected because of non-symmetric speed ratios are obtained.

Kinematic arrangements	1 st Transmission stage	2 nd Transmission stage	3 rd Transmission stage	4 th Transmission stage
18 = 3 * 3 * 2 * 1	1	1 3	1 3 9	1
18 = 3 * 3 * 1 * 2	1	1 3	1	1 3 9
18 = 3 * 1 * 3 * 2	1	1	1 3	1 3 9
18 = 1 * 3 * 3 * 2	1	1	1 3	1 3 9
18 = 3 * 2 * 3 * 1	1	1 3	1 2 3 6	1
18 = 3 * 2 * 1 * 3	1	1 3	1	1 2 3 6
18 = 3 * 1 * 2 * 3	1	1	1 3	1 2 3 6
18 = 1 * 3 * 2 * 3	1	1	1 3	1 2 3 6
18 = 2 * 3 * 3 * 1	1	1 2	1 2 3 6	1
18 = 2 * 3 * 1 * 3	1	1 2	1	1 2 3 6
18 = 2 * 1 * 3 * 3	1	1	1 2	1 2 3 6
18 = 1 * 2 * 3 * 3	1	1	1 2	1 2 3 6

Table A.2 Possible E(i) values for 18 speed 5 shaft train

APPENDIX B

SOLUTION ALGORITHM FOR DESIGN SYNTHESIS

B.1 Introduction

For a particular design problem, every design can be represented by a point in a n-dimensional space, which is termed as the design space. The design synthesis is the selection of a point in the design space. The change in the design is obtained as a move from one point to another in this space. Any point in the space is a "design" even though it may represent some impossible configuration. The designs represented by impossible configurations violates the design requirements, but in some region of the design space the requirements do satisfy. The surface that separates both the acceptable and impossible designs is termed as constraint surface. The region where the acceptable designs are found, is termed as the feasible design space. The parameters that are varied to obtain a design is termed as design variables.

In order to select a best design involving the vector of n independent design variables $\mathbf{x} = (x_1, x_2, x_3 \ldots x_n)$, the function whose value is a measure of merit of the design is defined as the objective function and denoted by $\Phi(\mathbf{x})$. Conventionally, by obtaining the lower value for the objective function, better design is achieved. A general mathematical model for a objective function that involves s number of different design objectives can be written as:

$$\text{Minimize } \Phi(\mathbf{x}) = [\Phi_1(\mathbf{x}) + \Phi_2(\mathbf{x}) \ldots \Phi_s(\mathbf{x})]$$

The requirements for the constraint surface is derived through r number of equations $F_1(\mathbf{x})$, $F_2(\mathbf{x})$, $F_3(\mathbf{x})$, ... $F_{r-1}(\mathbf{x})$, $F_r(\mathbf{x})$ in the form of equality and inequalities. More generally, a design with n independent design variables and r number of constraints is a feasible design if and only if

$$F_i(\mathbf{x}) \leq 0 \quad \text{for } i = 1,2,3,\ldots, r.$$

The vector of n independent design variables $\mathbf{x} = (x_1, x_2, x_3 \ldots x_n)$ is governed by upper and lower bound vectors **U**,**L** respectively.

$$\mathbf{U} \leq \mathbf{x} \leq \mathbf{L}$$

There is no single method available for solving all optimization problems efficiently. Hence a number of optimization methods have been developed for solving different types of optimization problems. The efficiency of the optimization method is based on obtaining the best optimum value in least number of searches. Unfortunately none of the classical methods can guarantee the global optimum in finite number of searches.

B.2 Development of non linear integer goal programming technique

In this section, a non-linear integer goal programming algorithm is presented which is capable of solving kinematic design of gear trains and many other similarly formulated design problems with integer design variables. The algorithm has been formulated as a constrained minimization problem, that is converted to a sequence of unconstrained minimization. The described solution assumes that a feasible starting point has been found in the design space. In developing the solution method, s number of objectives and r number of constrains are treated as form of m goals where m = s + r. A mathematical expression that is called as an achievement function **a**, is found by combining these m goals and minimized through the NLIGP method. Before see the details of the method the general formulation for the problem is given as:

Find $\mathbf{x} = x_1, x_2, x_3 \ldots x_n$

so as to minimize

$$\mathbf{a} = [(g_1(\mathbf{n},\mathbf{p}), g_2(\mathbf{n},\mathbf{p}), \ldots, g_K(\mathbf{n},\mathbf{p}))]$$

$$f_t(\mathbf{x}) + n_t - p_t = b_t \quad ; t = 1, 2, \ldots, m$$

$$\text{where } \mathbf{L} \leq \mathbf{X} \leq \mathbf{U}$$

$$\mathbf{n}, \mathbf{p} > \mathbf{0}$$

Once the set of n design variables of **x** and a set of m objectives of $f(\mathbf{x})$ are specified, the method specifies preemptive priorities for ea .i objectives in the achievement function. The priority levels are established to group the objectives in various levels. The concept of grouping them is to ensure which set has to achieve their goals first in searching the optimum value. A set of K priority levels are possible, which are denoted as P_1, P_2,P_3 .. P_K, were the subscript of P is identified as the priority level. The lower subscript is obviously be in higher priority level.

$$P_1 >>> P_2 >>> P_3 .. >>> P_k$$

Goals are found with one - one correspondence with objectives. The goals made from constraints are immeasurably preferred to the achievement of the objective function goals. In this way, the constraints are always satisfied in preference to the attainment of a minima or maxima for the objective function. In goal programming, the constraint set appears as the set of rigid constraints, which must be assigned to the priority level one. This leads all other set of goals to be in the feasible region.

There are 'm' aspiration levels are specified for all of the 'm' number of goals. The aspiration levels are like an attainment level for the objective functions. Knowing the nature of objective functions, reasonable values for aspiration levels is to introduced, so that the availability for goal of optimization domain is ensured. Additionally the goal carries a pair of deviation variables denoted by 'p' and 'n'. These parameters measure the deviation of the objective from aspiration level.

The components of the method can be listed as it follows:

-- A set of design variables

$\mathbf{x} = x_1 + x_2 + x_3 ..... x_n$

-- A set of priority levels

$P_1, P_2, P_3 ... P_k$. where $P_1 >>> P_2 >>> P_3 ... >>> P_k$.

-- A set of goals ($G_1, G_2, G_3, ..., G_m$) which correspond with

$f_1(\mathbf{x}), f_2(\mathbf{x}), f_3(\mathbf{x}) ..... f_m(\mathbf{x})$ respectively

-- A set of aspiration levels (b_1, b_2, b_3, ... b_m) for each goal

-- A set of goals (n_1,p_1), (n_2,p_2), (n_3,p_3) .... (n_m,p_m) to find the deviation away from the aspiration level from goals.

Mathematically, this can be represented:

$$
\begin{array}{ll}
P_1: & \left|\begin{array}{ll} G_1: & f_1(\mathbf{x}) + n_1 - p_1 = b_1 \\ \vdots & \vdots \\ G_a: & f_a(\mathbf{x}) + n_a - p_a = b_a \end{array}\right. \\
P_2: & \left|\begin{array}{ll} G_{a+1}: & f_{a+1}(\mathbf{x}) + n_{a+1} - p_{a+1} = b_{a+1} \\ \vdots & \vdots \\ G_c: & f_c(\mathbf{x}) + n_c - p_c = b_c \end{array}\right. \\
\vdots & \\
P_k: & \left|\begin{array}{ll} G_{c+1}: & f_{c+1}(\mathbf{x}) + n_{c+1} - p_{c+1} = b_{c+1} \\ \vdots & \vdots \\ G_m: & f_m(\mathbf{x}) + n_m - p_m = b_m \end{array}\right.
\end{array}
$$

Here all goals are only assigned to the priority level and no other prescribed ordering is imposed. That is within a priority level P_k the subscripts on G does not has any order , where k = 1, 2, ... K.

An achievement function is a mathematical expression of preemptive priorities. A vector representation denoted as **a** , is able to express the degree of attainment at each priority level. The **a** is a row vector of K components. Mathematically, **a** is expressed as

$$\mathbf{a} = [\ (g_1(\mathbf{n},\mathbf{p})),\ (g_2(\mathbf{n},\mathbf{p})),\ (g_3(\mathbf{n},\mathbf{p})),\ .....\ \ (g_K(\mathbf{n},\mathbf{p}))\ ]$$

Where $g_j(\mathbf{n},\mathbf{p})$ j =1... K is a linear function of deviation variables assigned to the j^{th} priority level.

The appearance of deviation variables **n**,**p** in the achievement function is based upon the nature of goal. Achievement is measured as follows:

(i) If the t^{th} goal is less than or equal type, $f_t(x) \leq b_t$, p_t appears in the achievement function.

(ii) If the t^{th} goal is grater than or equal type, $f_t(x) \geq b_t$, n_t appears in the achievement function.

(iii) If the t^{th} goal involves an equality expression, $f_t(x) = b_t$, then $n_t + p_t$ appears in the achievement function.

It should be noted that $f_i(x)$, i = 1,2, ... m is not restricted to be convex, linear, nonlinear, continuously differentiable, etc. Also **X** is unrestricted in sign. It may be continuous, discrete, or a mix of continuous or discrete variables. [3]

B.3 Pattern search algorithm for non linear goal programming

In performing the optimization, the design variables often pose conflicting behavior among themselves or with the objective function. The vector of design variables is to be checked by a small increment for improvement of the objective function in each direction and then only the overall design vector is evaluated. Pattern search techniques are able to handle this type of optimum search with high efficiency. The Hooke and Jeeve method for pattern search is present in this section. The method is one of the earliest and most successfull methods of optimum seeking techniques. Each in this search method consists of two kinds of moves, one is called as the exploratory move and the other is pattern move. The exploratory move is to explore the local behaviour of the objective function and the pattern move is to take advantage of the pattern direction. In order to present the concept of the pattern search strategy of the Hooke and Jeeve method, an algorithm is listed below. For clarity, the optimization surface for two design variables x_i and x_j is shown in Figure B.1. The contour lines are represented by constant values of Φ where the search starts from an initial point towards an optimum. The unsuccessful search path is shown in dashed lines.

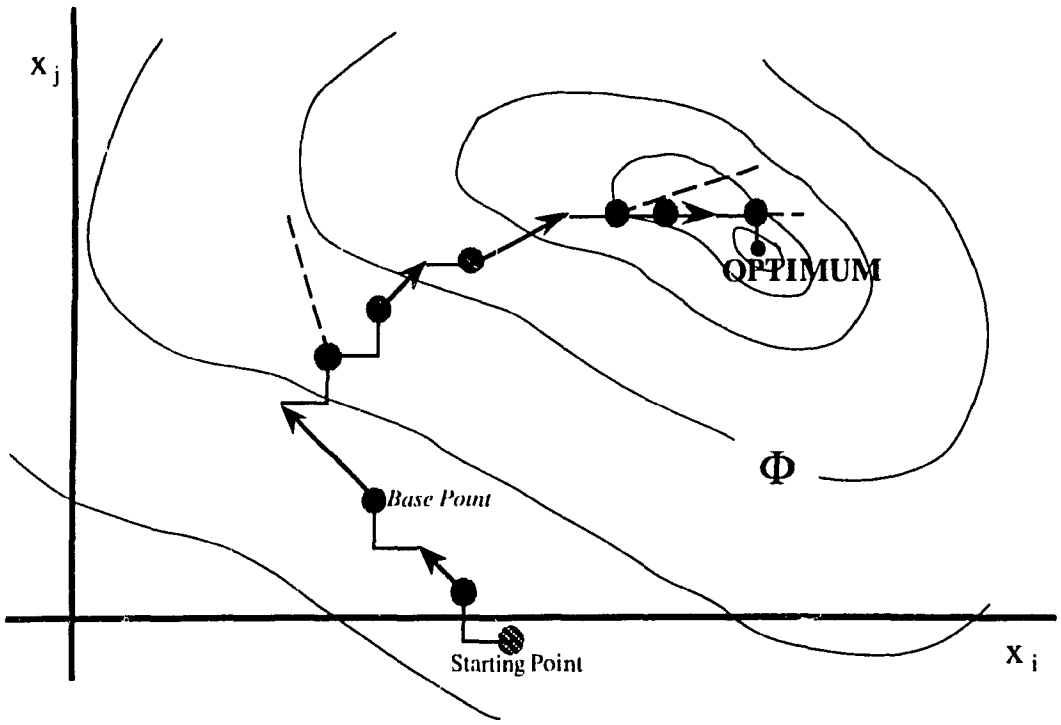

Figure B.1 Search strategy of the Hooke and Jeeve method

Algorithm:

Step 1- An arbitrary starting point (initial base point) is selected and the objective functoin Φ is evaluated.

Step 2- An exploratory search from the base point is begun by giving one design variable a small predetermined step length. If this improves the value of Φ, it is retained; else a corresponding negative step value is taken. The final result of the exploratory search yields a temporary base point.

Step 3- Patern move is made by changing each design variable from the temporary head an amound equal to the difference between the temporary base point and the base point. From the new point make an exploratory search.

Step 4- If the exploratory search fails to improve , it is cancelled and repeated by a new seach from the previous base point. If it succeeds, the final result is taken as the new base point followed by a patern move.

Step 5- The iteration continues until the exploratory search fails to locate a better point. The step length is then reduced, and the search is repeated. After each failure the step length is reduced an additional fraction until it reaches some predetermined minimum. The base point where that minimum occure is called then the optimum.

Flowchart of the above mentioned algorithm is illustrated in Figure B.2.

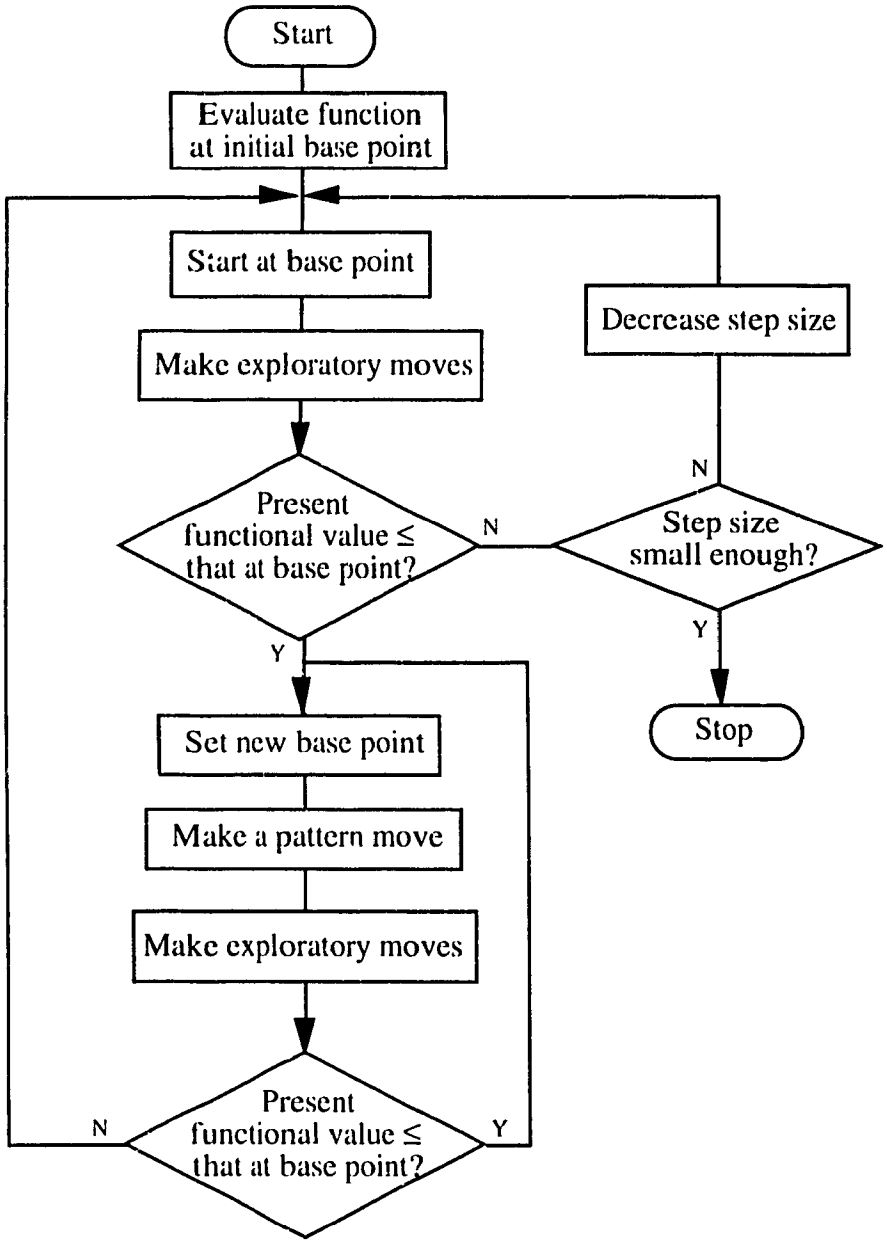

Figure B.2 Flowchart of Hooke and Jeeve method

The pattern search is performed successfully in an unconstrained nonlinear design space. The method is not suitable for a design space with nonlinear constraints.

B.4 Hooke and Jeeve method for non linear goal programming

A Hooke and Jeeve method for pattern search in the context of non linear goal programming algorithm is presented here.

Finding the design variable vector **x** as to minimize

$\mathbf{a} = [\ (g_1(\mathbf{n},\mathbf{p})),\ (g_2(\mathbf{n},\mathbf{p})),\ (g_3(\mathbf{n},\mathbf{p})),\ .....\ \ (g_K(\mathbf{n},\mathbf{p}))\ ]$

such that $f_i(\mathbf{x}) + n_i - p_i = b_i;$

$n_i,\ p_i \geq 0 \quad \text{for} \quad i = 1,2,3, ..., m$

Where $g_k(\mathbf{n},\mathbf{p})$ is a function of deviation variables associated with the objectives at the k^{th} priority level and $f_i(x)$ is the left hand side of the i^{th} goal.

Step 1: Initialization

(i) Set the index on the pattern search number $r = 0$

(ii) Set the index on the **x** vector $q = 0$

(iii) Select the first base point $\mathbf{x}^{(1)}$

(iv) Set the initial variable pertrurbation step size δ

(v) Set the minimum δ for termination δ_{min}

(vi) Set ε, the convergence factor two successive evaluations of **a**

(vii) Set the acceleration factor α

(viii) Set the step reduction factor β

(ix) Set the number of search iterations R_{max}.

Step 2: evaluation of initial achievement function and test base point.

(a) Set $h = q + 1$

(b) Compute the initial achievement function value $\mathbf{a}(\mathbf{x}^{(h)})$ for $\mathbf{x}^{(1)}$.

(c) Let $\mathbf{t}_{h,0} = \mathbf{x}^{(1)}$ as the initial test base point.

Step 3: Increment the indices set in step 1

(a) $q = q+1$

(b) $r = r +1$

Step 4 : Exploratory Search

Perform explorations about (i.e., about $\mathbf{t}_{h,0}$).

(a) Initialize the index for variable subscripting; set j = 1

(b) If $\mathbf{a}(\mathbf{t}_{h,0} + \delta_j) < \mathbf{a}(\mathbf{t}_{h,0})$ then $\mathbf{t}_{h,j} = \mathbf{t}_{h,0} + \delta_j$ proceed to step 4(d) otherwise, $\mathbf{t}_{h,j} = \mathbf{t}_{h,0}$: proceed to step 4(c)

(c) If $\mathbf{a}(\mathbf{t}_{h,0} - \delta_j) < \mathbf{a}(\mathbf{t}_{h,0})$ then $\mathbf{t}_{h,j} = \mathbf{t}_{h,0} - \delta_j$ proceed to step 4(d) otherwise, $\mathbf{t}_{h,j} = \mathbf{t}_{h,0}$: proceed to step 4(d)

(d) Set $\mathbf{t}_{h,0} = \mathbf{t}_{h,j}$; if j = n, go to step 5. Otherwise set j = j + 1 and return to step 4(b).

Step 5: Achievement function determination test

Compare the achievement function value at $\mathbf{t}_{h,0}$ with the $\mathbf{a}(\mathbf{x}^{(h)})$.

(a) If $\mathbf{a}(\mathbf{t}_{h,0}) + \varepsilon < \mathbf{a}(\mathbf{x}^{(h)})$, the test base point $\mathbf{t}_{h,0}$ becomes the permanent base point. Set $\mathbf{x}^{(q+1)} = \mathbf{t}_{h,0}$ and then proceed to step 6

(b) Otherwise, $\mathbf{x}^{(q+1)} = \mathbf{x}^{(h)}$ and then proceed to step 7.

Step 6: Pattern Search

(a) If $r \geq R_{max}$, the number of pattern searches limit has been exceeded, proceed to step 9

(b) otherwise set h = q+1 and set $\mathbf{t}_{h,0} = 2\mathbf{x}^{(h)} - \mathbf{x}^{(h-1)}$, proceed to step 3.

Step 7: Step size reduction

(a) Set $\delta = \beta.\delta$ and proceed to step 8.

Step 8: Minimum step size test

(a) If $\delta \leq \delta_{min}$ proceed to step 3

(b) otherwise set, h = q+1 and $\mathbf{t}_{h,0} = \mathbf{x}^{(q+1)}$ proceed to step 3

Step 9: Search termination step

Best solution attained is at $\mathbf{x}^{(q)}$.

B.5 Integer conversion heuristic

There are many methods available to obtain an integer solution during a pattern search. In the presented NLIGP approach the integer conversion is obtained using rounding heuristic. The algorithm, which can be adopted with the exploratory search of a NLIGP, is presented below:

$\mathbf{t}_{h,0}$ is the test base point

if $\mathbf{a}([\mathbf{t}_{h,0} + \delta_j + 0.5]) < \mathbf{a}([\mathbf{t}_{h,0}])$ then

$\mathbf{t}_{h,j} = [\mathbf{t}_{h,0} + \delta_j + 0.5]$

$\mathbf{t}_{h,0} = \mathbf{t}_{h,j}$

else

if $\mathbf{a}([\mathbf{t}_{h,0} + \delta_j]) < \mathbf{a}([\mathbf{t}_{h,0}])$ then

$\mathbf{t}_{h,j} = [\mathbf{t}_{h,0} + \delta_j]$

$\mathbf{t}_{h,0} = \mathbf{t}_{h,j}$

else

$\mathbf{t}_{h,j} = \mathbf{t}_{h,0}$

endif

endif

The '[ ]' brackets in the expressions mean the largest integer contained in. For example [9.3] translates into 9; while [- 4.5] translates to -5.

B.6 The algorithm for a NLIGP

An algorithm for non-linear integer goal programming method is presented here. The algorithm is the combination of the NLIGP method with the rounding heuristic.

Step 1: Initialization

(i) Set the index on the pattern search counter, r = 0

(ii) Set the index on the x-vector, q = 0

(iii) Select the first base point $x^{(1)}$.

(iv) Set the initial variable pertrurbation step size δ

(v) Establish the minimum δ for termination δ_{min}

(vi) Set the convergence factor ε for two successive evaluations of **a**

(vii) Select the acceleration factor α and the step reduction factor β

(viii) Set the number of search iterations not exceed R_{max}.

(ix) Set KFLAG = 0, a value used to distinguish an exploration about an accelerate test point.

Step 2: Compute the initial achievement function value for $\mathbf{x}^{(1)}$, $\mathbf{a}(\mathbf{x}^{(1)})$. Let $t_{1,0} = x^{(1)}$ be the initial test base point; set h = q+1

Step 3: Increment the indices set in step 1; q = q+1; r = r+1

Step 4: Exploratory search perform explorations about $\mathbf{x}^{(h)}$ (i.e., about $\mathbf{t}_{h,0}$) so as to determine $\mathbf{t}_{h,n}$ (the best $\mathbf{a}(\mathbf{x}^{(h)})$ attributable to this method of search) as follows:

(a) Initialize the index for variable subscript; set j = 0

(b) Increment j; j = j +1

if all variables have been processed (j > n), goto step 5

else continue

(c) Compute $\mathbf{t}_{h,j}$ as follows:

$$\mathbf{t}_{h,j} = [\, \mathbf{t}_{h,0} + \delta_j + 0.5]$$

(d) Check if the upper limit on x_j has been reached. If $\mathbf{t}_{h,j} > d_j$ goto step 4(f)

(e) If the value of achievement function at $\mathbf{t}_{h,j}$ represent an improvement in solution ($\mathbf{a}(\mathbf{t}_{h,j}) < \mathbf{a}(\mathbf{t}_{h,0})$) goto step 4(i); else continue

(f) Compute $\mathbf{t}_{h,j}$ as: $\mathbf{t}_{h,j} = [\mathbf{t}_{h,0} - \delta_j]$

(g) Check if the lower limit on x_j has been reached. If $\mathbf{t}_{k,j} < c_j$ goto step 4(b); else continue

(h) If the value of achievement function at $\mathbf{t}_{h,j}$ represent an improvement in solution ($\mathbf{a}(\mathbf{t}_{h,j}) < \mathbf{a}(\mathbf{t}_{h,0})$) goto step 4(i) ; else goto 4(b)

(i) Set new $\mathbf{t}_{h,0}$ as $\mathbf{t}_{h,0} = \mathbf{t}_{h,j}$; goto step 4(b)

Step 5: Compare the achievement function value at $\mathbf{t}_{h,0}$ with the $\mathbf{a}(\mathbf{x}^{(h)})$.

If $\mathbf{a}(\mathbf{t}_{h,0} + \varepsilon < \mathbf{a}(\mathbf{x}^{(h)})$, the test base point $t_{h,0}$ become the permanent base point: set $\mathbf{x}^{(q+1)} = \mathbf{t}_{h,0}$, KFLAG = 0, and goto step 6;

else $\mathbf{x}^{(q+1)} = \mathbf{x}^{(h)}$ then if KFLAG = 0, set KFLAG = 1, h = q+ 1 and set $\mathbf{t}_{h,0} = \mathbf{x}^{(q+1)}$ goto step 3;

If KFLAG = 1, reset KFLAG = 0 and goto step 7

Step 6: (pattern search) If the limit on teh number of pattern searches has been exceeded ($r > R_{max}$), go to step 9; else set h = q + 1 and set $\mathbf{t}_{h,0} = 2\,\mathbf{x}^{(h)} - \mathbf{x}^{(h-1)}$ and go to step 3

Step 7: (Step size reduction) set $\delta = \beta \,.\, \delta$ and go to step 8

Step 8: (minimum step size test) If $\delta < \delta_{min}$ goto step 9; else h = q + 1 and $\mathbf{t}_{h,0} = \mathbf{x}^{(q+1)}$ and goto step 3

Step 9: (Search termination step) Best solution attainable is at $\mathbf{x}^{(q)}$

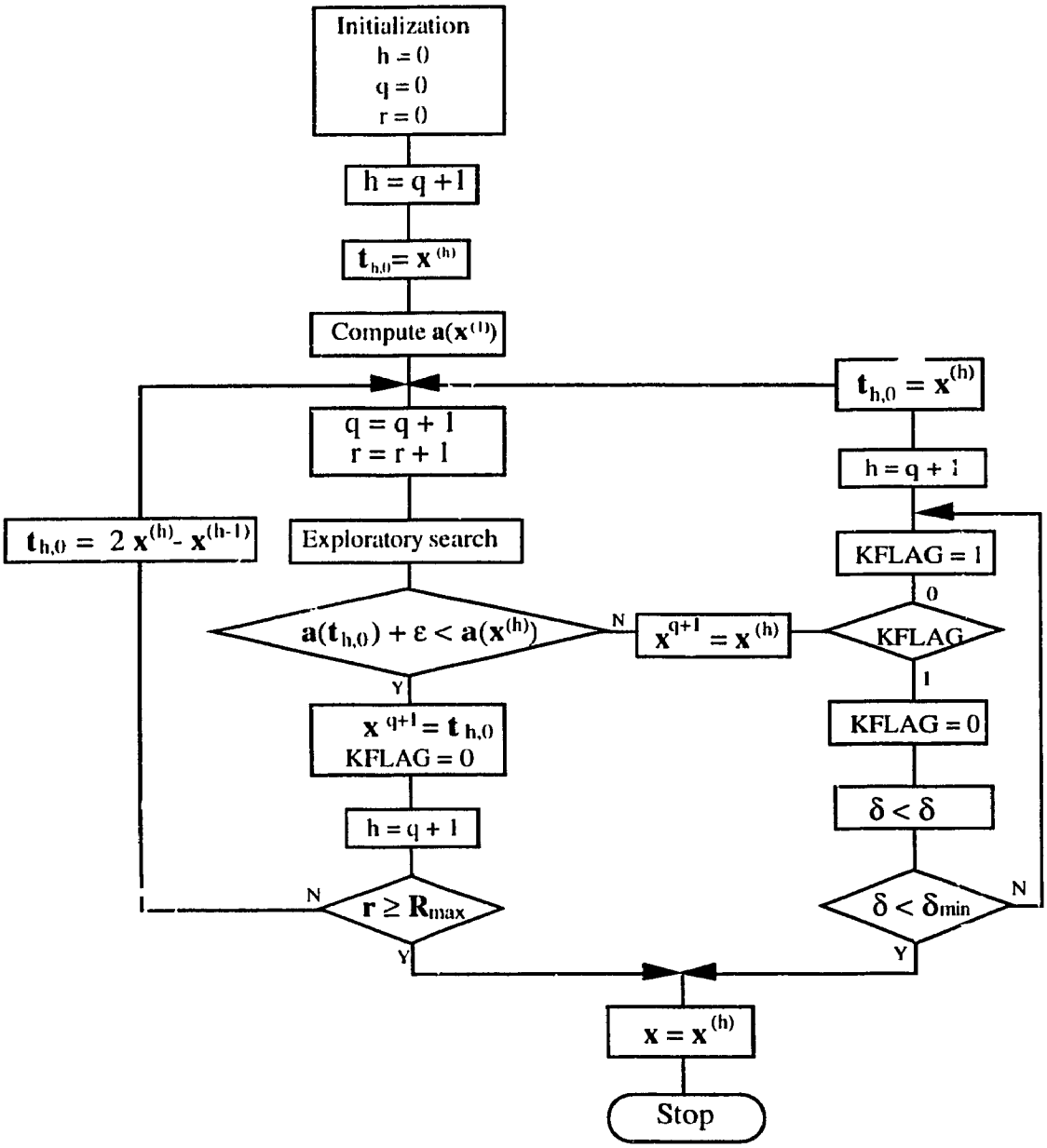

Figure B.3 Flow chart for NLIGP

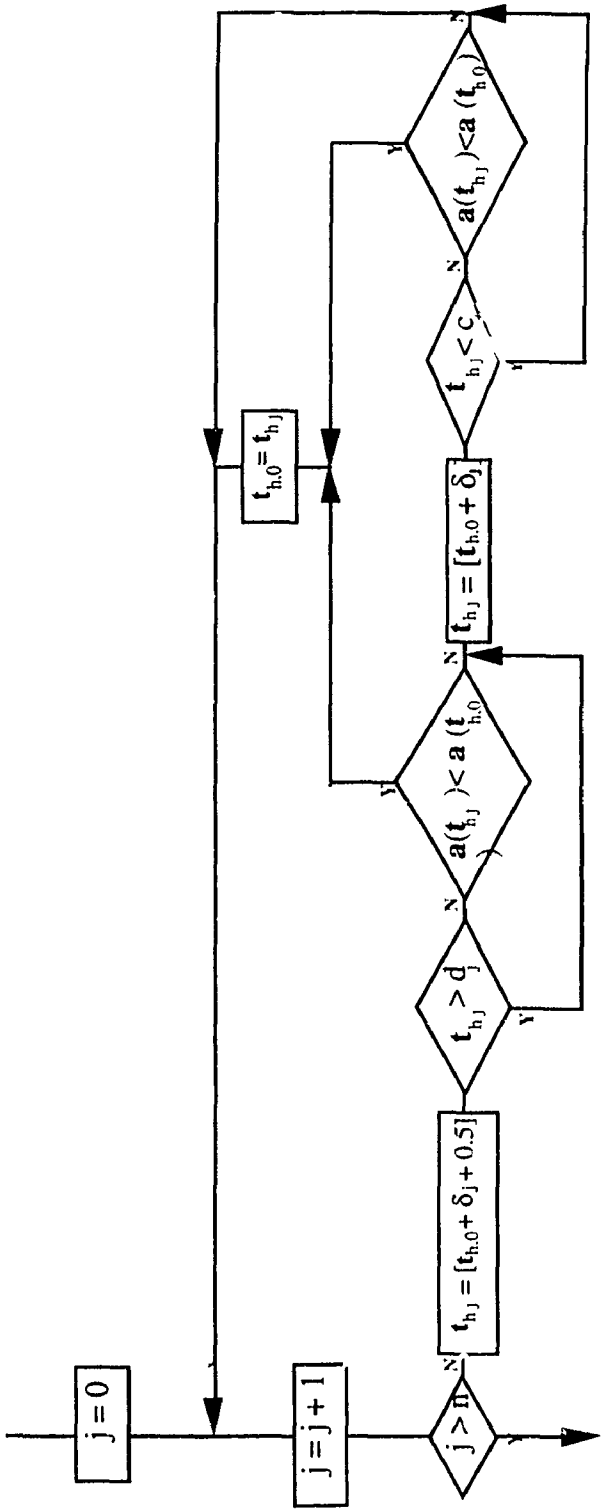

Figure B.4 The exploratory search step

When exercising the solution procedure, the optimization process often converges to the local minima. In finding the local minima, the optimized values must be examined for the design limits at which the procedure stops. In the selected NLIGP approach, the required design limits are specified as the goals to the solution procedure. In each minimization, a specified less critical quantities are treated as goals for the objective function and constraints. Usually, the goal to the objective function terminates the search process, even the procedure does not converges to the other goals exactly. When the search terminates in a local minima, the resulted value for the objective function may be inputed as a new goal and the entire process is repeated till no change between the objective function value and corresponding goal is notified. The limiting features associated with the constrains can also terminate the procedure in local minima. In such case, parametric variations in NLIGP algorithm are performed to allow the objective function to have higher priority. One of the other reasons for the convergence towards local minima seems to be the selection of the initial values for the design variables. Feasible starting points are often dictated knowing the approximate location of the optimum is known.

B.7 The NLIGP organization

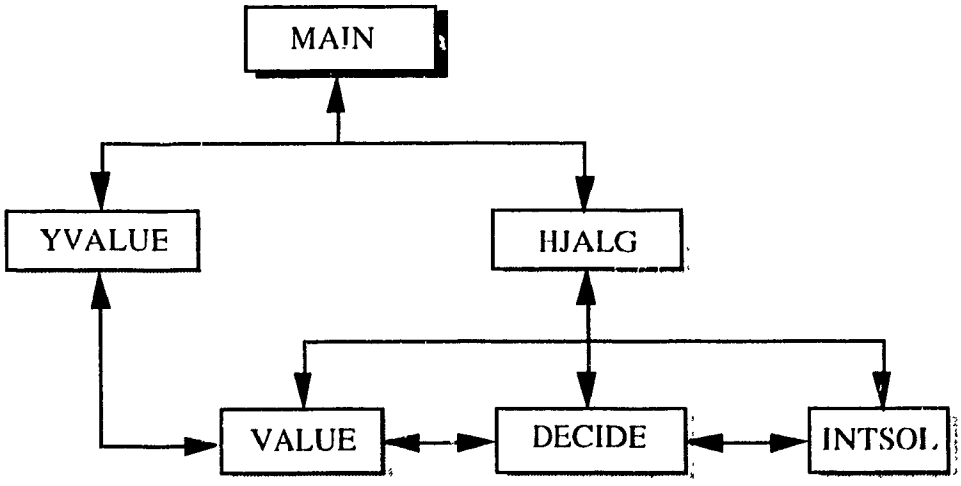

Figure B.5 Structure of NLIGP

Based on the algorithm described earlier, the computer code for NLIGP has been obtained. The main program calls 5 subroutines in order to perform the optimization. Figure B.5 shows the structure of the main program and NLIGP subroutines. The main program controls the overall execution by calling the two routines YVALUE and HJALG. The subroutine HJALG perform the pattern search, by sequentialy calling one of three subroutines VALUE, DECIDE and INTSOL. The achievement function is computed by the VALUE routine. DECIDE is to compare the achievement function values in different stages. It takes the value of the test point, evaluates achievement function and decides if the test point leads to an improvement. The INTSOL controls the integer modifications. The objectives are inputed in the subroutine YVALUE which is called by VALUE. For every new problem, the main program alters the objective functions according to the kinematic arrangement.

APPENDIX C

SOLUTION ALGORITHM FOR PENALTY FUNCTION METHOD

C.1 Introduction

Optimization techniques available for the solution of constrained nonlinear problems is classified into two broad categories, namely, the direct methods and indirect methods [38]. The Penalty function is one of the powerful indirect methods for handling heavily constrained problems with equality, inequality and mixed constraints. The penalty function method transforms the basic optimization problem into alternative formulations such that numerical solutions are sought by solving a sequence of unconstrained minimization problems. Two types of Penalty function method are available as, (i) Interior penalty function and (2) Exterior penalty function. In interior penalty function method, the sequence of unconstrained minima is found in the feasible region and in the exterior method it is in the infeasible region.

Let the basic optimization problem be of the form:

Minimize $\Phi(\mathbf{x})$, where $\mathbf{x} = x_1, x_2, x_3, \ldots, x_n$

subject to $F_i(\mathbf{x}) \leq 0$ for $i = 1, 2, 3, \ldots, m$

and also $F_i(\mathbf{x}) = 0$ for $i = (m+1), (m+2), (m+3), \ldots, r.$

The proposed penalty function method seeks the unconstrained minimum using an alternate form of objective function, known as the achievement function. The achievement function, denoted as $\mathbf{a}(\mathbf{x}, s)$, is defined by the following form:

Find $\mathbf{x} = x_1, x_2, x_3 \ldots x_n,$

so as to minimize

$$\mathbf{a}(\mathbf{x}, s) = \Phi(\mathbf{x}) + s * \left\{ \sum_{i=1}^{r} G_i[F_i(\mathbf{x})] \right\}$$

where, $\Phi(\mathbf{x})$ is the original objective function; 's' is a positive constant known as penalty parameter and $G_i[\ F_i(\mathbf{x})\ ]$ is the penalty term that is some function of constraints $F_i(\mathbf{x})$.

Popularly used forms of penalty terms are

for interior:

$$G_i[\ F_i(\mathbf{x})\ ] = -\frac{1}{F_i(\mathbf{x})}$$

$$G_i[\ F_i(\mathbf{x})\ ] = \log[-\ F_i(\mathbf{x})\ ]$$

for exterior:

$$G_i[\ F_i(\mathbf{x})\ ] = \max[0\ ,\ F_i(\mathbf{x})\ ]$$

$$G_i[\ F_i(\mathbf{x})\ ] = \max[0\ ,\ F_i(\mathbf{x})\ ]^2$$

C.2 The algorithm for penalty function method

An algorithm based on penalty function method is given as in the following steps:

(i) Start with a vector of initial feasible points $\mathbf{x}_1$ satisfying all constraints with strict inequality sign, i.e. $F_i(x_1) \leq 0$ for i = 1 to r and an initial value of $s_1 > 0$; set k = 1

(ii) Minimize $a(\mathbf{x}, s_1)$ by using any of the unconstrained methods and get $\mathbf{x}_k^o$.

(iii) Test whether $\mathbf{x}_k^o$ is the optimum solution for the original problem. If $\mathbf{x}_k^o$ is found to be the optimum, terminate the process. Otherwise go to the next step.

(iv) Find the next penalty parameter $s_{(k+1)}$ where $s_{(k+1)} = C * s_k$ and $0 < C < 1$

(v) Set the new value for k as k = k + 1; take the new starting point as $\mathbf{x}_k^o$; go to step (ii).

C.3 Development of interior penalty function solution procedure

The general formulation for the optimization problem is given as:

Find $\mathbf{x} = x_1, x_2, x_3 \ldots x_n$

so as to minimize $\Phi(\mathbf{x})$

subject to the inequality constraints

$$F_i(\mathbf{x}) \leq 0 \; ; \; i = 1, 2, \ldots, r$$

where $\mathbf{L} \leq \mathbf{x} \leq \mathbf{U}$ (**L**,**U** are upper and lower bound vectors of design variables respectively.)

The inequality constrains are incorporated into unconstrained artificial achievement function **a** which can be optimized through interior penalty function method. The penalty term assumes that the vector of design variables **x** is a feasible point (i.e., $F_i(\mathbf{x}) \leq 0 \; ; \; i = 1, 2, \ldots, r$). The artificial achievement function is given as:

$$\mathbf{a}(\mathbf{x}, s_1) = \Phi(\mathbf{x}) + s_1 * \left\{ \sum_{i=1}^{r} - \frac{1}{F_i(\mathbf{x})} \right\}$$

where s_1 is a positive constant. As stated in step (iv) of the algorithm, the s_1 value is reduced by a constant factor *C* after each minimization performed. The values specified for *C* affect the rate of convergence but otherwise fairly problem independent. A reasonable starting value for s_1 may be taken as 1.

In order to allow an infeasible starting point , an alternate additional penalty term $G_i[\, F_i(\mathbf{x}) \,]$ is used for any $F_i(\mathbf{x}) > 0 \; ; \; i = 1, 2, \ldots, r$.

$$G_i[F_i(\mathbf{x})] = 10^{20} * (\, | - F_i(\mathbf{x}) | \,)$$

This modification of the achievement function is implemented to achieve the feasible solution rapidly. Hence, the new achievement function becomes:

$$\mathbf{a}(\mathbf{x}, s_1) = \Phi(\mathbf{x}) + s_1 * \left\{ \sum_{i=1}^{r} - \frac{1}{F_i(\mathbf{x})} \right\} + 10^{20} * \left\{ \sum_{i=1}^{r} (\, | - F_i(\mathbf{x}) | \,) \right\}$$

At this point, a new penalty parameter s_2 is selected so that $0 < s_2 < s_1$. Using this penalty parameter, another achievement function is formulated.

$$\mathbf{a}(\mathbf{x}, s_2) = \Phi(\mathbf{x}) + s_2 * \left\{ \sum_{i=1}^{r} - \frac{1}{F_i(\mathbf{x})} \right\} + 10^{20} * \left\{ \sum_{i=1}^{r} (\, | - F_i(\mathbf{x}) | \,) \right\}$$

Now, the solution from $\mathbf{a}(\mathbf{x}, s_1)$ is taken as feasible starting base point for minimizing $\mathbf{a}(\mathbf{x}, s_2)$ and the process is repeated as it is indicated in step (iv) of the algorithm. If any solution is not obtained during the first minimization, then it is assumed that there is no feasible solution. As in using the procedure, the method should be used with caution, particularly in selecting the convergence criterion. In the assumed value for convergence is not sufficiently small, a premature convergence could be resulted. Knowing this, the entire search can be terminated under one of the following convergence criteria:

(1) $$C * s_k \leq 1^{-20}$$

(2) $$\left| \frac{\mathbf{a}(\mathbf{x}, s_{(i+1)}) - \mathbf{a}(\mathbf{x}, s_i)}{\mathbf{a}(\mathbf{x}, s_i)} \right| \leq 10^{-8}$$